A PUSH STRENGTH PREDICTION MODEL FOR THE SHOULDER HEIGHT TRANSVERSE PLANE

A THESIS

Presented to

The Faculty of the Division

of Graduate Studies

By

Ralph Conway Underwood

In Partial Fulfillment

of the Requirements for the Degree

Master of Science in the School

of Industrial and Systems Engineering

Georgia Institute of Technology

June, 1978

A PUSH STRENGTH PREDICTION MODEL FOR THE

SHOULDER HEIGHT TRANSVERSE PLANE

Approved:

R. W. Schutz, Chairman

T. L. Sadosky

R. G. Heikes

Date approved by Chairman: _____

ACKNOWLEDGMENTS

Dr. Rodney K. Schutz contributed a great amount of time and effort to this thesis. I am indebted to him for his guidance and advice. I would also like to thank Dr. Thomas L. Sadosky and Dr. Russell G. Heikes for their advice and support as members of the reading committee. I am grateful to Mr. Fred Dixon for his assistance with apparatus-related problems.

Other individuals to whom I am extremely grateful are Loren P. Rees, Jane C. Ammons, and Randy C. Maxwell. They supported me with their excellent technical minds and their strong friendship. I received valuable assistance from many other friends at Georgia Tech, for which I am grateful.

I am the most indebted to my family, whose sacrifices, understanding, and love will always be appreciated.

TABLE OF CONTENTS

Appendix Page

LIST OF TABLES

LIST OF ILLUSTRATIONS

SUMMARY

The purpose of this study was to develop a mathematical model of human arm strength. The specific type of strength studied was isometric push strength in a transverse plane located 20 inches above the seat reference point.

Data was collected on one male subject in 22 radial directions around the body, at 10 hand locations in each radial direction. The subject was seated. His hand was in the semi-pronated position during exertion.

The apparatus used for data collection was a framework housing a piezo-electric force transducer.

The subject employed a free-push exertion technique which provided minimal body support or restriction. General conclusions concerning strength capabilities were derived from the data.

The following criteria were considered in developing the mathematical prediction model.

1. Consideration for the ultimate user of the model
2. Realistic data collection techniques
3. Intuitive parameters in the model
4. Computational simplicity
5. Predictive flexibility
6. Acceptable predictive accuracy

The laboratory procedures were evaluated to determine the

effect of secondary factors such as fatigue and learning.

A sequential model building process was used, wherein curves were fitted to data in individual directions. The individual curves were then integrated into a single general model. The general model utilizes four parameters.

CHAPTER I

INTRODUCTION

The purpose of this thesis is to develop a mathematical model of human static push strength for a seated person. The particular location in the reach sphere which was studied is the transverse plane located 20 inches above the seat reference point. This study is a part of an ongoing research effort at the Georgia Institute of Technology. Lower (1976) initiated this research with the design and construction of the strength testing apparatus, which was used in this study in modified form.

Objectives

The objectives of this thesis were to satisfy the following criteria:

1. Consider the ultimate user of the model and develop the model in such a way that it can be easily applied by these users. In this case, the user can be assumed to be the workplace designer, industrial designer or machine designer, with or without access to a digital computer.
2. Use data which are collected with realistic techniques--that is, without constraints on body position.

3. Develop a model which employs parameters which have clear, intuitive meanings.
4. Ensure that the model is computationally simple. This means that the predictions can be obtained quickly and easily without the need for advanced technical experience or access to a digital computer.
5. Develop a model which is robust enough to predict patterns of strength at all directions around the body.
6. Ensure that the model has good predictive accuracy.

Procedures

Maximum strength values were collected on a seated male subject using his right (preferred) hand. His hand was oriented in the semi-pronated position. The apparatus consisted of a steel framework housing a piezo-electric force transducer (load cell) which measured isometric pushing force. Values of strength were collected in 22 different radial directions around the body, with approximately 10 data points in each direction. All of the data points were located in a transverse plane 20 inches above the seat reference point.

The subject was instructed to use a free push position, the restrictions of which are:

1. Keep both feet on the floor
2. Keep both buttocks on the seat
3. Keep at least one point of the back on the chair back at all times.

A four parameter model was initially fit to the data on individual radial directions. Then expressions for the parameters were derived which were functions of the radial angle. Finally, these expressions were integrated into the general model, which predicts strength as a function of hand location, expressed as angle around and distance from the right shoulder.

Factors affecting the subject's performance were analyzed by performing an analysis of variance on data collected at two test points. The effects studied were hand location, fatigue, time of day, and learning.

Conclusions

From examination of the data, several characteristics of pushing forces were observed. The location of the largest forces was in the right front quadrant of the transverse plane. Strength profiles on individual radial directions took one of two general shapes: A centrally humped form which varied in height and skewness from one radial direction to the next, or a highly skewed form which was highest close to the body and sloped downward at more distant locations.

The distance from the body to the location of maximum strength in each direction was smallest behind the subject's left shoulder, but gradually increased as the hand location moved forward and around the body to the right.

There was a small statistically significant effect in the data due to fatigue. There was a significant negative "learning" effect. This effect was probably due to soreness and declining motivational levels of the subject. The free push criteria were probably responsible for some of the variability of the data but this effect was not pronounced enough to affect the general utility of the model.

The final model was as follows:

$$S = S_m \left(\frac{R}{R_m}\right)^{BR_m} \left(\frac{m-R}{m-R_m}\right)^{B(m-R_m)}$$

where

S = strength

S_m = maximum strength in one direction

R = distance to hand in one direction

R_m = distance to maximum strength in one direction

B = shape parameter of strength profile

m = distance to maximum reach in one direction

CHAPTER II

LITERATURE REVIEW

This chapter reviews the strength literature with emphasis on the following areas:

1. Patterns observed in pushing strength
2. Pushing techniques used by experimental subjects
3. Quantitative models of arm strength.

For a more general review of strength literature including other directions of exertion, definitions of terms, and historical perspectives, the reader is referred to Lower (1976) and Hunsicker (1955).

General Push Strength Patterns

The purpose of this thesis is to describe pushing strength with a mathematical model. There have been many studies on human strength, but a limited number have studied pushing strength as a combination of the individual efforts of several muscle groups. The majority of the studies which have thought of pushing strength in this way did not develop mathematical models. Various patterns of strength were observed in these studies, however, and a successful mathematical model should predict these patterns. For this reason a brief review of the patterns of strength found by other researchers has been made.

Push Strength Patterns of Standing Subjects

Standing push strength has been most completely investigated by Kroemer (1969). In one experiment, the subject braced both shoulders against a back wall and pushed forward with one hand. It was noted that his arm was straight at 80-90 percent of his maximum reach. The strength values increased to a point in the middle of his reach and then tapered off (Figure 2-1).

In another experiment, the subject braced one shoulder against the back wall and pushed forward with his opposite hand. Even though the same humped form resulted (Figure 2-1), this position was considered to be inefficient because of the rotation of the trunk at all distances except from 70 to 90 percent of reach, when the arm was straight and pushing was done with the shoulders.

When the subject placed one point of his back against the back wall and pushed forward with both hands, the hump of the curve moved closer to the body. At farther distances a slight upward trend was noted (Figure 2-1).

If the subject pushed with both shoulders contacting the back wall with two hands, the hump moved further away (Figure 2-1). In this condition the subject could lock his arms, resulting in the high maximum force. In Kroemer (1974) several general conclusions were made. First, it was noted that posture, support, and the force path through the body all have gross effects on push force. If the subject can wedge

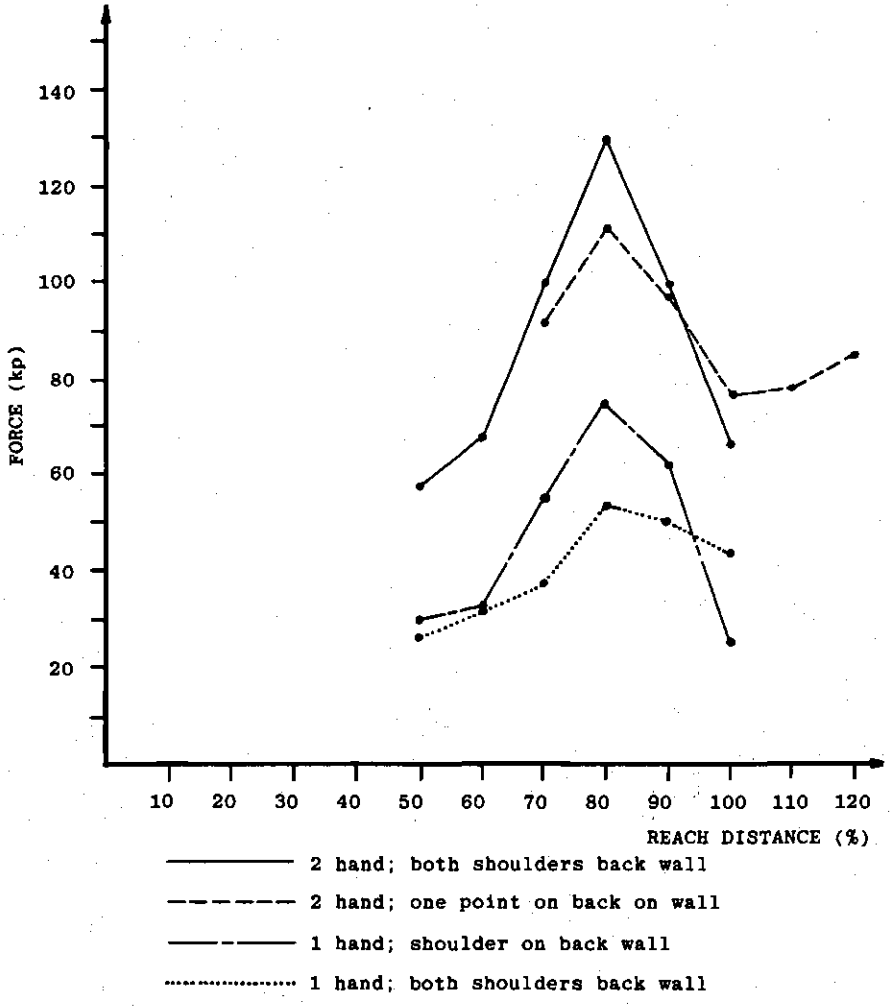

Figure 2-1. Push Strength with Varying Bracing Conditions (after Kroemer, 1969)

himself between the point of application and a wall or foot-rest, he can exert higher force. This is especially true if the force path through his body approaches horizontal.

It was noted that bracing against a rear wall and pushing forward with two arms is efficient, but bending of the arms tends to decrement force. Oblique force paths and one-handed pushes (even if braced) also decrement force. The highest observed forces were observed when the operator pushed with his back, with his legs pushing rearward against the rearwall. In general, maximum push strength was observed at 80 percent of the maximum reach. Laubach (1976) studied push strength differences between males and females. The results in push strength from that study are given in Table 2-1.

Push Strength Patterns of Seated Subjects

Hugh Jones (1947) studied push strength in the mid-sagittal, left-, and right-shoulder sagittal plane, and a sagittal plane outside the right shoulder. The hand was located 15 inches above the seat plane. Strength was observed to increase to hand locations 29 inches from the body and decrease from 29 to 33 inches, where the arm was straight. This pattern was attributed to the mechanical advantage at the intermediate positions outweighing the muscle's loss of power due to shortening. Strength in the mid- to right-shoulder-sagittal and outside-right-shoulder sagittal planes had less strength.

Table 2-1. Push Strength Comparison Between Males and Females (after Laubach, 1976)

Direction	Number of Hands	Brace	5%**	Mean	95%**
Forward	2	Foot Rest	31*	38	40
Forward	2	Vertical Wall	39	43	44
Rearward	1	Vertical Wall	39	35	35
Lateral	1	Vertical Wall	25	43	50
Forward	1	Vertical Wall	43	47	49

*Percentile of male strength exerted by females

**Female percentile rank

Hugh Jones detected a "toggle" effect in pushing wherein the streightening of the arm to a peak or "limiting" angle of 135° greatly increased push force. He noted that, because of this effect, push forces can be stronger than pull forces. Subjectively, however, pushing force was less comfortable for the subjects because of increased intra-thoracic pressure associated with pushing.

Hunsicker (1955) established a nomenclature system for pushing in the right shoulder sagittal plane. By this system, 180° corresponded to pushing horizontally directly ahead, 90° corresponded to pushing downward, and 0° corresponded to a horizontal rearward push. In the shoulder sagittal plane, maximum strengths were recorded at 180°. These values decreased to 90° and slightly increased to 60° (see Figure 2-2). Percentile tables for sitting position push were developed on a sample size of 55. This information is given in Table 2-2.

Thordsen, et al. (1972) studied seated push strength in the following aircraft oriented locations:

Stick:	in centerline of seat, 13 inches
	in front of SRP, 12 inches above SRP
Throttle:	10 inches left of seat centerline
	20 inches forward of SRP
	12.4 inches above SRP
Collective:	14 inches left of seat centerline
	10.3 inches forward of SRP
	4.75 inches above SRP

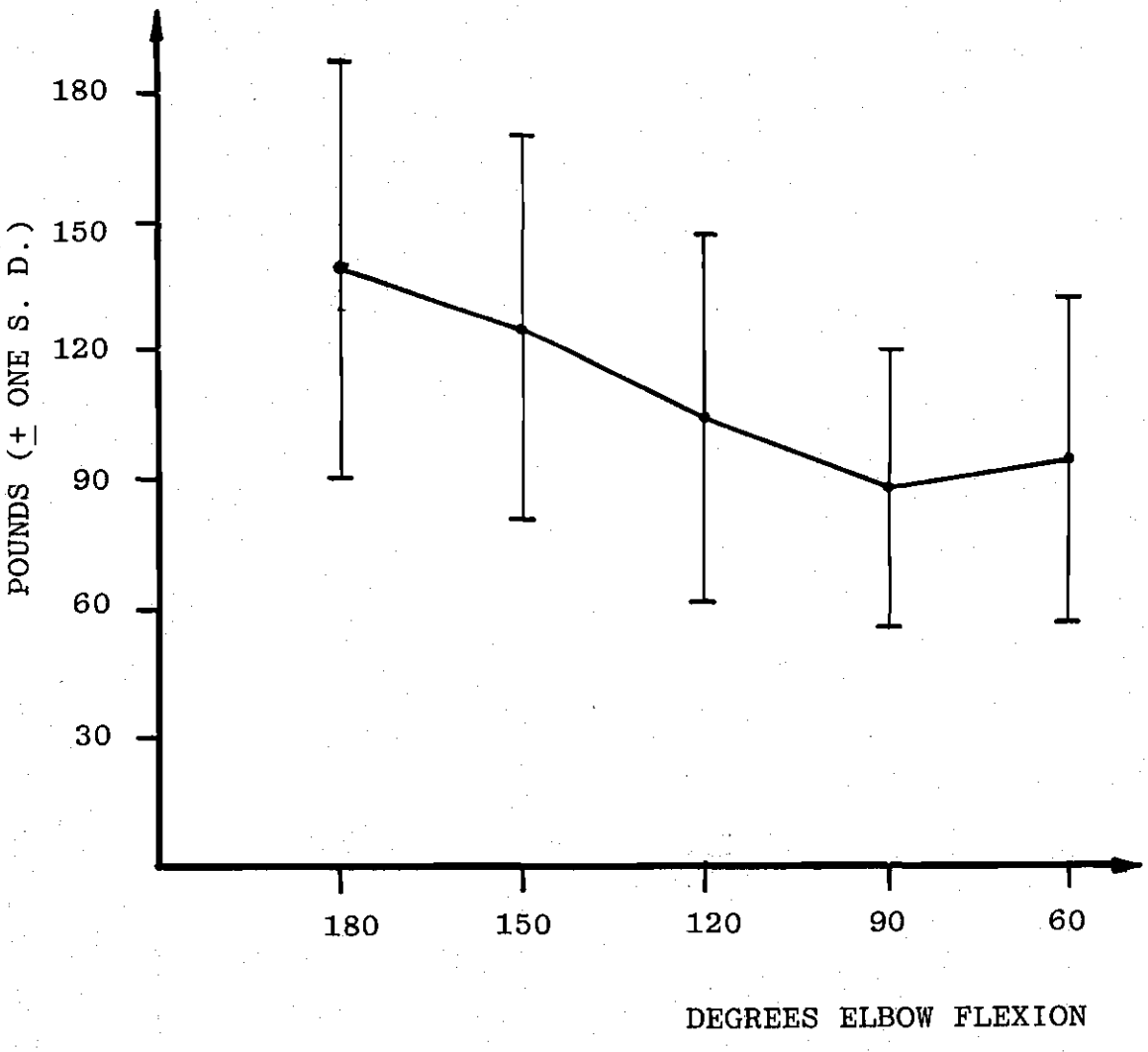

Figure 2-2. Sitting Position Push (after Hunsicker, 1955)

Table 2-2. Sitting Position Push Percentile Data* (after Hunsicker, 1955)

Percentile	Elbow Flexion				
	180°	150°	120°	90°	60°
5	50	42	36	36	34
10	76	62	44	47.5	47
20	82	118	65	54	54
30	101	90	78.5	66	62.5
40	132	116	87	77	76
50	139.5	128.5	95.5	84	93
60	156	136	112	89	97
70	164.5	149	121.5	101.5	113
80	177	164	131	112	123
90	206	181	150	125	143.5
95	210	194	172	154	150
Min	33	34	30	25	24
Max	215	210	220	178	174
μ	138.0	123	103.5	86.5	92.3
σ	48.9	45.1	43.3	32.8	37.7

*In pounds, N = 55, right arm.

Overhead control:	10 inches left of seat centerline
	0.0 inches forward of SRP
	47.3 inches above SRP
Panel Control:	10 inches left of seat centerline
	24.7 inches forward of SRP
	23.0 inches above SRP
Hatch Control:	13 inches right of seat centerline
	13 inches forward of SRP
	23 inches above SRP

These data were collected on a sample size of 51, using the left hand in the mid-position, except for collective and overhead controls, which were in the pronated position. Percentile data from this study are given in Table 2-3.

Laubach and Kroemer (1974) completed a study using similar control locations. They concluded that the strongest push forces occurred on the line between the shoulder and the handle. Weaker forces occurred in directions perpendicular to that line. They also noticed high variance between force directions at the same hand locations.

Pushing Techniques Used by Experimental Subjects

The importance of the pushing criteria used by subjects in strength studies is a point which has been mentioned in the literature (Kroemer, 1969). The question of the restricted versus non-restricted pushing criteria is a major area of concern, because of its implications on the applicability of

Table 2-3. Percentile Data for Selected Seated Push Forces*
(after Thordsen, et al., 1972)

Percentile	Stick	Throttle	Collective	Overhead	Panel	Hatch
99	124.8	238.2	98.5	65.9	245.1	60.4
95	100.3	208.6	94.2	51.8	219.6	56.8
75	79.9	180.2	79.2	38.2	194.8	44.0
50	67.9	162.5	66.5	31.3	174.8	34.0
25	54.9	140.7	54.6	25.4	148.6	25.3
5	36.3	93.8	41.4	17.7	103.2	16.2
1	29.2	44.9	36.2	12.9	74.5	11.8
μ	68.8	157.7	67.1	32.5	169.8	35.0
σ	20.4	34.8	16.0	10.5	36.3	12.5

*In pounds, N = 51, left arm.

the data generated. The following paragraphs briefly review the pushing criteria used in past studies.

Standing Push Force Techniques

It seems that in studies where subjects were standing fewer restrictions were imposed on their individual pushing techniques.

Ayoub (1974) tested standing push strength with an adjustable-height bar. No foot rest was provided for the subjects--only friction between the shoes and the floor was relied on to transmit reaction forces. This is an extreme case of the experimental simulation of real pushing conditions. Body weight was found to have a positive effect on pushing force at conditions where the feet were far from the bar and the bar was at a high position. The highest push forces were found to be exerted when the foot distance from the bar was 90-100 percent of the shoulder height, and the bar height was 70-80 percent of the shoulder height.

Kroemer (1969) utilized various realistic, non-restricted pushing situations. These conditions were tested with and without foot rests. Because the subjects assumed a variety of bracing positions between the load and a rear wall, no muscle group isolations were attempted. These positions resulted in more realistic forces than studies which restricted the subject to stand erect. This condition limits the force exerted because of the tendency to fall over.

Streimer and Springer (1963, in Kroemer, 1969) also

allowed subjects to assume natural positions in pushing. Pushing strengths were recorded at the knee, waist, chest, and overhead positions.

The natural position criteria was also used for pushing at the two inch, 24 inch, and overhead level by Fox (1967, in Kroemer, 1969). The subject was allowed to push with his shoulders or hands. The Schanne model (1972) calculated the optimal position for pushing with an iterative computer program. His approach was somewhat restricted, however, because his human voluntary forces were calculated on the basis of isolated muscle groups. Because of this approach, complex areas, such as regions behind the mid-frontal plane, were not investigated. In complex areas such as those behind the body, interaction between muscle groups is inevitable, and the isolation of muscle groups is impossible. A correction factor was included in the model to correct for inter-group interaction in areas in front of the subject.

Sitting Push Force Techniques

Because seated pushing is more dependent on the seat structure, more restricted pushing studies have occurred on seated subjects than when subjects are standing. Pushing strength with an adjustable back-rest was studied by Caldwell (1962). The force exerted was very apparatus-dependent. It was found that higher backrest positions resulted in higher forces exerted. He noted that force exerted was dependent on the resistance force at the shoulder. The toggle effect

mentioned by Hugh Jones (1947) was also observed. These results suggest that strength forces may vary between studies simply on the basis of the experimental apparatus. Therefore, a nonrestrictive, non-apparatus-dependent approach would seem to be as valid an approach as the restricted approach.

Another example of a restricted push study was that by Thordsen, et al. (1972). In this study, a limited number of aircraft control locations were studied. A rigid seat structure was used, with a high, hard backrest and footrest. The pushing convention used was as follows: Both feet were to remain on the footrest, and at least one point on the upper back must always be in contact with the seat back. This convention restricted the subject considerably. There would be a need to modify the push convention if more remote test locations were to be considered.

A rigid seat and footrest was used in the Hunsicker (1955) study also. Because all of the push forces were directed forward in the shoulder sagittal plane, the subject's back always contacted the seat-back. No long reaches occurred, because the locating index was arm angle rather than hand location. Hence, the seat back had a definite effect on the forces measured.

An example of a very free pushing criteria was that used by Gaughran and Dempster (1956). The subject sat freely on a bench with no back or foot contact with any surface. It was found that maximal push force could be

exerted when the moment arm of the couple formed by (1) the upward resistance force of the bench and (2) the downward force through the center of gravity of the body was maximized (see Figure 2-3). This moment arm could be lengthened by muscle tension which would move the contact area on the buttocks and thighs forward while keeping the location of the center of gravity the same. The addition of a backrest increased the amount of force exerted by providing resistance. This increase in force was highest when the backrest was at the shoulder position.

Other studies which used the free push criteria were Lower (1976) and Lower et al. (1977). These studies used the following criteria: Both feet were on the floor at all times, both buttocks on the seat at all times, and at least one point on the entire back was to contact the backrest at all times. This criteria allowed the subject to rotate his body for pushing at positions behind his back, and to reach to longer distances in front of him. These loose restrictions led to slightly increased data variance, but the increased realism was considered to have offset the variance increase.

Conclusions on Pushing Techniques

From examining the data it seems that non-restrictive push criteria are seen more frequently in the studies for standing subjects than seated subjects. Strength data on seated subjects in specialized settings, i.e., aircraft,

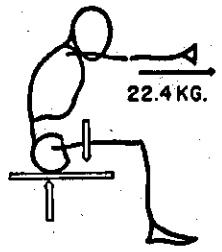

MAXIMUM PUSH POSITION

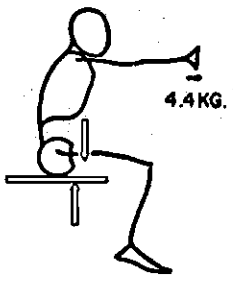

MINIMUM PUSH POSITION

Figure 2-3. Push Positions for Maximum and Minimum Force (from Gaughran, Dempster, 1956)

tend to use restrictive criteria. In the studies which are directed toward ultimate use in industry, there are efforts toward the use of general, non-restrictive push criteria.

A problem exists now because the majority of the seated push data has been collected in restricted conditions. It is difficult to apply this data to the more general pushing forces found in industry. Until more data is collected using free push criteria on seated subjects, this problem will remain.

Models of Strength

There are several types of models which have been developed to predict strength. The types which can be used to predict arm pushing strength include computerized models, models in equation form, and rigorous kinematic models.

Computerized Models

The model developed by Chaffin and Baker (1970) predicted static arm forces in the saggital plane. It consisted of a computer program which utilized the following inputs (see Figure 2-4):

1. Subject body dimensions: body height, weight, center of gravity of the hand-wrist combination, lower arm length, lower leg length, foot length, and elbow height when standing. These data were used in Dempster's (1964) equations to derive eight body link lengths and masses. These links

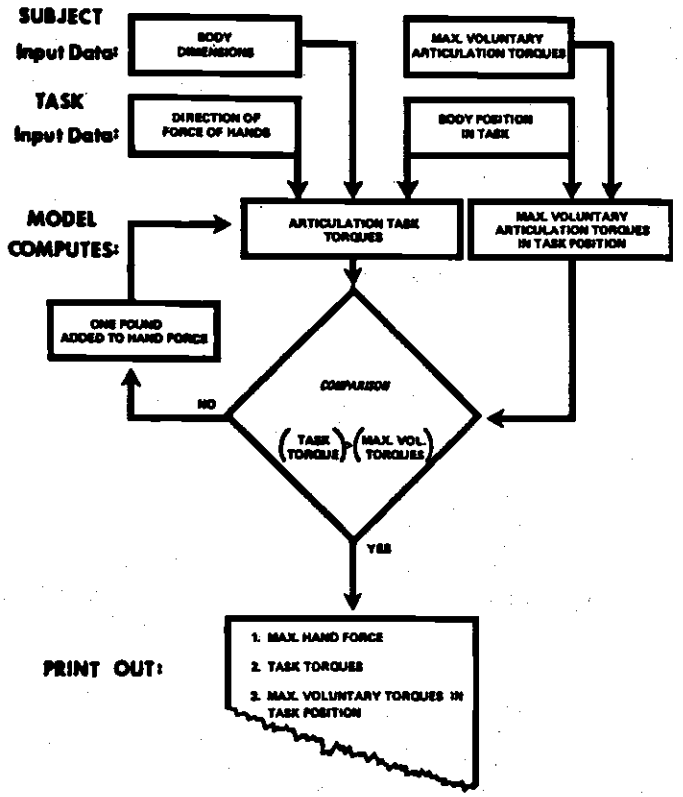

Figure 2-4. Flow Chart of Strength Model (from Chaffin, Baker, 1970)

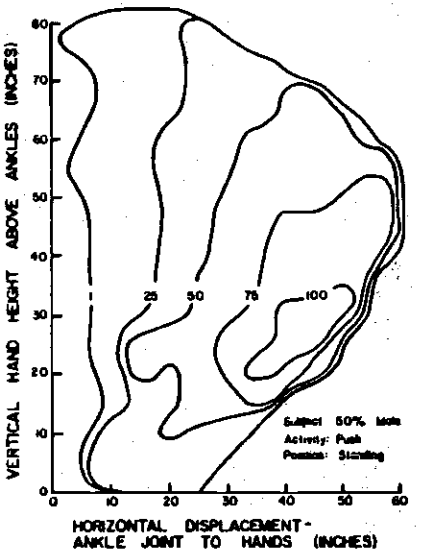

Figure 2-5. Push Strength Contours (from Martin, Chaffin, 1972)

composed a simplified "stick-man" representation of the body.

2. Body position of the specific task to be studied: this was composed of various angles between links. These angles were determined from photographs of the subject or drawing table templates.
3. Force direction of task to be studied: for a lifting task, this direction would be a downward force acting at the hands.
4. Maximum voluntary torques: these torques were computed from force data collected directly from the subject. The following forces were measured:
   a. ankle plantar flexion
   b. knee extension
   c. hip extension
   d. shoulder extension
   e. shoulder flexion
   f. elbow extension

A cable, pulley and load cell force measuring device was used to collect these values.

Following the input of the above data, the program computed task torques for each joint based on the anthropometric subject data and an initial external force value to be acting, say, downward at the hands.

The program then compared each computed task torque with each inputted voluntary torque. The stopping criteria

were as follows: (1) if any task torque exceeded its corresponding voluntary torque, (2) if the computed torque at the L5-S1 vertebral level exceeded given fracture limits (1284 lbs for males, 784 lbs for females). The current external force at the hands was considered to be the predicted maximum strength if either stopping criteria was satisfied. If neither of these conditions existed, the program incremented the external force by one pound, and the process iterated until one of the stopping conditions was satisfied. This model predicted the data with a least squares standard deviation estimate of 32.4 pounds.

Martin and Chaffin (1972) expanded this model to include two important features. The first feature was that their model iterated over many body positions for each hand location to find the optimal position. The task torques at this position were then compared to the voluntary torques. Also checked at each position were spine fracture conditions and body balance. Body balance was evaluated by examining torques at the ankle joint, so that no hand force and body position would result in the body becoming unbalanced.

The second new feature of the Martin and Chaffin (1972) model was the binary search procedure used in choosing successive external hand force values. Instead of simply incrementing the force by one pound after every iteration, the search procedure either halved or doubled the current value. This is a more efficient technique for converging

on the optimal force value.

Using input data from other sources, rather than directly measuring a subject, push prediction contours were developed (see Figure 2-5). This figure illustrates one of the conclusions stated in the report which asserted that push strength increases with horizontal displacement of the hands from the body.

Three dimensional prediction capability was the result of the Garg, Chaffin (1975) model. This model was similar in concept to the two previous models, but performed in modes using one or two hands.

Validation for this model was performed on subjects at Wright Patterson Air Force Base in the same hand locations that were examined in Thordsen, et al. (1972). These studies indicated that the model was good as a first approximation model, but a correction factor, which was a function of handle location and force direction, was needed.

Schanne (1972) utilized the same task torque approach as the above models. He also developed regression equations for torque at each joint. These equations predicted torque as a function of various joint angles. The voluntary torques used by Chaffin, Baker (1970) were replaced by these prediction equations.

Dynamic Strength Modeling

The above models dealt with static forces, or forces in which the muscles involved do not appreciably change in length. An example of a dynamic force model is the Pearson,

Butzel (1963) model. This model is a rigorous kinematic study of arm strength. For general applications among machine, industrial, and workplace designers, its use would be somewhat limited, due to its computational and theoretical complexity.

Models in the Form of Predictive Equations

Lower (1976) developed a model for predicting static push forces in the transverse plane located 20 inches above the seat reference point. This model expressed strength as a function of hand location in the plane. The lower model, which is parabolic in form, is as follows:

$$\text{Log}_e(S) = 2.837 - .003438\ (X-10.5)^2 - .002649\ (Y-.5)^2$$

$$+ .137\ \sqrt{(X-10)^2 + (Y-.1)^2}$$

where X and Y are coordinates of the hand in the transverse plane.

This model over-predicts in areas in front of the body and under-predicts maximum strengths in areas to the right of the mid-sagittal plane.

Figure 2-6 shows contours drawn from the data collected by Lower and equal strength contours generated from the parabolic model. The model predicted the data with an $R^2 = .9040$.

Lower, et al. (1977) developed a push strength model

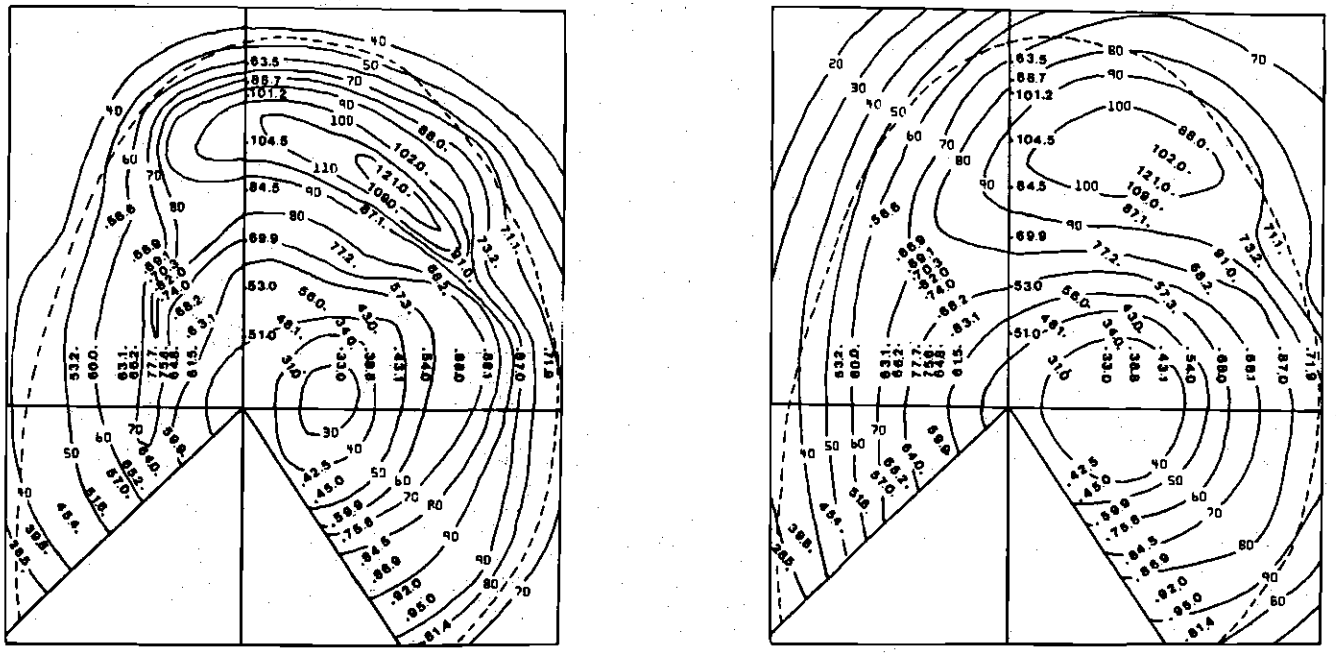

DATA CONTOURS

CONTOURS PREDICTED
BY MODEL

Figure 2-6. Data and Predicted Strength Contours
(from Lower, 1976)

for the 20 inch transverse plane which used parameters with clear physical interpretations. This model is as follows:

$$S = S_m e^{b_o R((R/R_m)-1)^2}$$

where:

$$R = ((X-X_o)^2 + (Y-Y_o)^2)^{\frac{1}{2}}$$

$$R_m = b_1 + b_2 (\theta^2 - b_3)^2$$

$$S_m = b_4 e^{b_5 \theta}$$

$$\theta = 90° - \arctan (Y/X)$$

and:

(X,Y) = coordinates of the hand (from SRP as origin)

(X_o,Y_o) = coordinates of the shoulder

θ = angle of hand about shoulder (to right)

R = radial distance from shoulder to hand

R_m = radial distance from shoulder to maximum strength in one direction

S_m = maximum strength in one direction

This model gave the poorest fit of the models investigated in the study (R^2 = .80). Because of the clear, intuitive interpretations of parameters R_m and S_m, however, this model

was considered to be the most promising of several models presented.

Figure 2-7 includes plots of predicted strength versus hand distance from the shoulder, S_m versus θ, and R_m versus θ, respectively. The strength versus distance plot of Figure 2-7 suggests a tendency for strength to remain at high levels, and possibly even increase at points close to the shoulder. This is a result which detracts from the intuitive appeal of the model. The S_m versus radial angle plot of Figure 2-7 demonstrates that maximum strength is highest almost directly in front of the shoulder. Equal strength contours plotted in Figure 2-8 further illustrate the S_m and R_m curves in Figure 2-7.

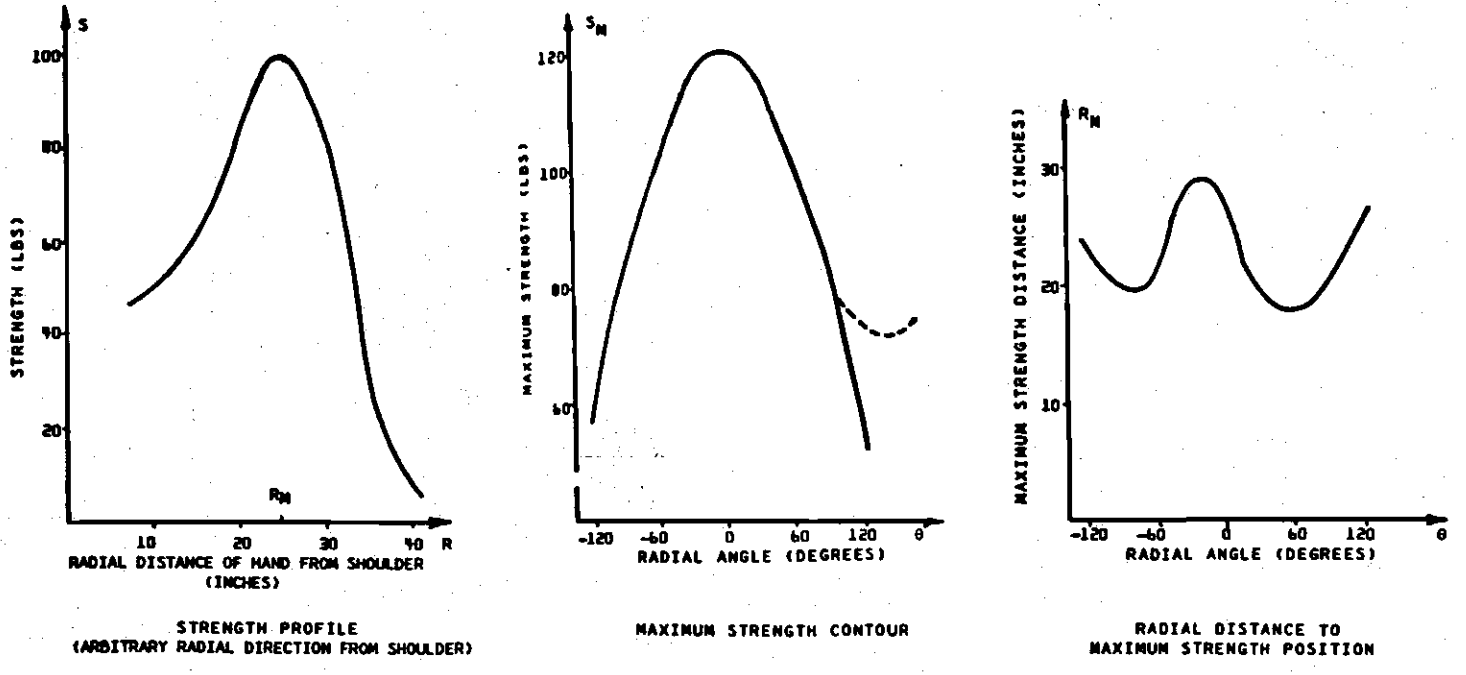

Figure 2-7. Strength Versus Distance and Parameter Versus Angle Plots (from Lower, et al., 1977)

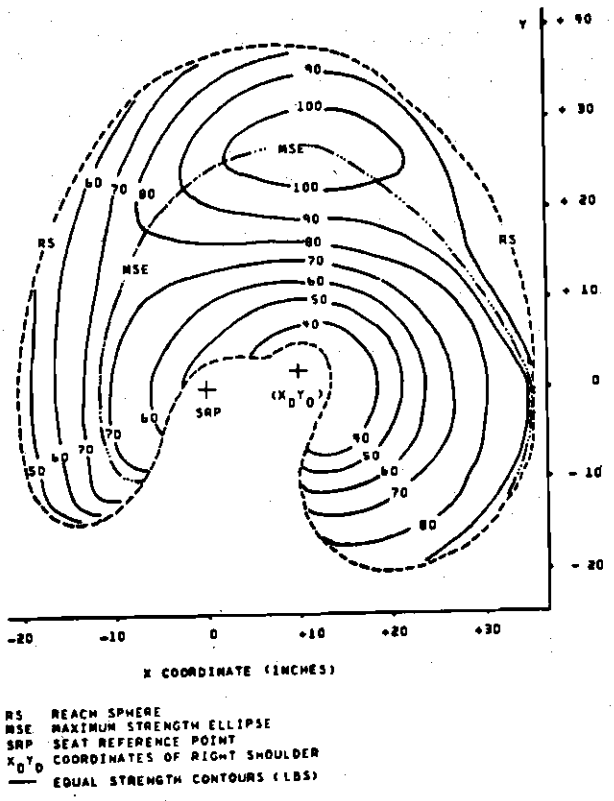

Figure 2-8. Predicted Strength Contours (from Lower, et al., 1977)

CHAPTER III

APPARATUS AND PROCEDURES

This study involved the collecting of arm strength data using an electronic force recording apparatus. The apparatus could be adjusted so that exertions could be made by a seated subject at different hand locations. Pushing force was measured at hand positions in the transverse plane located 20 inches above the seat plane. As suggested by Caldwell et al. (1974), the exertions were scheduled over four minute intervals. The measurements were analyzed for learning, fatigue, and session effects.

Apparatus

Physical Description of Apparatus

The positioning apparatus consists of a rectangular framework fabricated from 1-5/8 inch "Unistrut" steel channel (Figure 3-1). This is a modified version of the apparatus used by Lower (1976). Two channels were bolted to the floor parallel to each other extending between two walls of the laboratory. At the end of each floor channel, vertical channels were bolted to the walls. The distance between the walls is five feet four inches. The distance between the floor and wall channels was 23 and 11 inches, respectively.

Mounted on the floor channels is a rolling trolley,

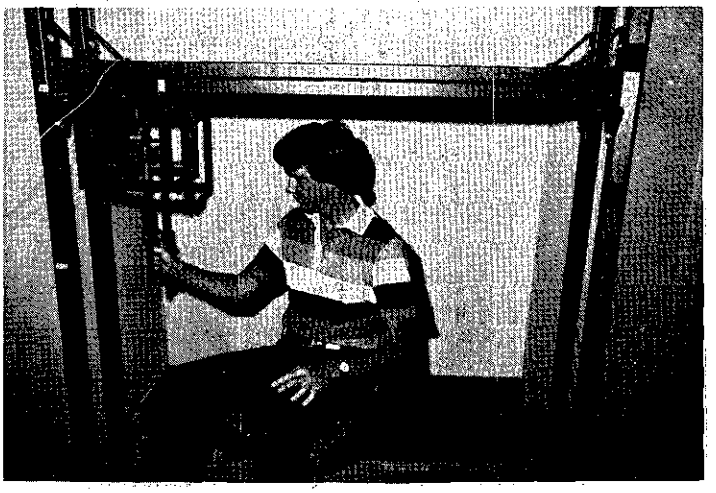

Figure 3-1. Experimental Apparatus: Long Reach Configuration

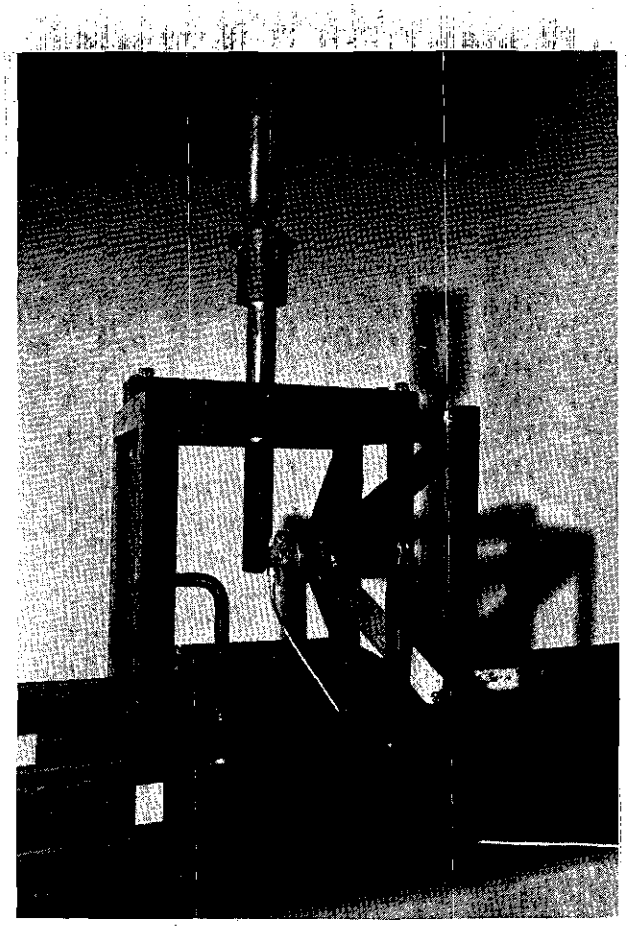

Figure 3-2. Subframe Containing Load Cell

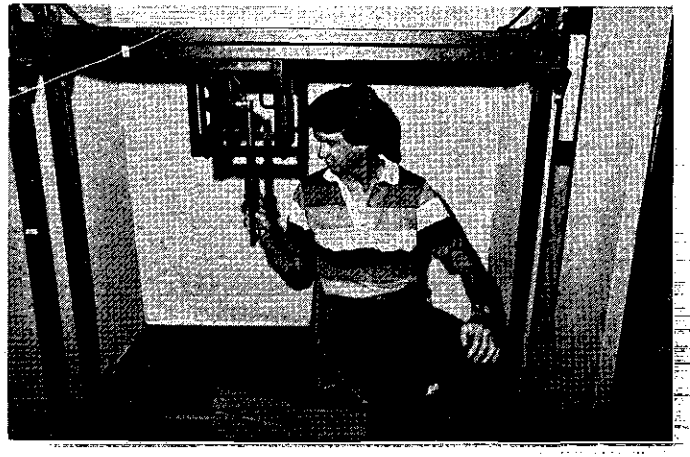

Figure 3-3. Experimental Apparatus: Short Reach Configuration (Radian 9)

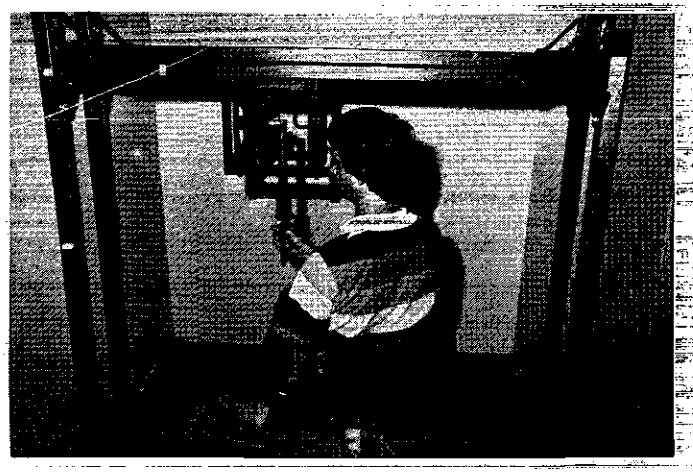

Figure 3-4. Experimental Apparatus: Short Reach Configuration (Radian 20)

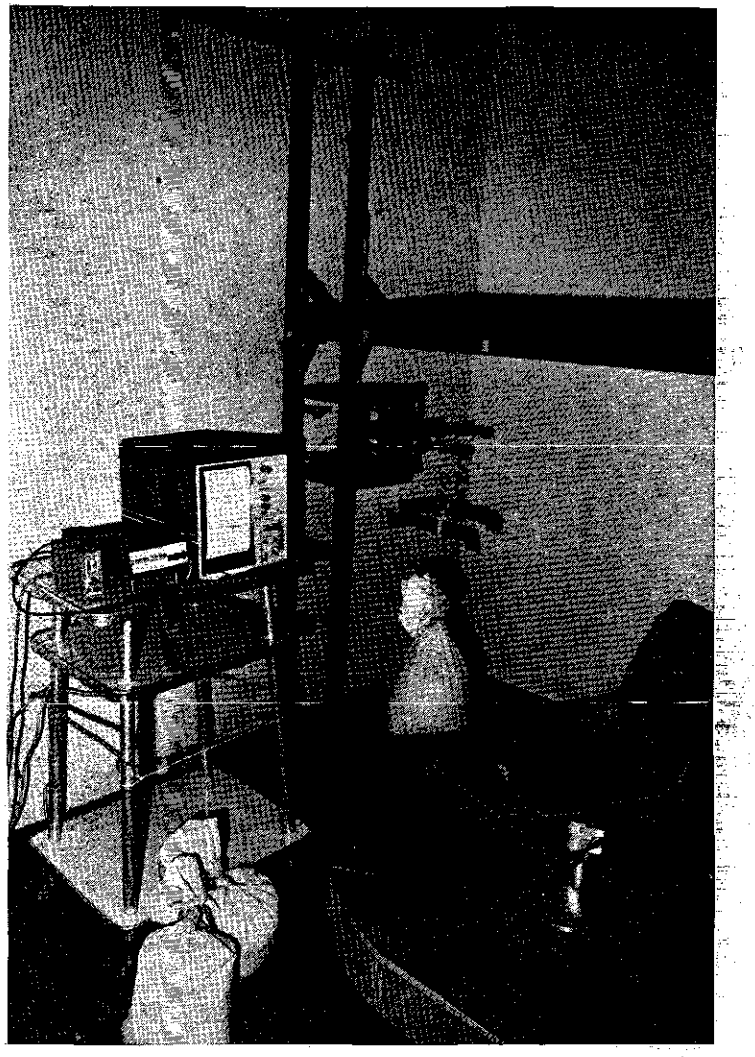

Figure 3-5. Calibration of Experimental Apparatus

on which is mounted the subject's chair. The trolley can be moved along the floor channels to any point between the walls and locked into position.

The chair dimensions are as follows:

seat width:	17 inches
seat length:	14.5 inches
backrest height:	14.0 inches
SRP height:	15.75 inches
base width:	three feet
base height:	three feet

The chair can be rotated and locked in any angle. The back of the chair is made of 1 8 inch plastic and flexes two to three inches under maximum stress. A foot rest is mounted on the trolley. It is inclined approximately 26 degrees. Suspended between the two walls at a height of 56.75 inches above the floor are two more channels, which are bolted to the vertical wall channels.

The force measuring instrument is a Piezotronics 208A03 Piezoelectric load cell force transducer. Constructed by Lower (1976) the frame also contains a handle located such that force exerted on the stirrup-shaped grip of the handle by the subject is transferred by the handle to the load cell. This is accomplished by pivoting the handle around a center mounted fulcrum pin. The load cell is attached to the handle with elastic berrylium copper studs. It emits a voltage of 10 mv per pound force. The load cell is a rigid structural

unit and can accept loadings to 500 lb (linear).

Operational Modes

The frame containing the handle and load cell can be mounted to the wall of overhead channels for testing. By (1) moving the trolley, (2) the handle, and (3) rotating the chair on the trolley, data points at varying angles and distances from the shoulder can be collected (Figures 3-1,3,4). For points close to the shoulder, the frame containing the handle is inverted and suspended from the overhead channels at a point near the center of their span (Figures 3-3,4). For points far from the shoulder, the frame containing the handle is inverted and suspended from the overhead channels at a point flush with the wall (Figure 3-1).

For calibration of the apparatus, the frame containing the handle is mounted directly to the wall channels so that the handle points perpendicularly away from the wall (Figure 3-5). In this position, weights are hung from the handle for calibration. Twenty-five, fifty and seventy-five pounds were hung from the handle before each test session to check the accuracy of the strip chart recorder.

Other Apparatus

The signals from the load cell are sent via coaxial cable to a PCB Piezotronics 484B power supply which is connected to a Hewlett-Packard 5306A multimeter. The voltages are read directly from the multimeter or sent to a Hewlett-Packard 7402A strip chart recorder for permanent recording.

A tape recorder was used to time the exertions. This tape is referred to as the "exertion sequence tape." Every 30 second interval of the four minute rest period was announced by the tape. For the last 10 seconds to the rest, every second was announced. At that time the tape gave the command "touch," which instructed the subject to touch, but not push, the grip of the handle. Five more seconds were counted, and the command "push" was given by the tape. Five more seconds were counted, and the tape gave the command "release." Then the four minute rest began. (The subject had been initially instructed to build to his maximum effort in one or two seconds after the "push" command, and to sustain the effort until the "release" command was given.)

Procedures

Nomenclature

The study consisted of measuring the maximum push strength of the subject at each of 215 locations in a transverse plane 20 inches above the seat reference point (SRP). The data points can be seen in Figure 3-6 and Tables 4-1 and 3-1. Table 4-1 lists the data by radian and Table 3-1 lists the data points in the order tested, by test session.

The data points were located approximately every three inches along 22 radial directions. On each radial direction, or "radian," 10 data points were located, with the exception of radian 13 (behind the left shoulder) which contained only

Table 3-1. Data Points in Order of Testing

TEST SESSION 1		TEST SESSION 2		TEST SESSION 3		TEST SESSION 4		TEST SESSION 5	
9.0	29.0	26.0	15.0	18.0	14.0	16.5	18.0	14.5	26.0
16.0	6.5	23.0	-9.0	25.0	-4.5	22.0	1.0	22.0	5.0
18.5	-12.0	-15.0	-9.0	-2.0	-6.0	-28.5	15.0	9.0	-12.0
-9.0	0.0	-10.0	24.0	-20.0	21.5	9.0	14.0	-16.0	5.0
-2.0	24.0	18.0	21.0	12.0	16.0	28.0	10.0	5.0	20.0
22.0	18.0	23.0	0.8	32.0	5.0	17.5	-10.0	32.0	18.0
31.0	-8.0	-3.0	-16.0	9.0	-4.0	-14.0	-1.5	26.0	-12.0
-8.0	-12.0	-4.0	8.0	-21.0	5.0	4.0	14.0	-10.0	-6.0
-22.5	23.0	9.0	26.0	4.0	24.0	30.0	26.0	3.0	11.0
11.0	12.0	18.0	7.0	23.0	13.0	28.0	-6.0	14.0	14.0
30.0	5.0	21.0	-16.0	22.0	-8.0	-11.0	-15.0	27.0	0.0
9.0	-22.0	-20.0	-3.0	-6.0	-4.0	-14.0	18.0	-1.0	-12.0
-9.0	5.0	1.5	18.0	-6.0	20.0	16.0	31.0	-14.0	11.0
4.8	21.0	16.0	12.0	12.0	10.0	38.5	5.0	9.0	21.0
28.0	16.0	22.0	-3.0	25.0	0.5	9.0	-16.0	21.0	8.0
16.0	-2.0	-9.0	-13.0	-4.0	18.0	-31.0	5.0	18.0	-11.0
-22.0	-13.0	-18.0	20.0	-20.0	12.5	3.0	26.0	-24.0	-4.0
-4.0	-18.0	13.5	22.0	9.0	22.0	16.0	9.0	2.0	17.0
20.0	24.0	16.0	5.0	30.0	10.5	14.0	0.0	28.0	24.0
30.0	-1.0	9.0	-18.0	20.0	-14.0	-18.0	-10.5	16.0	1.0
2.0	-7.0	-26.0	5.0	-18.0	-2.5	-14.0	28.0	-10.0	-14.0
-18.0	12.0	5.5	18.0	-3.0	26.0			-2.0	11.0

TEST SESSION 6		TEST SESSION 7		TEST SESSION 8		TEST SESSION 9		TEST SESSION 10	
9.0	18.0	14.0	8.0	24.0	20.0	19.0	22.0	15.0	28.0
26.0	9.5	24.0	-10.0	33.0	-9.0	19.0	2.0	28.0	5.0
16.5	-8.0	-12.0	-7.0	-6.0	-10.0	-16.0	11.5	9.0	-29.0
-22.0	-3.5	-5.0	19.0	-4.0	12.0	9.0	12.0	-20.0	5.0
-5.0	29.0	17.0	19.0	11.5	14.0	36.0	12.0	4.5	22.0
26.0	22.0	16.0	3.0	34.0	5.0	22.0	-18.0	35.0	20.0
19.0	-1.0	-10.0	10.0	9.0	-14.0	-29.5	-5.5	25.0	-11.0
-4.0	-8.0	9.0	16.0	-22.0	5.0	5.0	12.0	-24.5	-14.5
-6.0	13.5	38.0	12.5	2.5	28.5	14.0	10.0	2.0	12.0
13.0	20.0	13.0	-2.0	18.0	10.0	27.0	-5.5	16.0	17.0
26.0	5.0	-16.0	-2.0	29.5	-15.5	-15.5	-20.0	34.0	-2.0
9.0	-8.0	-1.0	22.0	-17.0	-10.0	0.0	10.0	0.5	-10.0
-14.0	5.0	20.0	16.0	-8.0	22.0	12.5	18.0	-12.0	10.5
7.0	12.0	24.0	-4.0	21.0	26.0	24.0	5.0	9.0	24.0
21.0	12.0	-12.0	-16.0	18.0	2.5	9.0	-24.0	24.0	9.0
18.0	-4.0	-8.0	14.5	-2.0	-14.0	-24.0	5.0	24.5	-22.5
-13.5	-8.0	14.0	23.5	-25.0	14.0	6.0	16.0	-26.0	-5.0
0.0	14.0	14.0	5.0	9.0	20.0	24.5	14.0	0.0	20.0
23.0	29.5	9.0	-20.0	32.0	11.0	20.0	-6.0	21.0	17.0
36.5	-2.5	-18.0	5.0	15.0	-6.0	-20.0	-12.0	26.0	-5.0
-22.0	13.0	6.5	14.0	-12.0	-1.0	-2.0	16.0	-14.0	-18.0
				-4.0	27.5			-12.0	17.0

Table 3-1 (continued)

TEST SESSION 11		12		13		14		15	
9.0	29.0	26.0	15.0	18.0	14.0	16.5	18.0	14.5	26.0
16.0	6.5	23.0	-9.0	25.0	-4.5	22.0	1.0	22.0	5.0
18.5	-12.0	-15.0	-9.0	-2.0	-6.0	-28.5	15.0	9.0	-12.0
-9.0	0.0	-10.0	24.0	-20.0	21.5	9.0	14.0	-16.0	5.0
-2.0	24.0	18.0	21.0	12.0	16.0	28.0	10.0	5.0	20.0
22.0	16.0	23.0	0.8	32.0	5.0	17.5	-10.0	32.0	18.0
31.0	-8.0	-3.0	-16.0	9.0	-4.0	-14.0	-1.5	26.0	-12.0
-8.0	-12.0	-4.0	8.0	-21.0	5.0	4.0	14.0	-10.0	-6.0
-22.5	23.0	9.0	26.0	4.0	24.0	30.0	26.0	3.0	11.0
11.0	12.0	18.0	7.0	23.0	13.0	28.0	-6.0	14.0	14.0
30.0	5.0	21.0	-16.0	22.0	-8.0	-11.0	-15.0	27.0	0.0
9.0	-22.0	-20.0	-3.0	-6.0	-4.0	-14.0	18.0	-1.0	-12.0
-9.0	5.0	1.5	18.0	-6.0	20.0	16.0	31.0	-14.0	11.0
4.8	21.0	16.0	12.0	12.0	10.0	38.5	5.0	9.0	21.0
28.0	16.0	22.0	-3.0	25.0	0.5	9.0	-16.0	21.0	8.0
16.0	-2.0	-9.0	-13.0	-4.0	18.0	-31.0	5.0	18.0	-11.0
-22.0	-13.0	-18.0	20.0	-20.0	12.5	3.0	26.0	-24.0	-4.0
-4.0	-18.0	13.5	22.0	9.0	22.0	16.0	9.0	2.0	17.0
20.0	24.0	16.0	5.0	30.0	10.5	14.0	0.0	28.0	24.0
30.0	-1.0	9.0	-18.0	20.0	-14.0	-18.0	-10.5	16.0	1.0
2.0	-7.0	-26.0	5.0	-18.0	-2.5	-14.0	28.0	-10.0	-14.0
-18.0	12.0	5.5	18.0	-3.0	26.0			-2.0	11.0

TEST SESSION 16		17		18		19		20	
9.0	18.0	14.0	8.0	24.0	20.0	19.0	22.0	15.0	28.0
26.0	9.5	24.0	-10.0	33.0	-9.0	19.0	2.0	28.0	5.0
16.5	-8.0	-12.0	-7.0	-6.0	-10.0	-16.0	11.5	9.0	-29.0
-22.0	-3.5	-5.0	19.0	-4.0	12.0	9.0	12.0	-20.0	5.0
-5.0	29.0	17.0	19.0	11.5	14.0	36.0	12.0	4.5	22.0
26.0	22.0	16.0	3.0	34.0	5.0	22.0	-18.0	35.0	20.0
19.0	-1.0	-10.0	10.0	9.0	-14.0	-29.5	-5.5	25.0	-11.0
-4.0	-8.0	9.0	16.0	-22.0	5.0	5.0	12.0	-24.5	-14.5
-6.0	13.5	38.0	12.5	2.5	28.5	14.0	10.0	2.0	12.0
13.0	20.0	13.0	-2.0	18.0	10.0	27.0	-5.5	16.0	17.0
26.0	5.0	-16.0	-2.0	29.5	-15.5	-15.5	-20.0	34.0	-2.0
9.0	-8.0	-1.0	22.0	-17.0	-10.0	0.0	10.0	0.5	-10.0
-14.0	5.0	20.0	16.0	-8.0	22.0	12.5	18.0	-12.0	10.5
7.0	12.0	24.0	-4.0	21.0	26.0	24.0	5.0	9.0	24.0
21.0	12.0	-12.0	-16.0	18.0	2.5	9.0	-24.0	24.0	9.0
18.0	-4.0	-8.0	14.5	-2.0	-14.0	-24.0	5.0	24.5	-22.5
-13.5	-8.0	14.0	23.5	-25.0	14.0	6.0	16.0	-26.0	-5.0
0.0	14.0	14.0	5.0	9.0	20.0	-24.5	14.0	0.0	20.0
23.0	29.5	9.0	-20.0	32.0	11.0	20.0	-6.0	21.0	17.0
36.5	-2.5	-18.0	5.0	15.0	-6.0	-20.0	-12.0	26.0	-5.0
-22.0	13.0	6.5	14.0	-12.0	-1.0	-2.0	16.0	-14.0	-18.0
				-4.0	27.5			-12.0	17.0

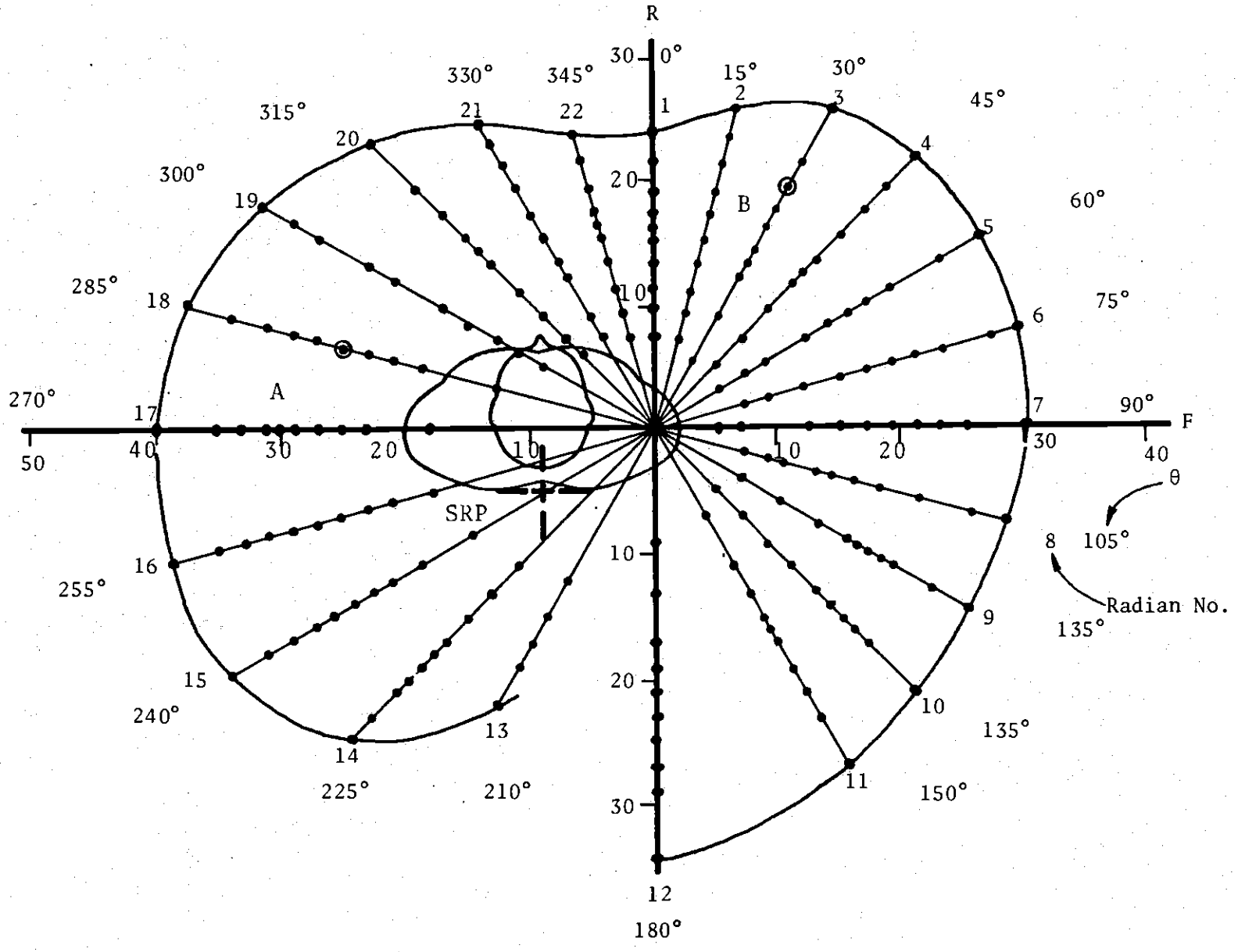

Figure 3-6. Locations of Data Points

five data points. The outermost data point on each radian was located near the maximum reach distance of an (approximate) fifth percentile male (Kennedy, 1964, in Vancott, Kincade, 1972). The radians were centered at a shoulder location nine inches to the right and five inches in front of the seat reference point. Each data point was located by means of an X,Y designation, with the origin being the seat reference point, positive X to the subject's right, and positive Y to the subject's front. Other nomenclature conventions are as follows (Figure 3-7):

1. The distance along each radian from shoulder point to hand location was designated "R".
2. The value of the strength recorded at each hand location was designated "S".
3. The distance from the shoulder to maximum reach was designated "M".
4. The angle between each radian and a point directly in front of the subject's right shoulder was designated "θ". A similar procedure for radial angle notation was used by Kennedy (1964, in Van Cott, Kinkade, 1972).

Subject Data

One subject was used in the experiment. Anthropometric data for the subject is as follows:

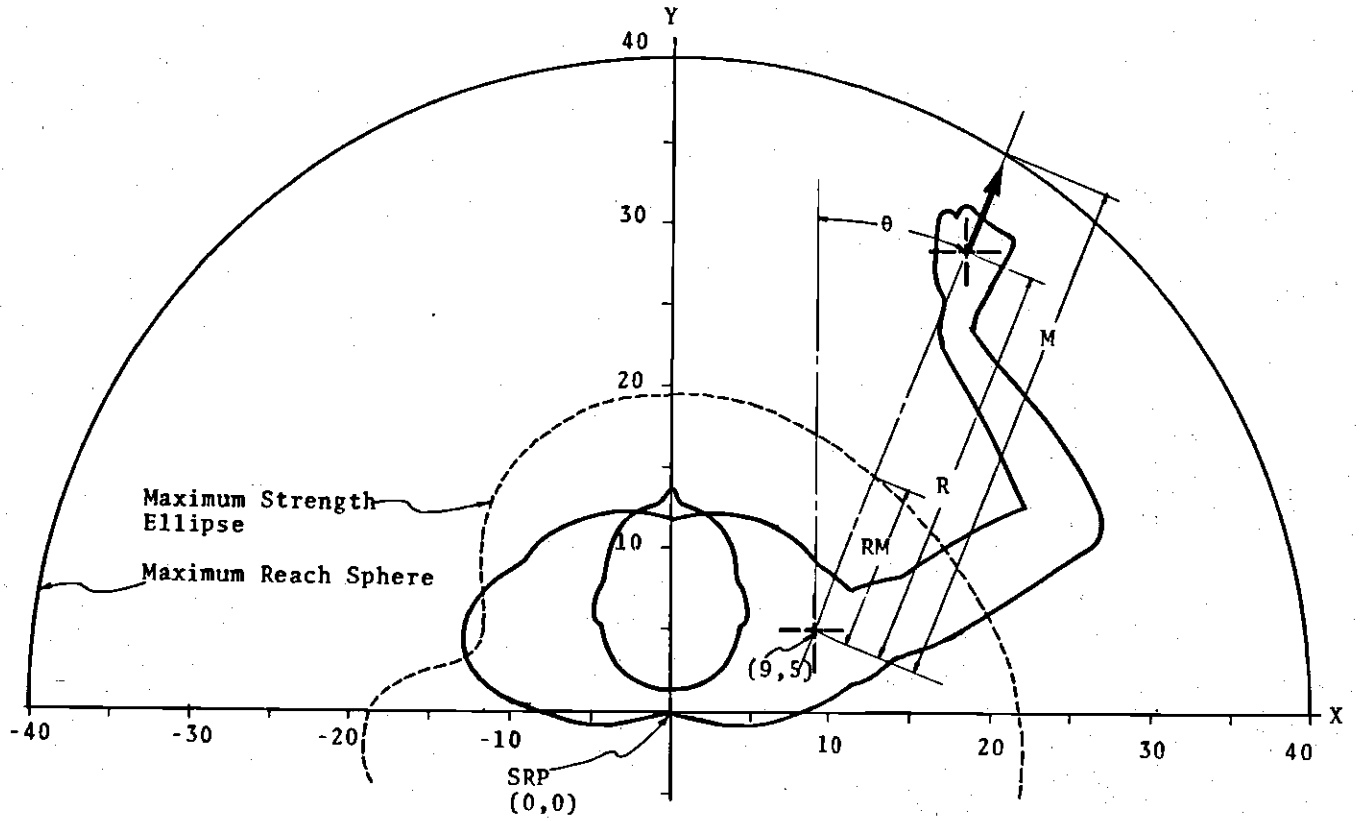

Figure 3-7. Nomenclature Used in Study

Age	25 years
Sex	Male
Height	6'0"
Weight	150 lb.
Neck	15.25 in.
Chest	27 in.
Forearm	10.5 in.
Wrist	6.5 in.
Waist	32 in.
Bicep (relaxed)	10.5 in.
Bicep (flexed)	12.0 in.
Hips	36 in.
Thigh	20 in.
Shoulder to elbow	14 in.
Shoulder width	18.38 in.
Somatotype	Ectomorphic
Preferred hand	Right

Test Sessions

Each test session measured maximum static push strength at 22 data points in a pseudo-random order. There were 20 test sessions, which resulted in one replication at each of the 215 data points. The experiment proceeded at the rate of two sessions per day: one in the morning, and one in the afternoon.

Each session proceeded in the following order:

1. Calibration of load cell at 25, 50 and 75 pound levels
2. Collecting strength data at two test positions for secondary effects sub-study
3. Collecting strength data at 22 data points for main strength study
4. Collecting strength data again at two test points for secondary effects sub-study.

The following paragraphs will discuss the four steps of each test session in detail.

Step One: Calibration

Each test session began by moving the frame containing the handle to the calibration position (Figure 3-5). Weights of 25, 50, and 75 pounds were hung from the handle in random order. The strip chart recorder was zeroed and calibrated for each weight.

Step Two: Test points for secondary-effects sub-study

After the calibration, strength at the following two test positions was recorded for use in the secondary sub-study (see Figure 3-6):

Test Point A: X = -11, Y = 10

Test Point B: X = 20, Y = 22

These positions were chosen to represent regions around the body in the transverse plane which were expected to have substantially different strength patterns.

Step Three: Data Points for Main Strength Study

After the first two secondary effects sub-study test points were collected, the 22 main data points were collected. These exertions proceeded according to the previously mentioned exertion sequence tape. The tape was a voice recording which counted four minute rest intervals, five second preparatory intervals, and five second exertion intervals. During the rest intervals, the subject rotated the chair and repositioned the trolley for the next exertion. He also recorded the value of the previous exertion. Chair angles and trolley locations could be read directly from scales mounted on the chair and floor.

The data forms and the computer program which converted the X,Y locations of the data points to actual trolley locations and chair angles are given in Appendices D and E.

A free form pushing convention was used in the data collection. The subject was allowed to push freely so long as both feet touched the trolley, both buttocks touched the seat of the chair, and at least one point on his back touched the back of the chair. Only the right arm was tested (the subject was right-handed), and the hand was held in the semipronated position.

No other attempt was made to locate or stabilize the subject. He was, however, instructed to avoid actively pushing with his feet. The strength value at each hand location was taken as the average of the middle three seconds of the five second exertion interval (see Appendix D).

Step Four: Test Points for Secondary-Effects Substudy

The test session was concluded with exertions at each of the two test points used in the secondary effects substudy. The results of the two test points before and after each session were analyzed later with an analysis of variance to monitor the effects of the following secondary factors.

1. Morning or afternoon test session time
2. Fatigue, or variation from beginning to end of each session
3. Learning, or variation from day to day over the course of the experiment.

CHAPTER IV

RESULTS

This chapter presents the results obtained from the experiment using the apparatus and procedures described in the previous chapter. The mathematical model which was derived from the data is given. Also, this chapter presents the results of the secondary effects sub-study.

Strength Data

The strength data collected during the 20 test sessions appears in Table 4-1. This data is presented in the form of equal strength contours in Figure 4-1. These contours were drawn using the average value of strength at each hand location. Some subjective estimation was used in completing these contours. The maximum strength elipse (MSE) indicated in Figure 4-1 represents the location of the highest strength readings on each radian. The perimeter of the contour is the approximate reach distance of a fifth percentile male (Kennedy, 1964, in Van Cott, Kinkade, 1972).

Data obtained along individual radians are presented in Figures 4-3 through 4-24. Each of these strength "profiles" shows two raw data points collected at each hand location, the predicted curve generated by the final model (discussed below) and a plot of σ_R. σ_R is the running

Table 4-1. Data Points and Strength Values by Radian

Hand Coordinates / Radian No.	1		2		3		4	
Strength Values								
	9,12	68,47	11,12	48,70	12,10	43,47	14,10	57,46
	9,14	53,50	11.5,14	53,57	14,14	60,56	16,12	47,70
	9,16	73,67	12,16	64,66	16,17	85,63	18,14	66,71
	9,18	85,72	12.5,18	92,74	16.5,18	70,72	20,16	82,87
	9,20	90,76	13,20	87,83	17,19	85,80	21,17	84,72
	9,21	84,78	13.5,22	72,80	18,21	68,85	22,18	70,85
	9,22	69,84	14,23.5	83,70	19,22	87,61	24,20	81,72
	9,24	78,77	14.5,26	76,65	20,24	62,75	26,22	82,75
	9,26	68,73	15,28	60,62	21,26	70,65	28,24	63,77
	9,29	60,65	16,31	52,51	23,29.5	45,55	30,26	38,61
	5		6		7		8	
	14,8	51,40	16,6.5	42,52	14,5	40,40	16,3	47,37
	16,9	51,42	18,7	44,78	16,5	42,50	18,2.5	47,40
	18,10	62,52	21,8	64,57	22,5	71,63	19,2	51,43
	21,12	83,92	24,9	83,74	24,5	77,70	22,1	51,58
	23,13	72,80	26,9.5	90,88	26,5	77,85	23,.75	56,70
	24.5,14	93,82	28,10	76,80	28,5	80,82	25,.5	60,69
	26,15	76,89	30,10.5	78,83	30,5	82,95	27,0	55,74
	28,16	67,83	32,11	80,80	32,5	83,85	30,-1	83,85
	32,18	75,61	36,12	83,52	34,5	85,76	34,-2	67,71
	35,20	68,35	38,12.5	46,36	38.5,5	74,55	36.5,2.5	60,52

Table 4-1 (continued)

9		10		11		12	
16,1	81,37	14,0	35,40	13,-2	42,31	9,-4	46,45
19,-1	52,45	16,-2	44,46	15,-6	44,36	9,-8	43,32
22,-3	52,70	18,-4	47,42	16.5,-8	57,42	9,-12	50,40
24,-4	68,63	20,-6	59,53	17.5,-10	46,50	9,-14	51,41
25,-4.5	76,72	22,-8	56,65	18,-11	56,48	9,-16	53,40
26,-5	73,67	23,-9	62,79	18.5,-12	55,65	9,-18	51,47
27,-5.5	86,80	24,-10	72,73	20,-14	59,62	9,-20	56,53
28,-6	74,59	25,-11	71,65	21,-16	57,77	9,-22	65,63
31,-8	85,90	26,-12	62,70	22,-18	76,70	9,-24	57,52
33,-9	56,55	29.5,-15.5	62,46	24.5,-22.5	42,45	9,-29	51,52

13		14		15		16	
2,-7	38,35	-2,-6	35,53	-6,-4	53,62	-9,0	61,66
.5,-10	30,39	-4,-8	55,45	-10,-6	59,46	-12,-1	52,52
-1,-12	40,27	-6,-10	52,43	-12,-7	57,50	-14,-1.5	43,57
-2,-14	40,31	-8,-12	38,51	-13.5,-8	55,42	-16,-2	55,43
-3,-16	32,30	-9,-13	35,35	-15,-9	40,43	-18,-2.5	47,57
		-10,-14	45,35	-17,-10	67,45	-20,-3	44,46
		-11,-15	37,36	-18,-10.5	43,50	-22,-3.5	57,47
		-12,-16	46,46	-20,-12	35,42	-24,-4	55,51
		-14,-18	27,42	-22,-13	40,36	-26,-5	54,47
		-15.5,-20	32,32	-24.5,-14.5	26,33	-29.5,5	62,47

Table 4-1 (concluded)

17		18		19		20	
-9,5	67,77	-4,8	80,76	0,10	72,67	3,11	53,54
-14,5	63,60	-10,10	64,63	-2,11	71,60	2,12	61,60
-16,5	71,57	-12,10.5	62,61	-4,12	70,67	0,14	67,61
-18,5	56,52	-14,11	61,61	-6,13.5	74,62	-2,16	82,68
-20,5	60,56	-16,11.5	70,60	-8,14.5	73,67	-4,18	56,60
-21,5	49,54	-18,12	55,63	-12,17	67,63	-5,19	75,61
-22,5	62,55	-20,12.5	52,58	-14,18	66,62	-6,20	64,70
-24,5	54,52	-22,13	52,55	-18,20	51,62	-8,22	72,66
-26,5	48,49	-25,14	57,51	-20,21.5	51,60	-10,24	53,71
-31,5	47,51	-28.5,15	52,52	-22.5,23	48,59	-14,28	62,67

21		22	
5,12	65,53	7,12	53,52
4,14	56,57	6.5,14	57,54
2,17	80,67	6,16	82,69
1.5,18	56,92	5.5,18	60,90
0,20	95,72	5,20	77,94
-1,22	87,87	4.75,21	64,92
-2,24	46,83	4.5,22	88,97
-3,26	63,70	4,24	86,70
-4,27.5	75,85	3,26	72,83
-5,29	70,60	2.5,28.5	76,65

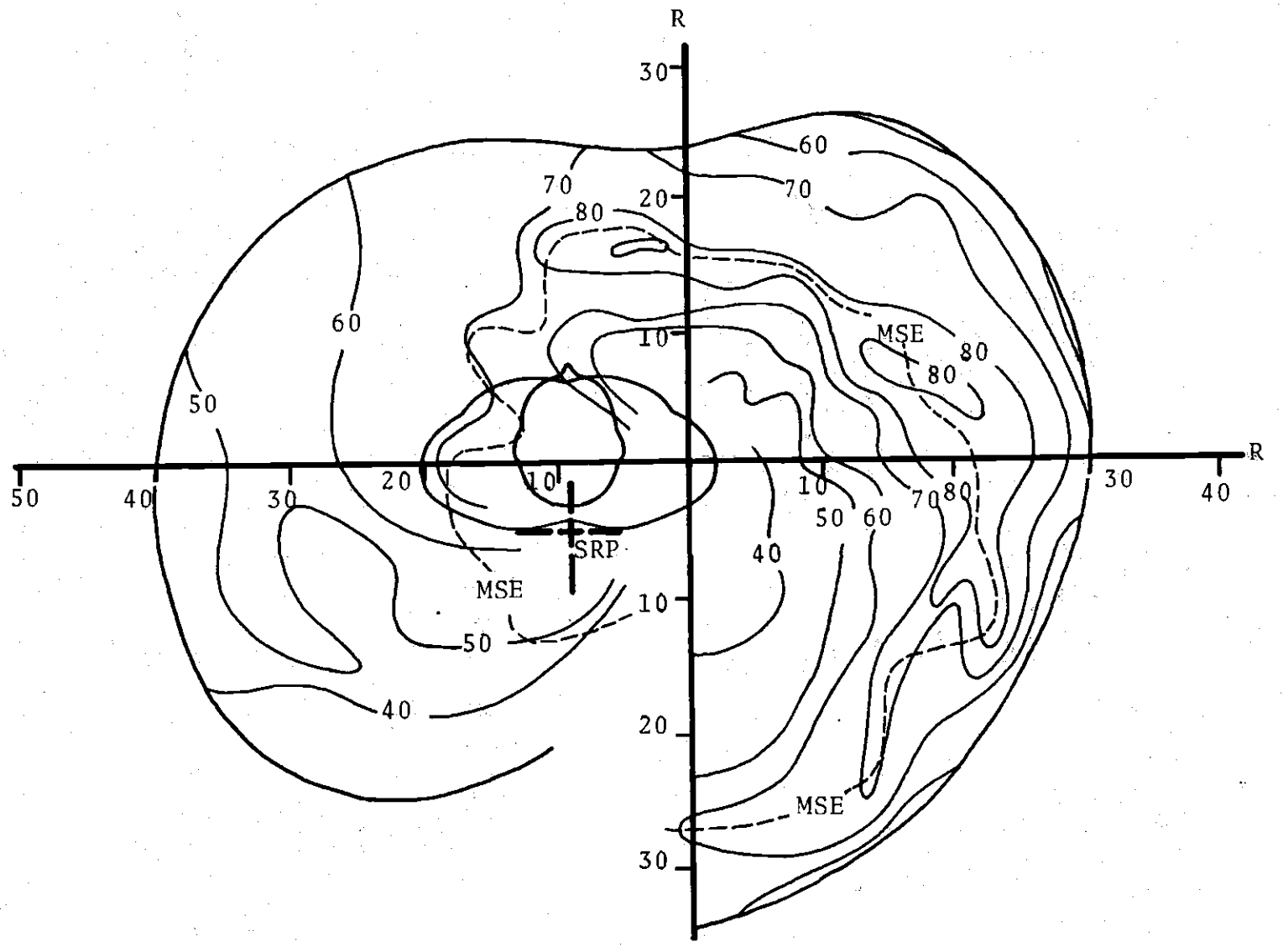

Figure 4-1. Raw Strength Data Contours

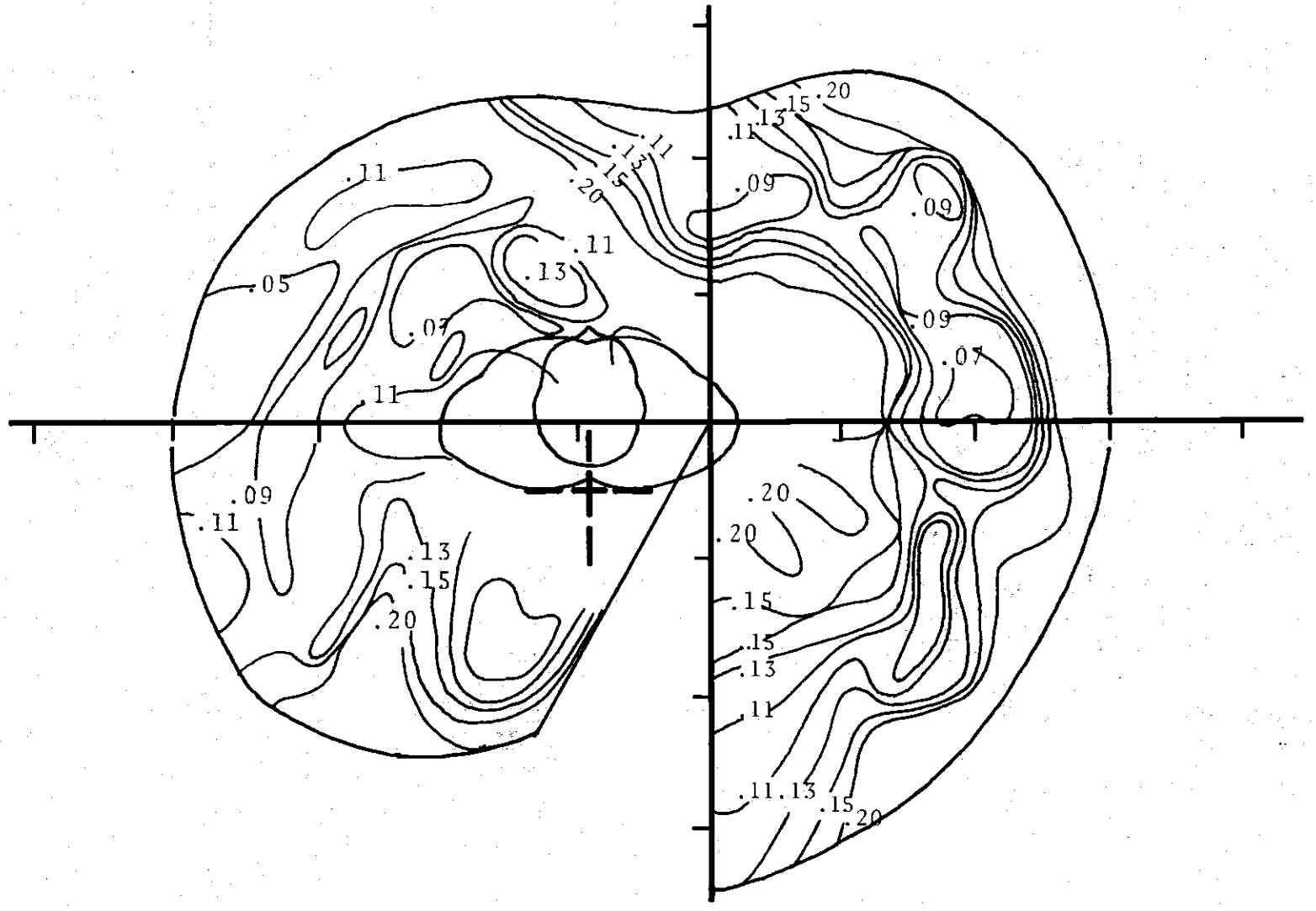

Figure 4-2. Contours of Running Average Coefficients of Variation (CV_R) of Strength Data

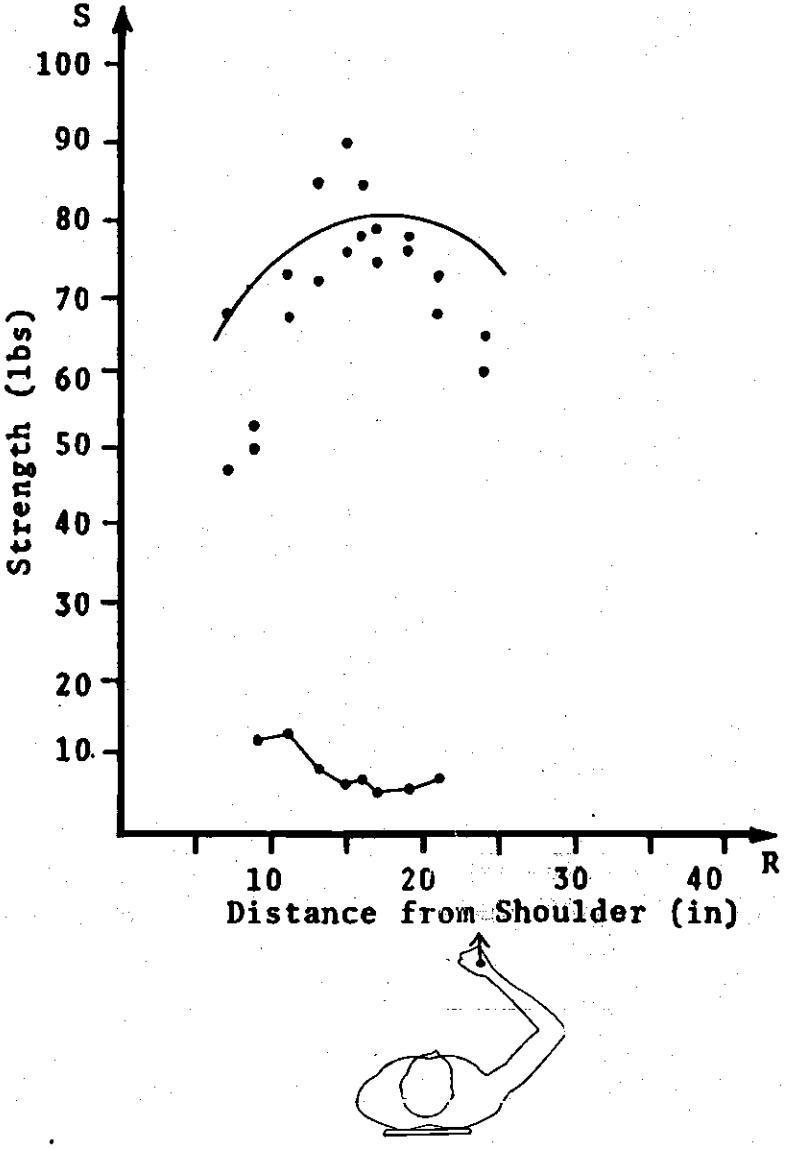

Figure 4-3. Strength Profile on Radian One

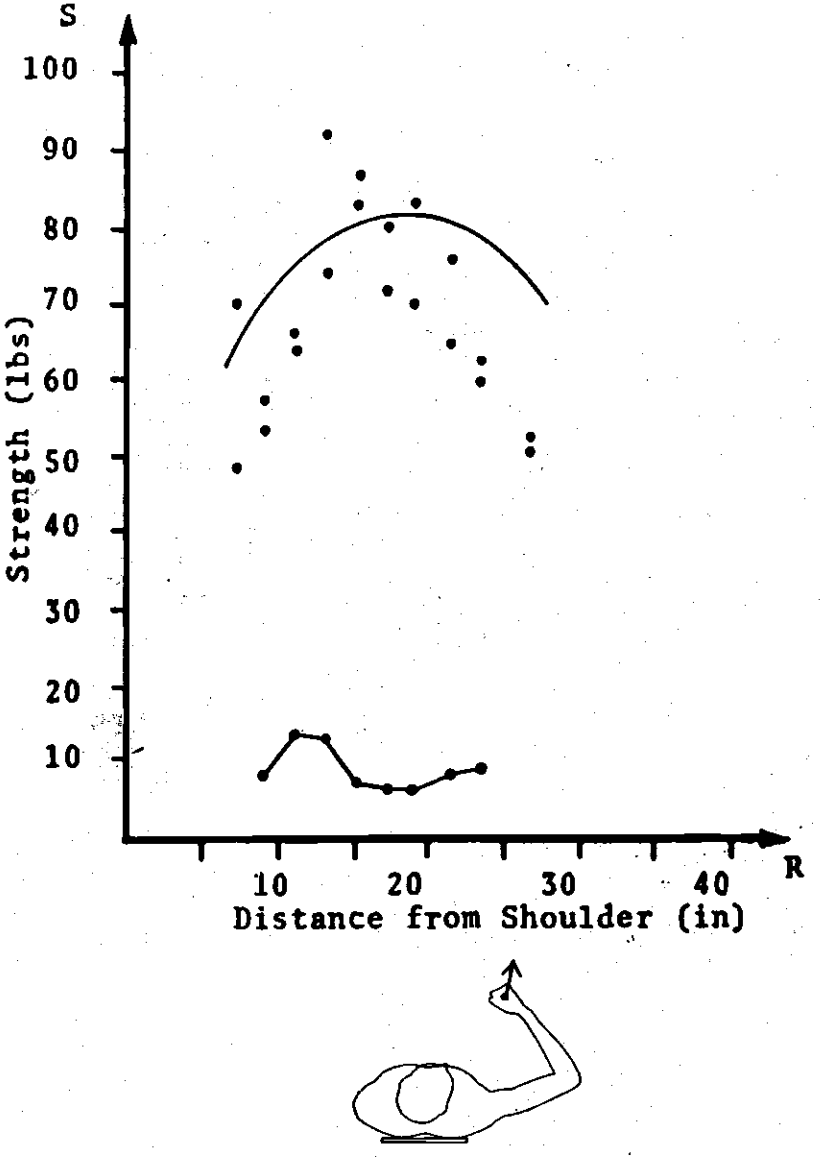

Figure 4-4. Strength Profile on Radian Two

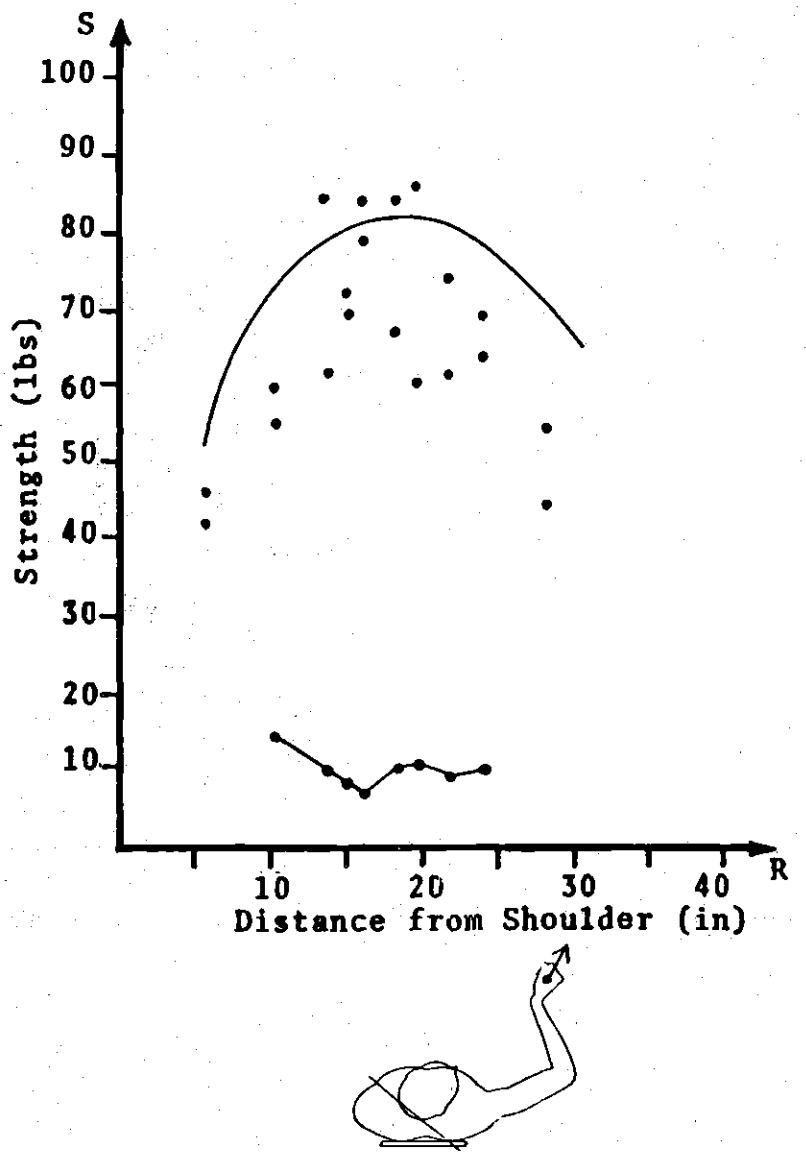

Figure 4-5. Strength Profile on Radian Three

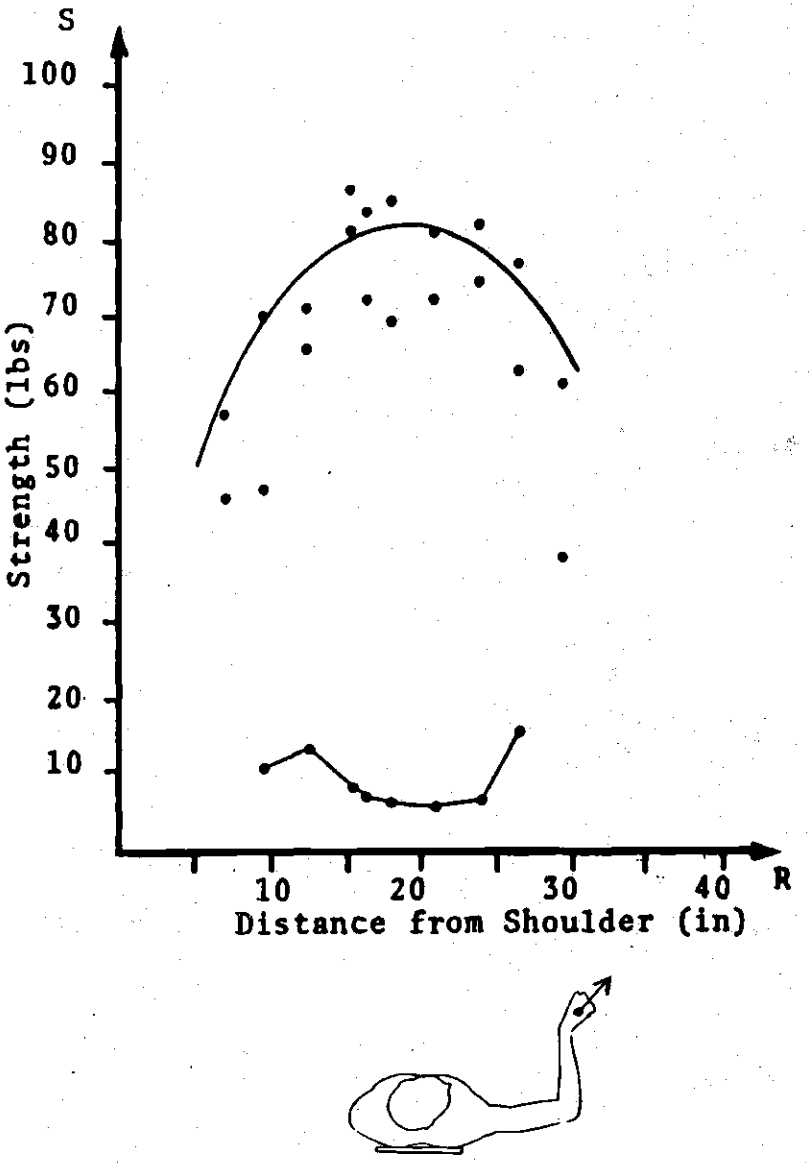

Figure 4-6. Strength Profile on Radian Four

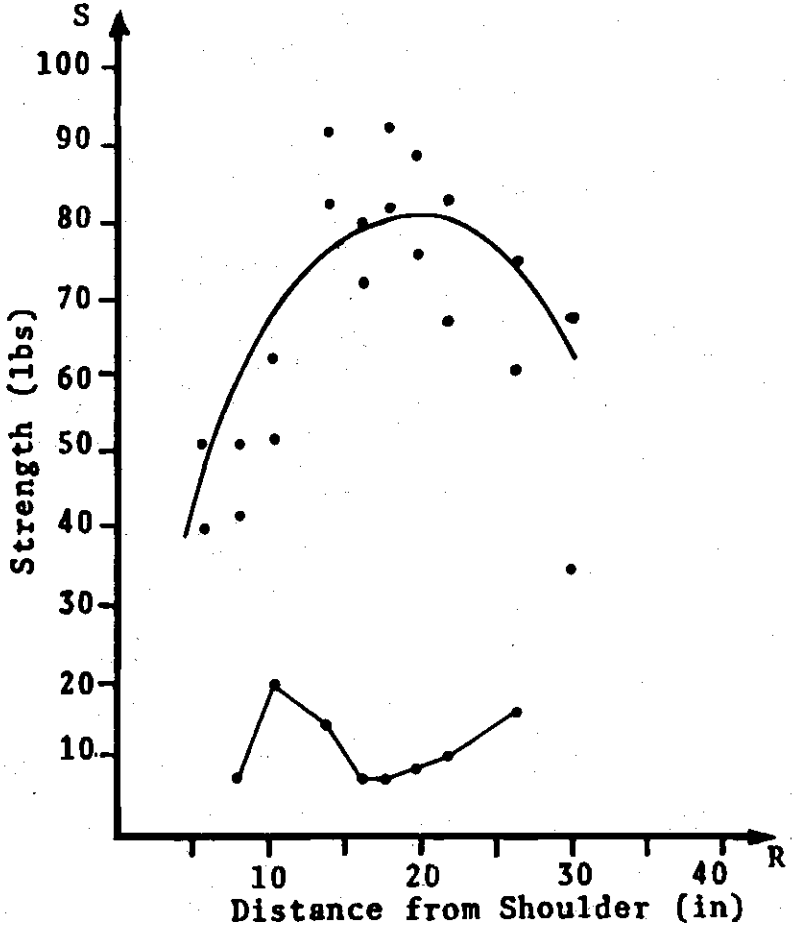

Figure 4-7. Strength Profile on Radian Five

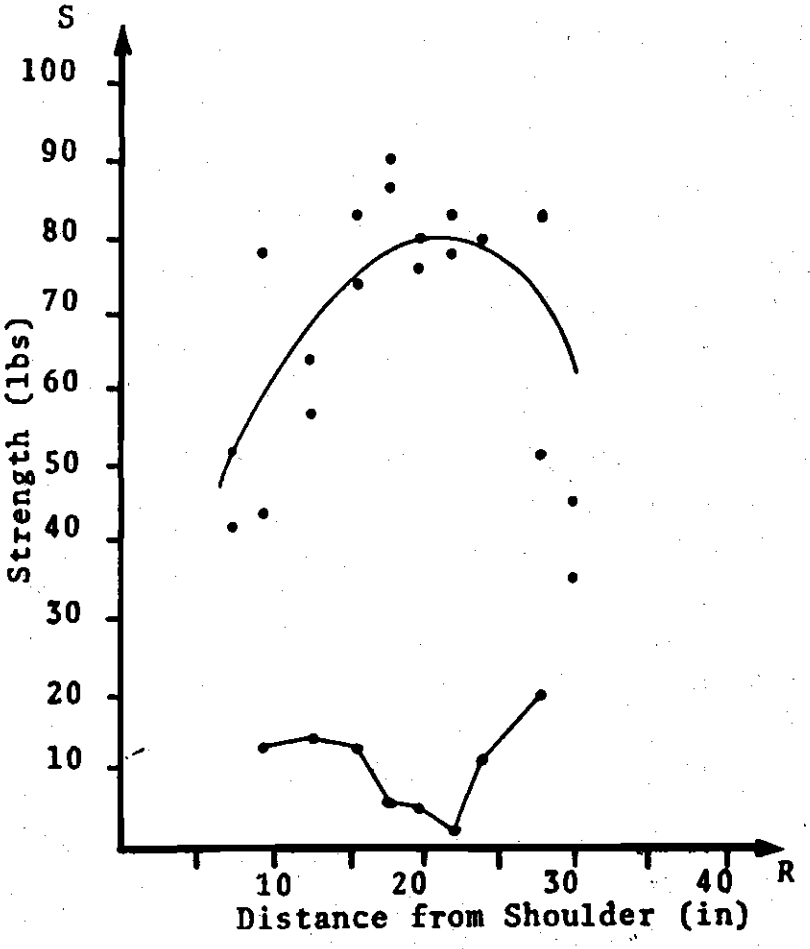

Figure 4-8. Strength Profile on Radian Six

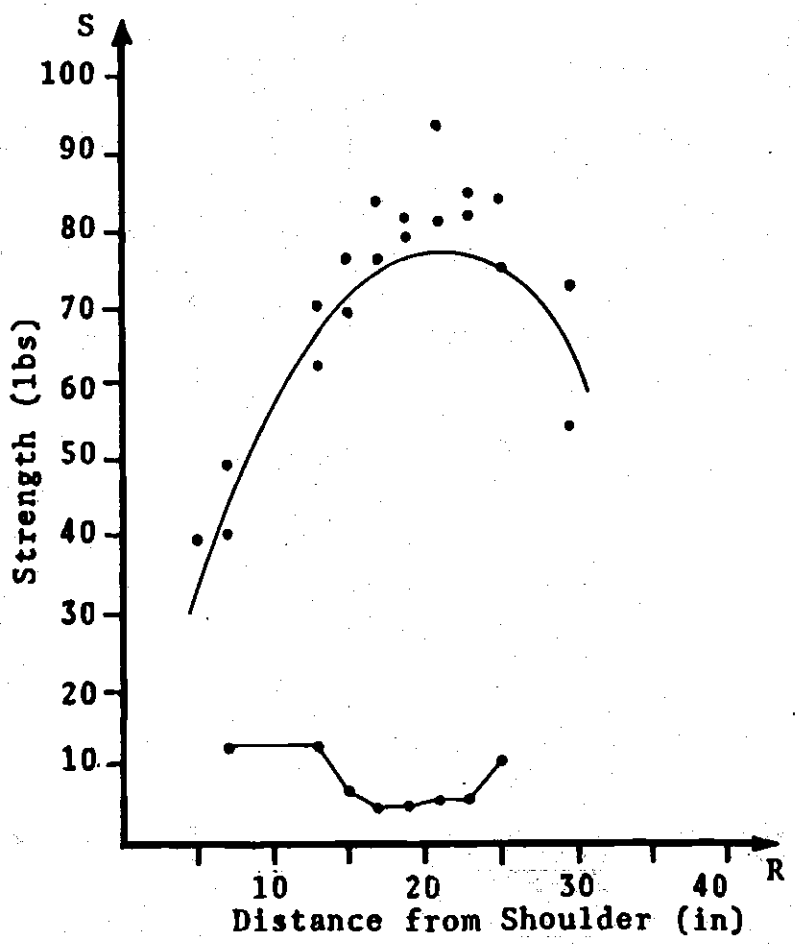

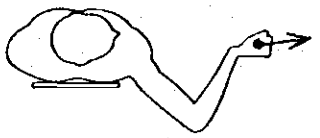

Figure 4-9. Strength Profile on Radian Seven

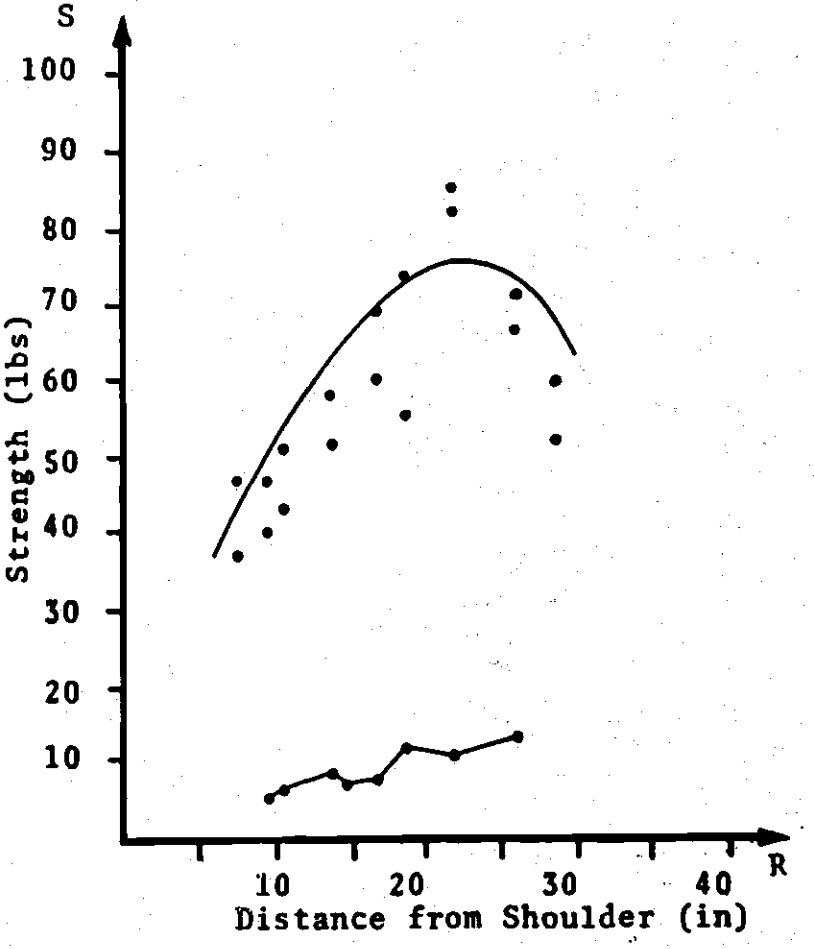

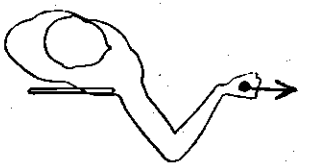

Figure 4-10. Strength Profile on Radian Eight

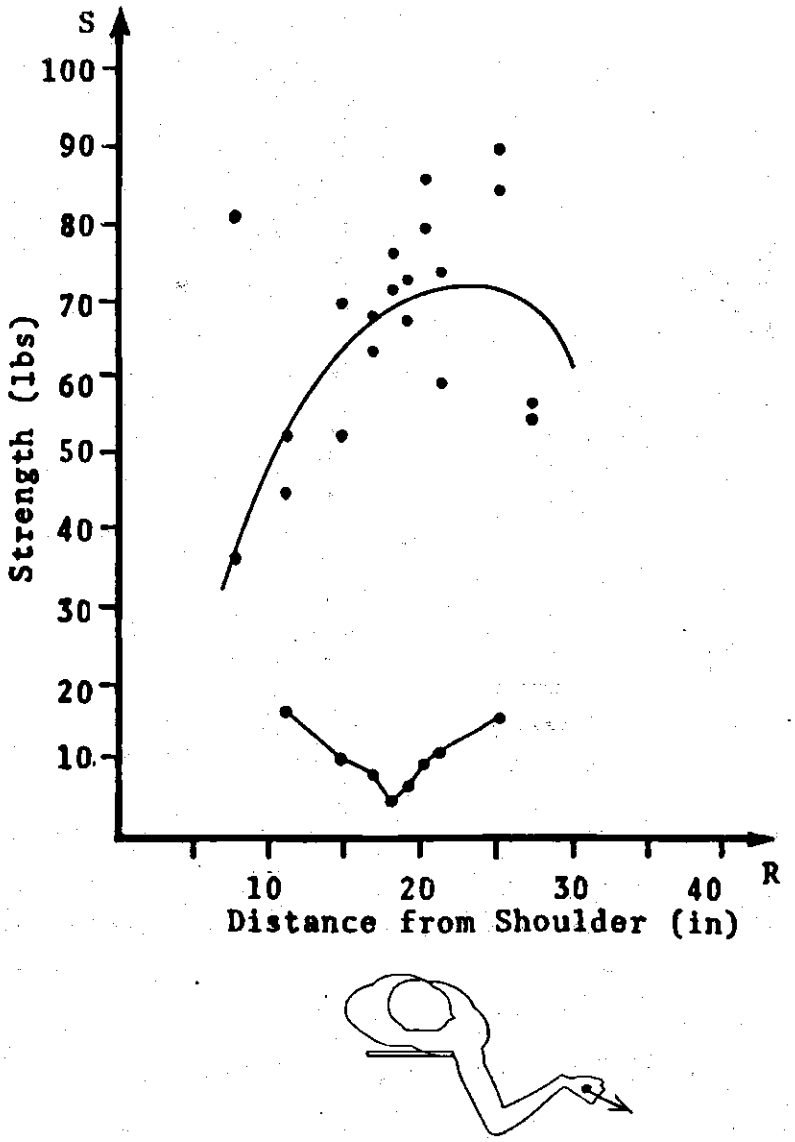

Figure 4-11. Strength Profile on Radian Nine

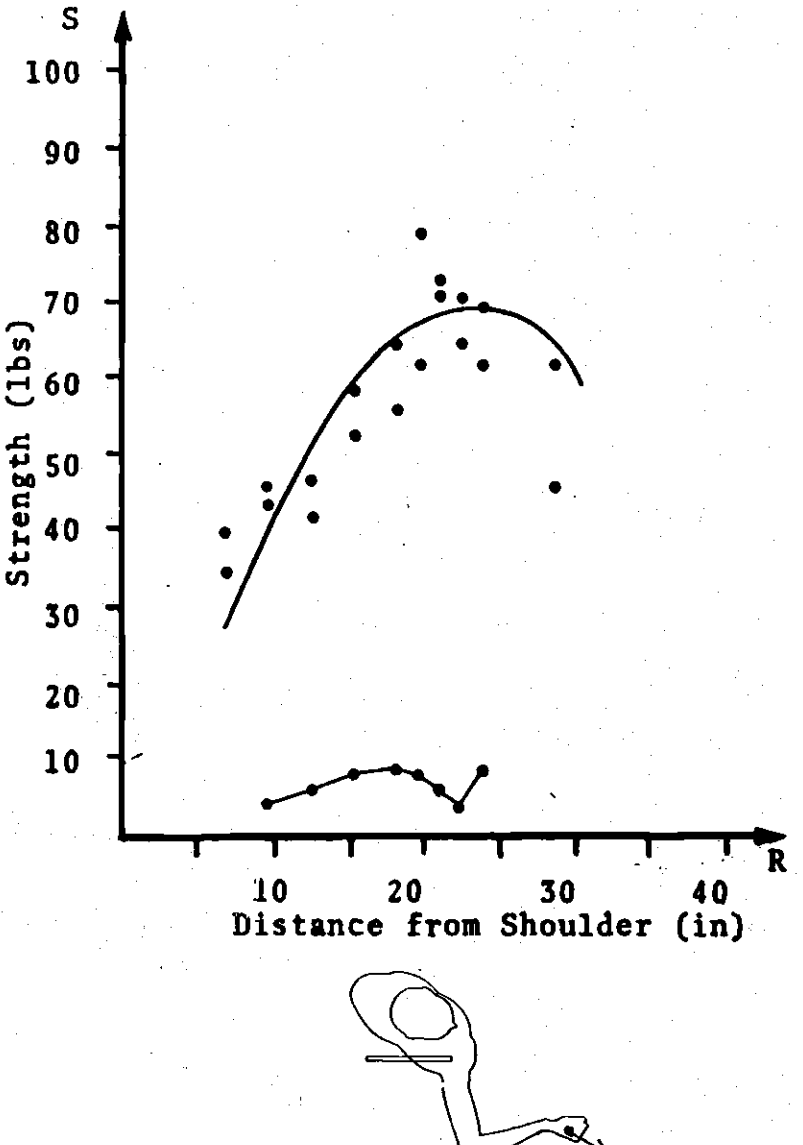

Figure 4-12. Strength Profile on Radian Ten

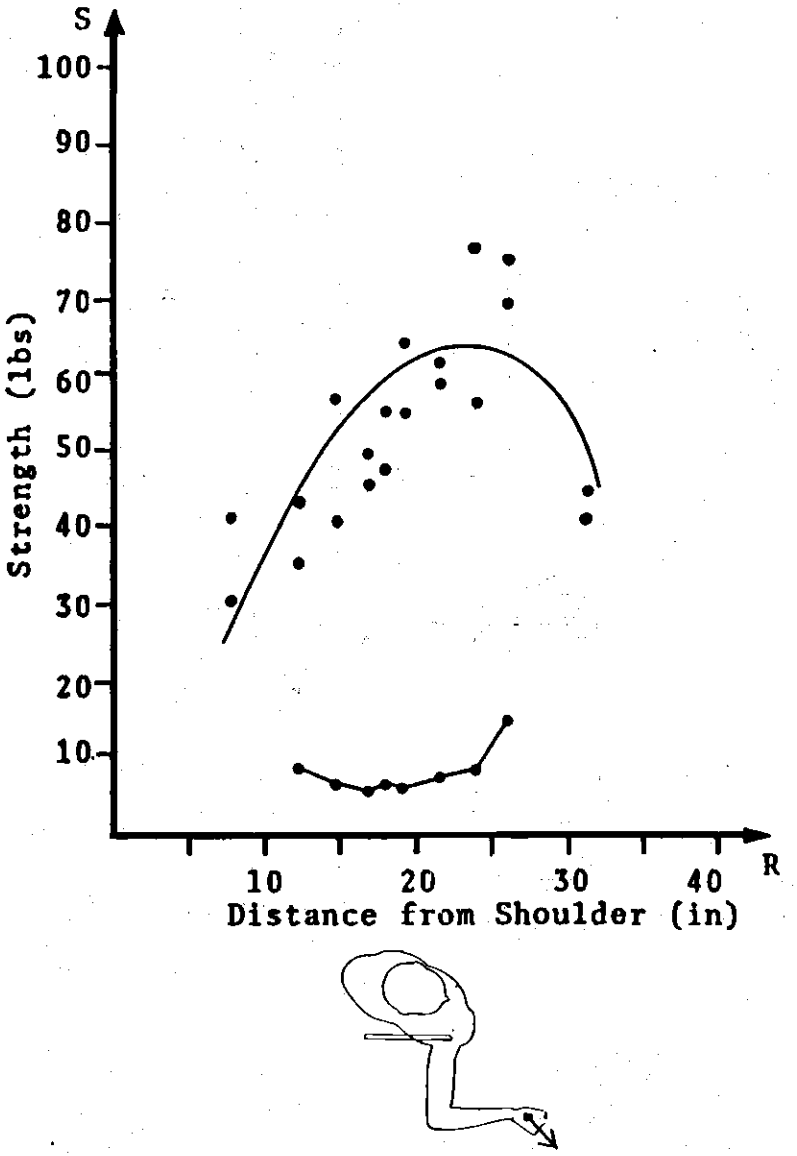

Figure 4-13. Strength Profile on Radian Eleven

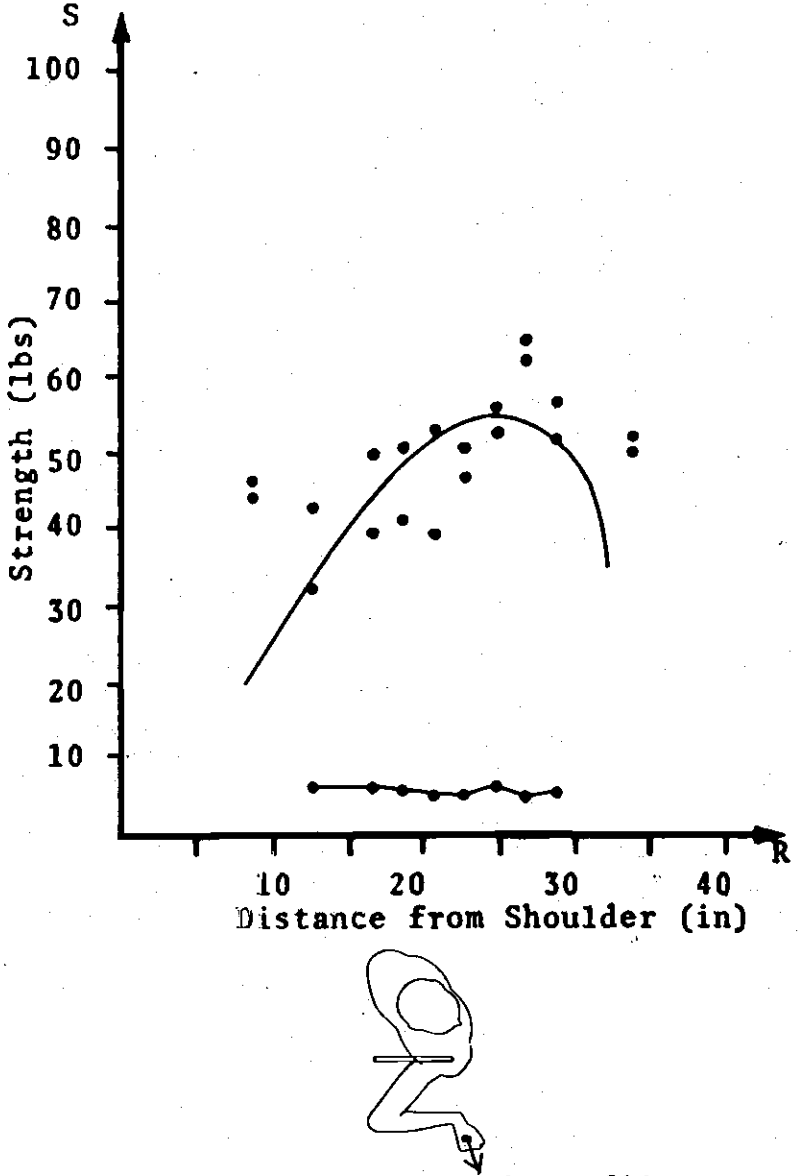

Figure 4-14. Strength Profile on Radian Twelve

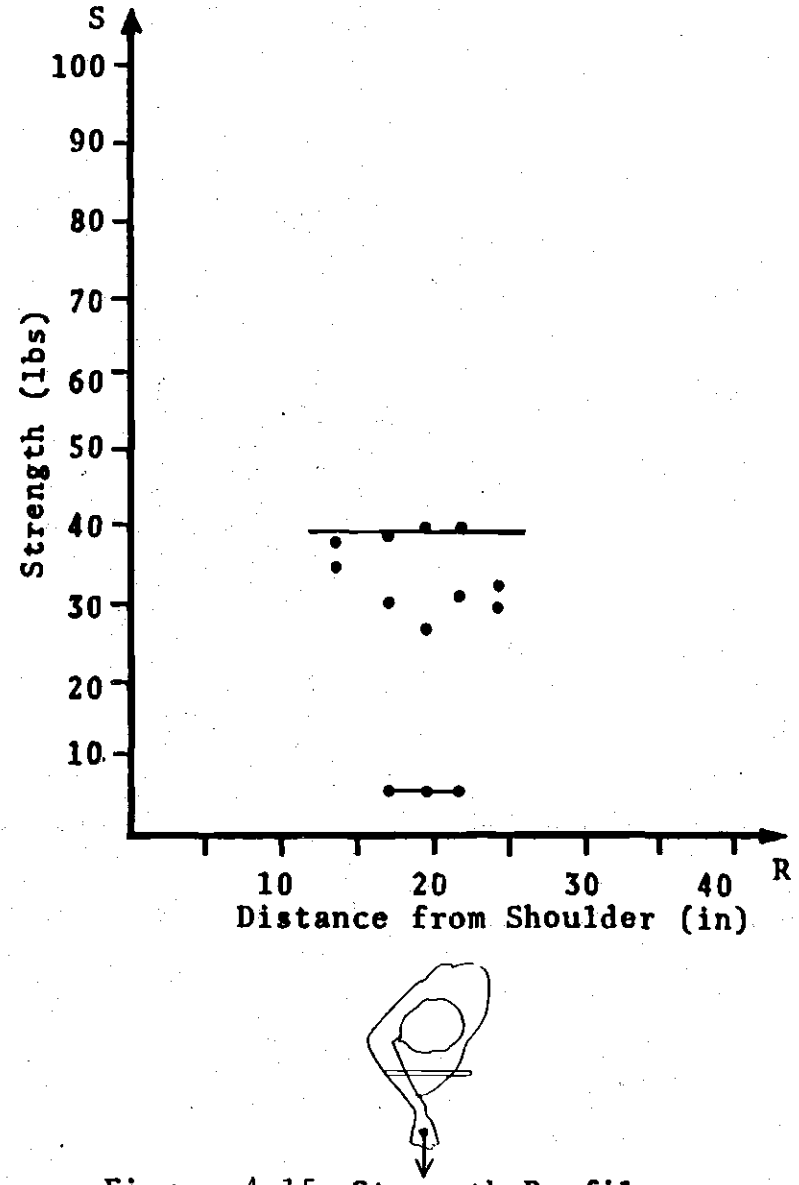

Figure 4-15. Strength Profile on Radian Thirteen

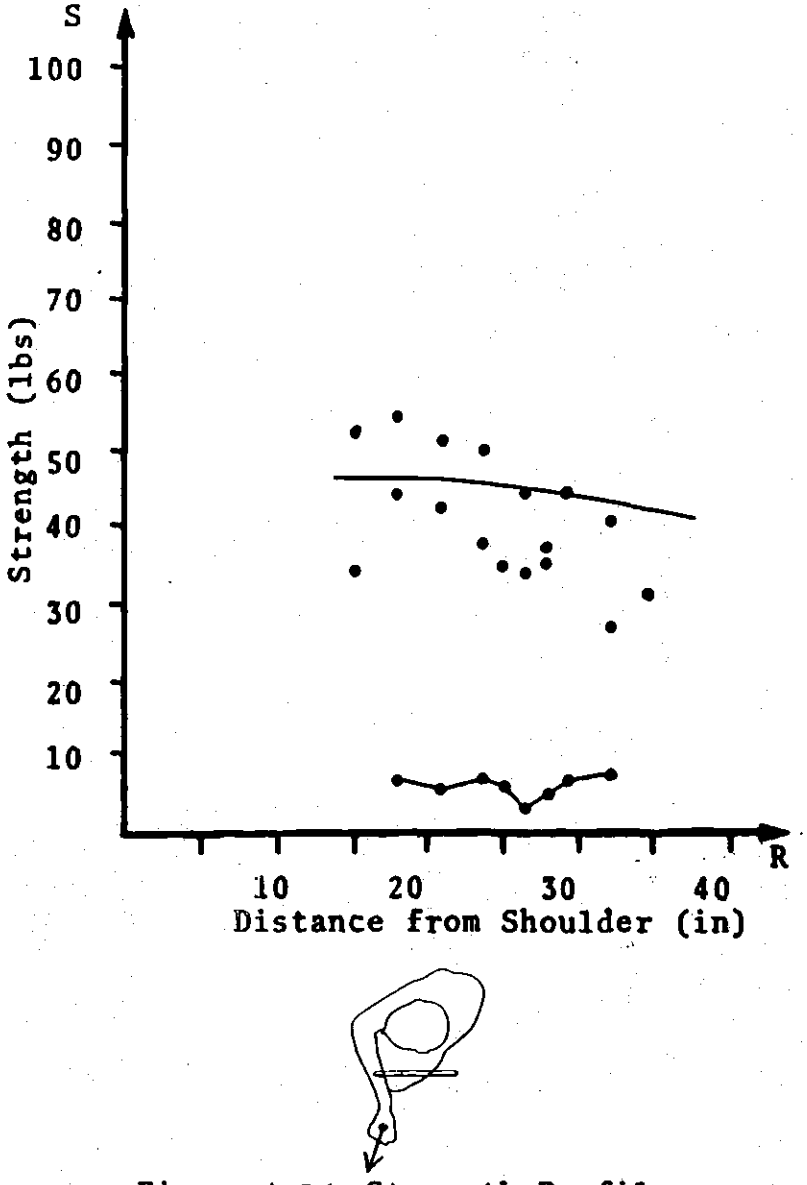

Figure 4-16. Strength Profile on Radian Fourteen

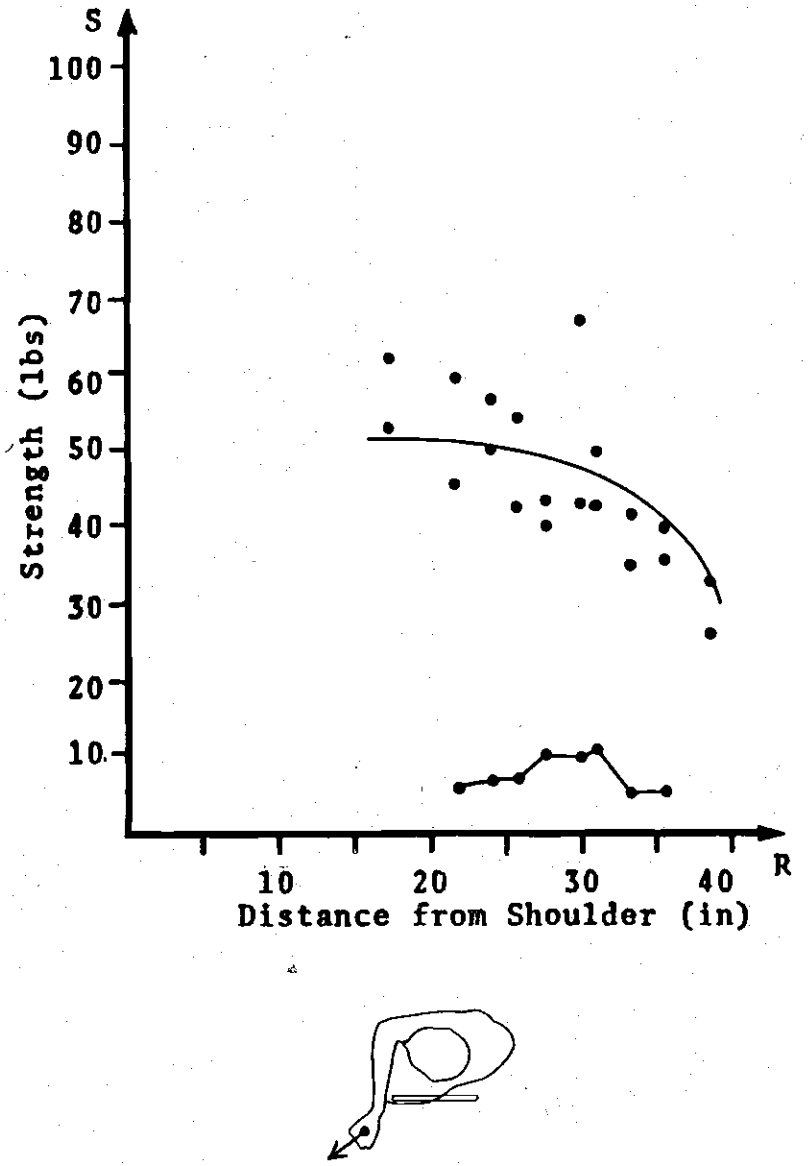

Figure 4-17. Strength Profile on Radian Fifteen

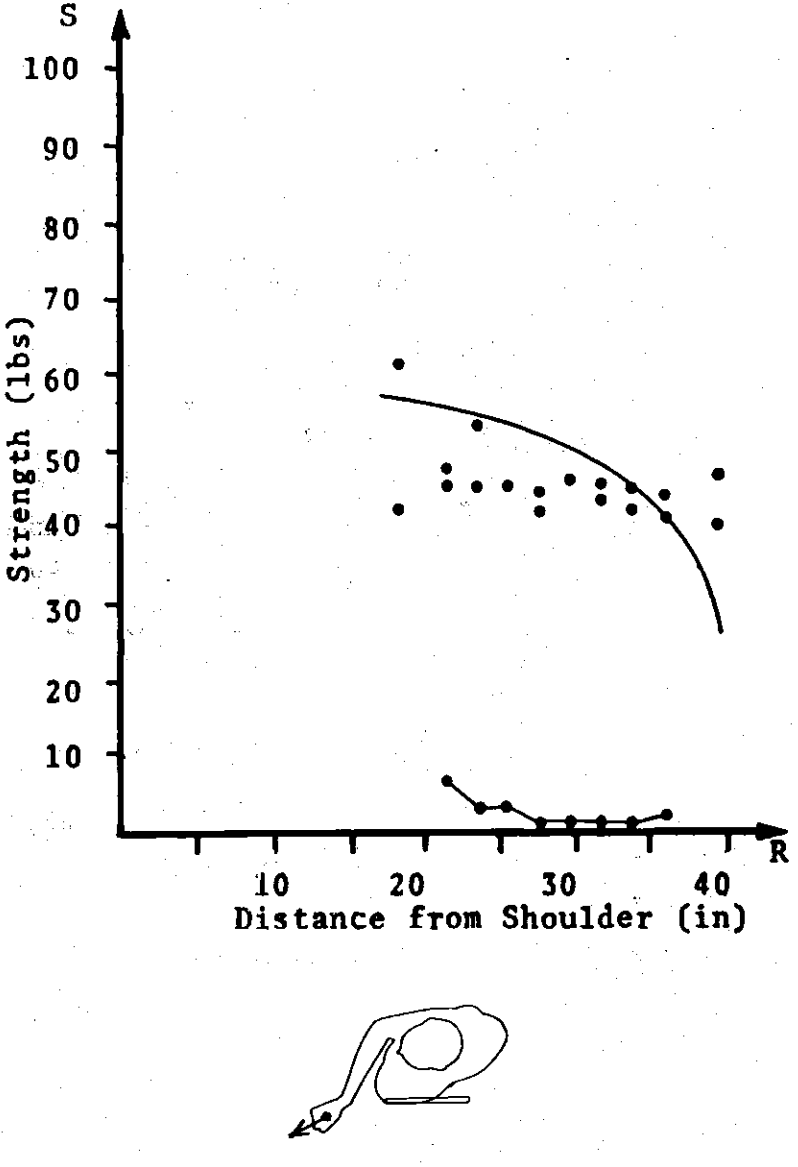

Figure 4-18. Strength Profile on Radian Sixteen

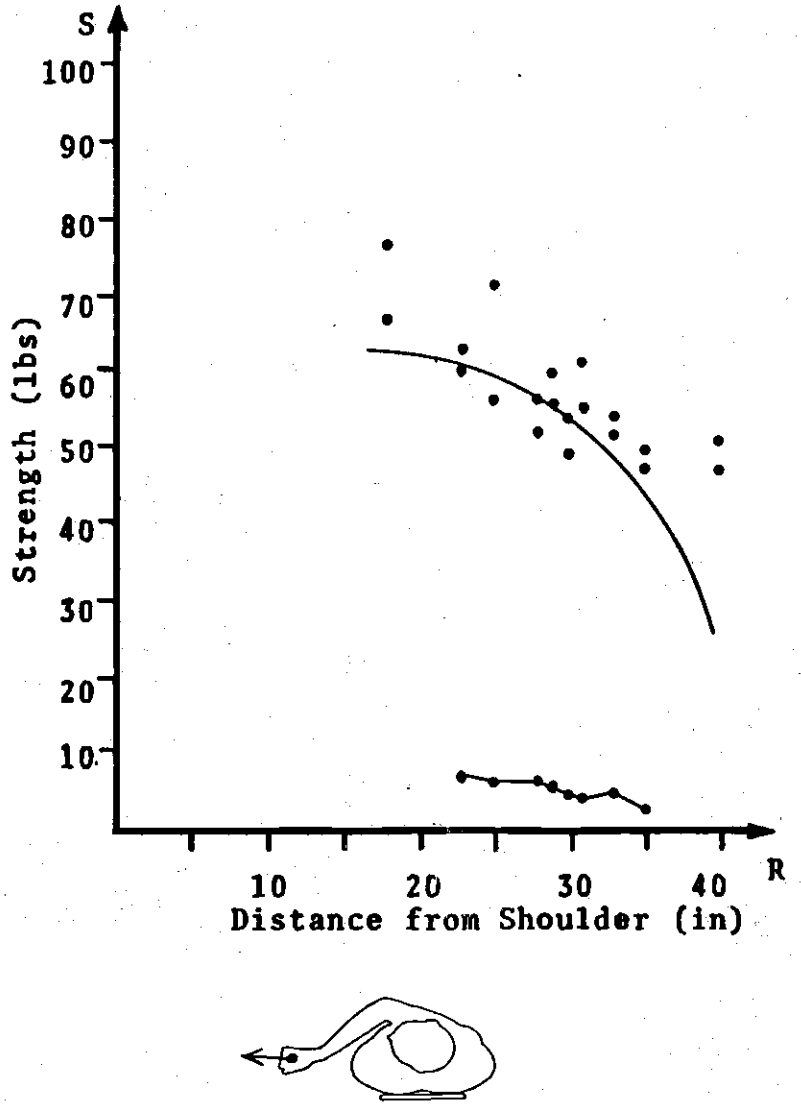

Figure 4-19. **Strength Profile on Radian** Seventeen

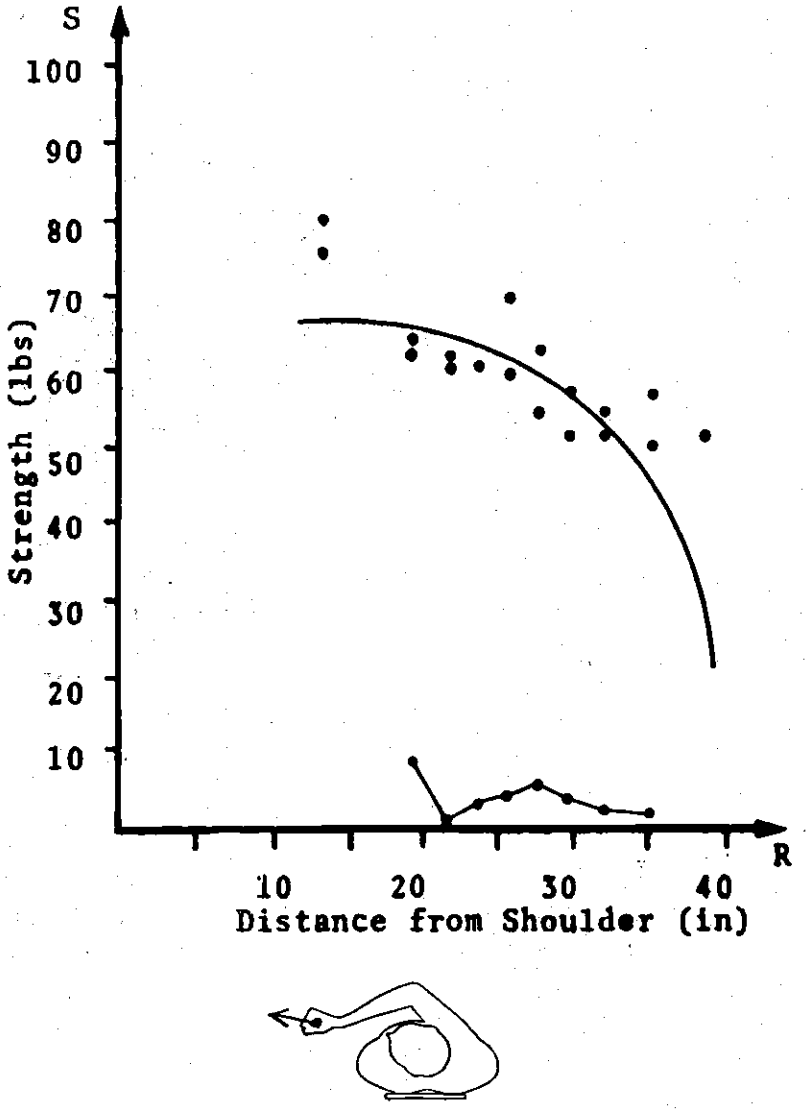

Figure 4-20. **Strength Profile on Radian** Eighteen

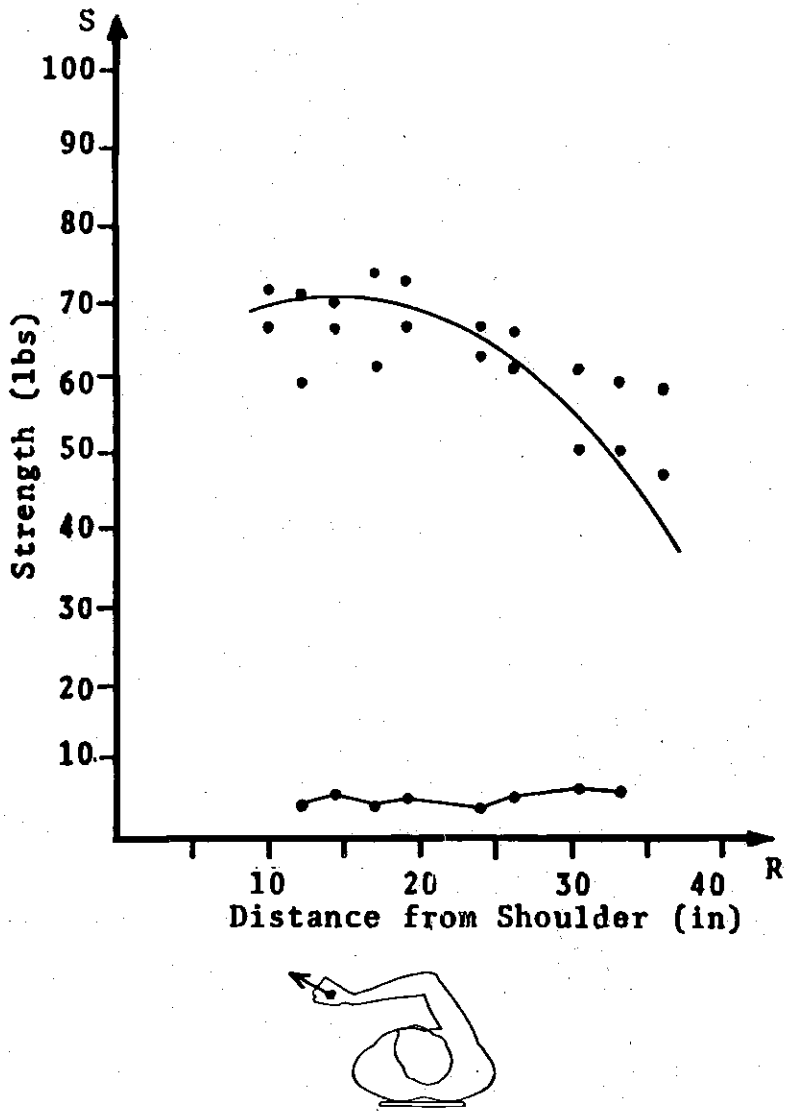

Figure 4-21. Strength Profile on Radian Nineteen

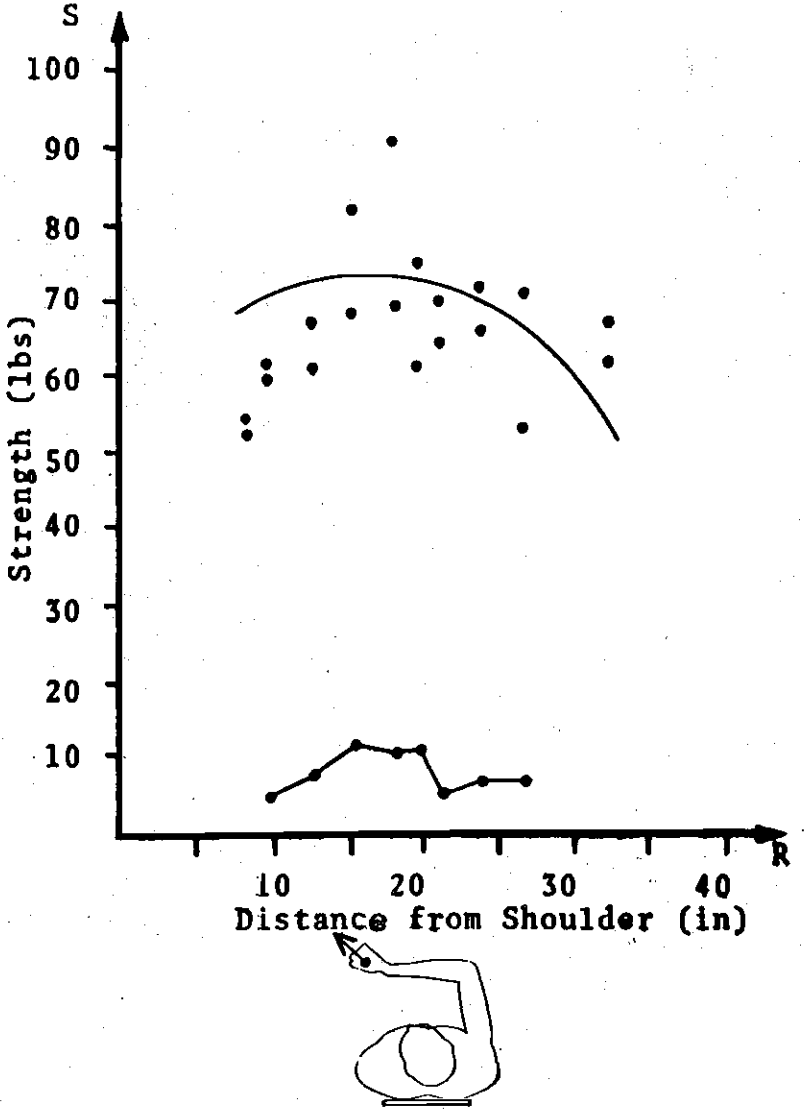

Figure 4-22. Strength Profile on Radian Twenty

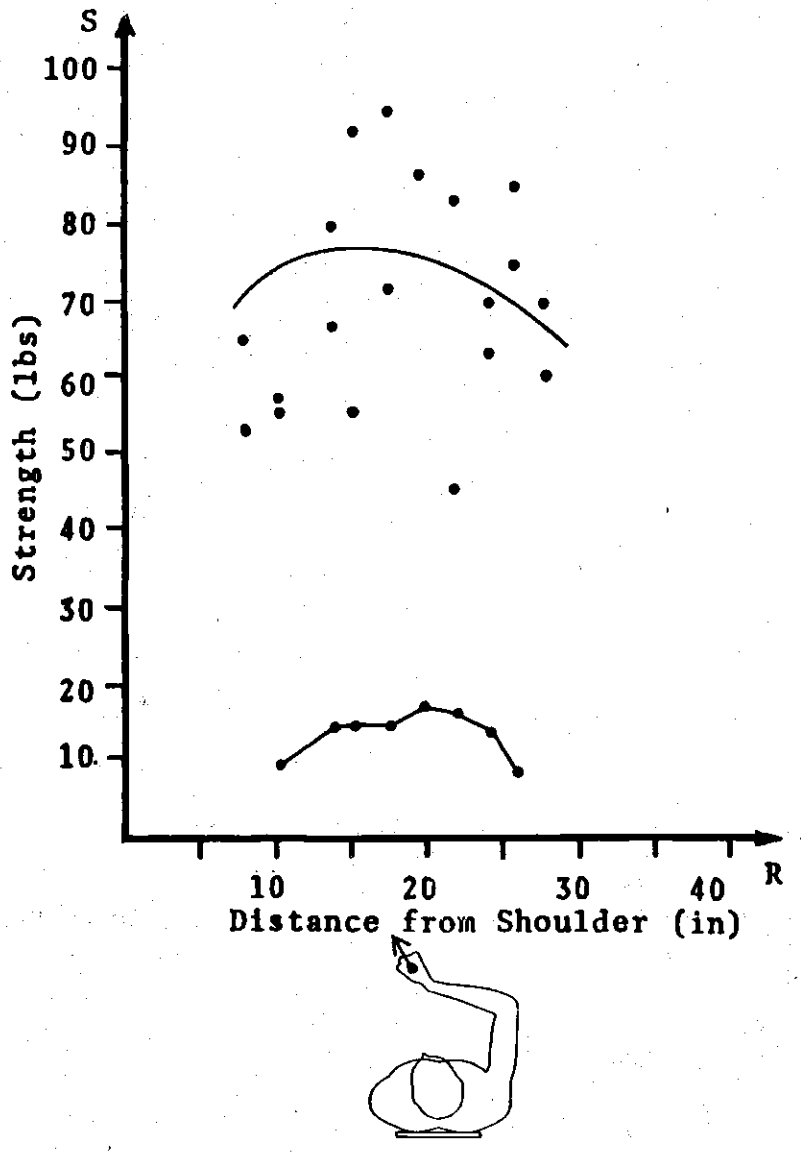

Figure 4-23. Strength Profile on Radian Twenty-one

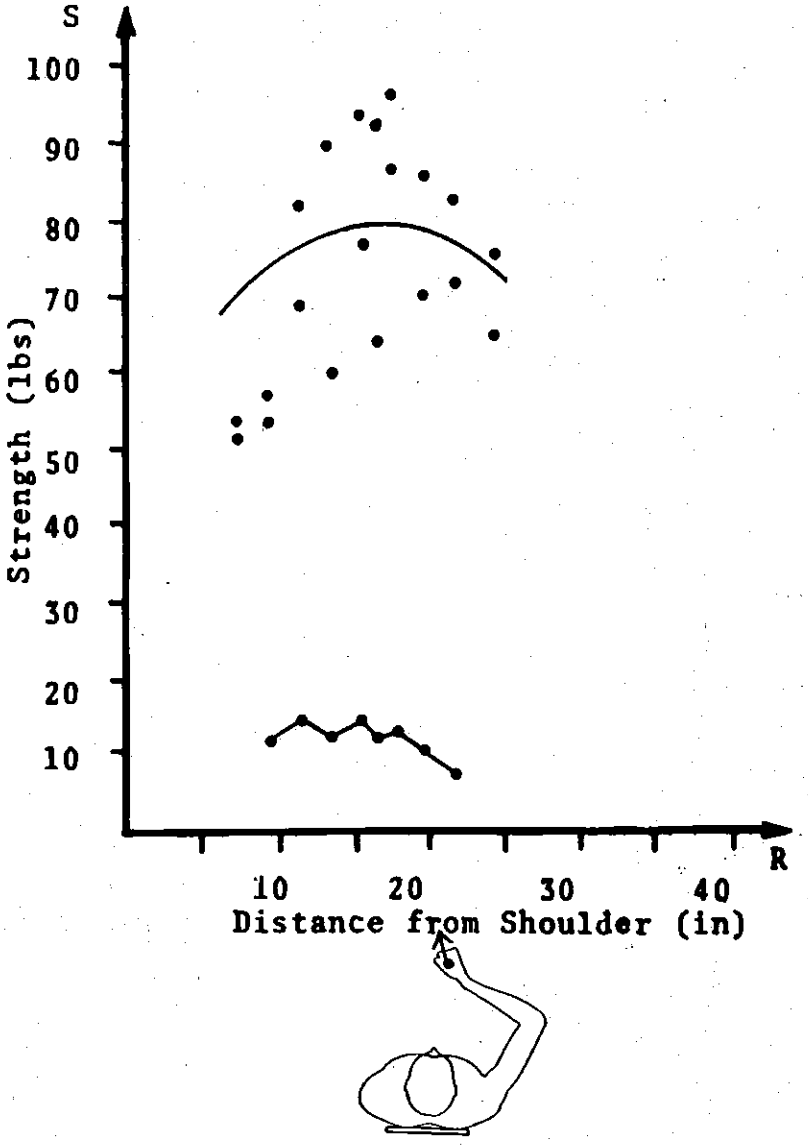

Figure 4-24. Strength Profile on Radian Twenty-two

average standard deviation of the six data points at any three adjacent locations along the radian. It is computed as follows:

$$\sigma_R = \sqrt{\frac{\sum_{i=1}^{3} \sum_{j=1}^{2} (S_{ij} - \bar{S}_j)^2}{5}}$$

where

S_{ij} = j^{th} data point in i^{th} adjacent hand location

$\bar{S}_j$ = average of two data points at i^{th} adjacent hand location

The plot of σ_R is located at the bottom of each strength profile. The silhouette below each strength profile indicates the approximate direction of push in which the data was collected. Note that the origin of these strength profiles represents the shoulder point.

Variation of the raw data is shown in contour form in Figure 4-2. These contours are plots of approximations of running average coefficients of variation (CV_R). The result of using the running average coefficient of variation is a slight smoothing effect along each radian. The running average coefficient of variation is computed as follows:

$$CV_R = \frac{\sigma_R}{\bar{S}_R}$$

where:

σ_R = running average standard deviation (defined above)

$\bar{S}_R$ = average of the six data points at any three adjacent hand locations.

An overview of all of the data appears in Figure 4-25. This illustration is a three-dimensional representation of all the strength profiles viewed from a point above the subject.

Mathematical Models of the Data

The Gamma-Based Model

Two major mathematical models were derived from the data. The first of these was a revised form of the gamma probability distribution. This model is summarized in Table 4-2. Because of several factors, this model was abandoned.

The expressions for major parameters such as maximum strength and the distance to maximum strength were awkward. Another problem was that the predicted curve would not skew left and right in response to manipulations of the parameters. This capability is essential for ensuring that all radians would be adequately fit by the model. Finally, the general form of the model did not have the necessary intuitive appeal. It appeared to be awkward and unnecessarily complex.

The Final Model

The final model was based on the beta probability distribution. Table 4-3 summarizes the characteristics of the model. Figure 4-26 defines the graphical meaning of

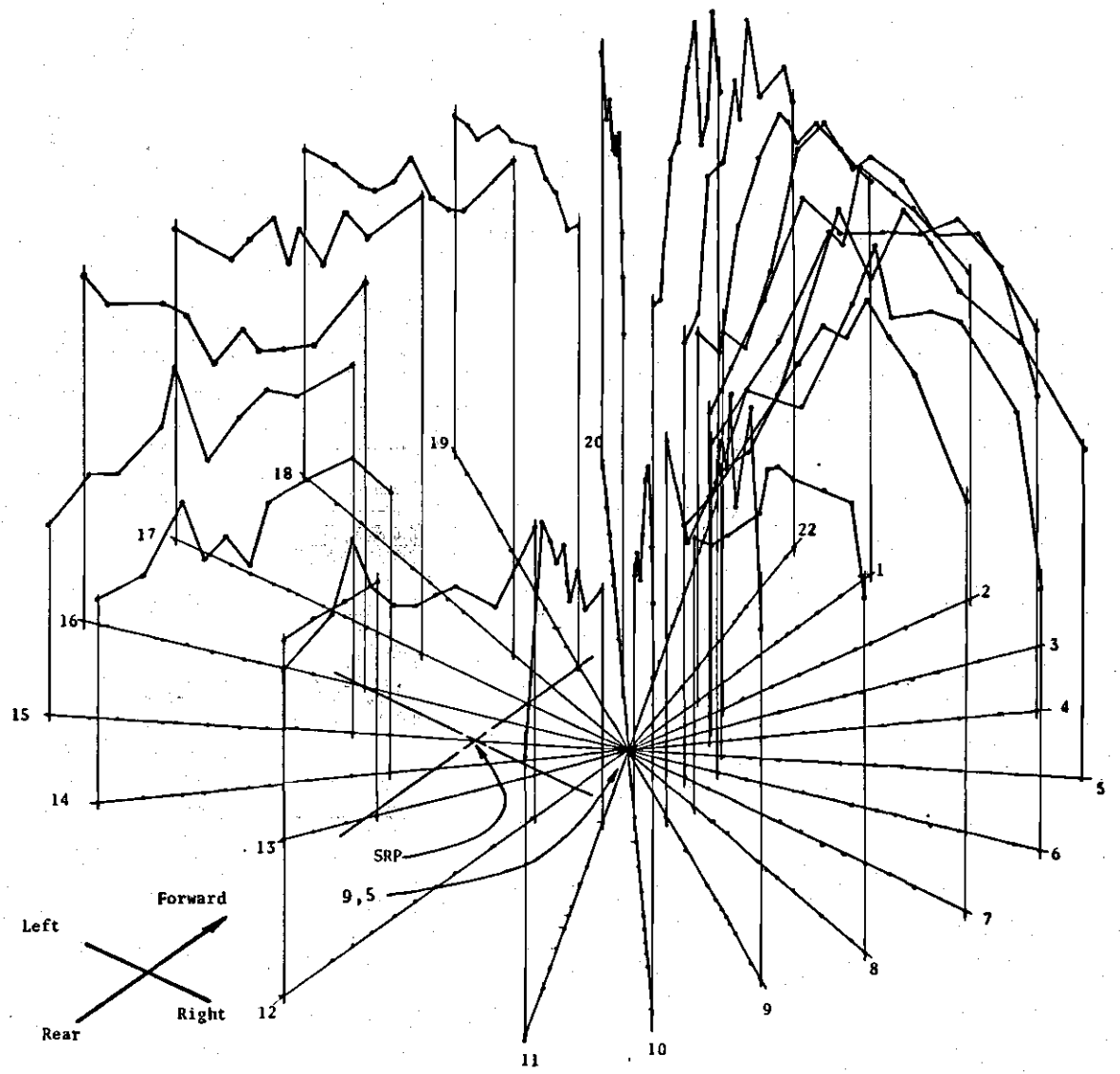

Figure 4-25. Three Dimensional View of all Strength Profiles

Table 4-2. Summary of Gamma-Based Model

Strength = $A(BR)^c e^{DR}$

Critical Points:

Max at R = -c/D if (A>0, c>0) or (A<0, c<0)

Min at R = -c/D if (A>0, c<0) or (A<0, c>0)

Discontinuous at R = 0

R = $+\infty$ tangent point if D<0

R = $-\infty$ tangent point if D>0

Strength at Critical Points:

$S|_{-c/D} = A(\frac{-Bc}{eD})^c$

$S|_0 = 0$

$S|_\infty = 0$

$S|_\infty = 0$

Intercepts: R = 0
R = $+\infty$
R = $-\infty$

Inflection Points: R = $-C/D + \sqrt{c}/D$ if c>1

$-C/D - \sqrt{c}/D$ if 0<c<1

Table 4-3. Summary of Final Model

Model:

$$\text{Strength} = S_m \left(\frac{R}{R_m}\right)^{BR_m} \left(\frac{m-R}{m-R_m}\right)^{B(m-R_m)}$$

where:

S_m = max strength on any radian

R_m = distance from shoulder to max strength on any radian

m = distance from shoulder to max reach

B = shape parameter

R = distance to hand from shoulder

Expressions for Parameters:

$$R = \sqrt{(X-9)^2 + (Y-5)^2}$$

where X and Y are coordinates of the hand location, with (0,0) being the SRP, X-axis lying in the frontal plane through the SRP, and Y-axis lying in the mid-saggital plane

$$S_m = 39.0 + .4759\phi - .0013\phi^2$$

$$R_m = 11.25 + .0417\phi$$

$$B = .00019\phi$$

$$m = 40.0 \text{ inches}$$

where:

Table 4-3 (concluded)

θ = direction of push in degrees (0° = in front of right shoulder, increasing to right)

ϕ = 0° at θ = 210°; increases clockwise around body

Extrema: Min at R = 0

Max at $R = R_m$

Min at R = m

$S|_{R=0} = 0$

$S|_{R=R_m} = S_m$

$S|_{R=m} = 0$

Shape: Increase B → increase peakedness

Skewness: Left → $R_m < m/2$

Right → $R_m > m/2$

Intercepts: R = 0, R = m

Error Sum of Squares (all data) = 45,101.00

Standard Deviation (all data) = 13.9 lb

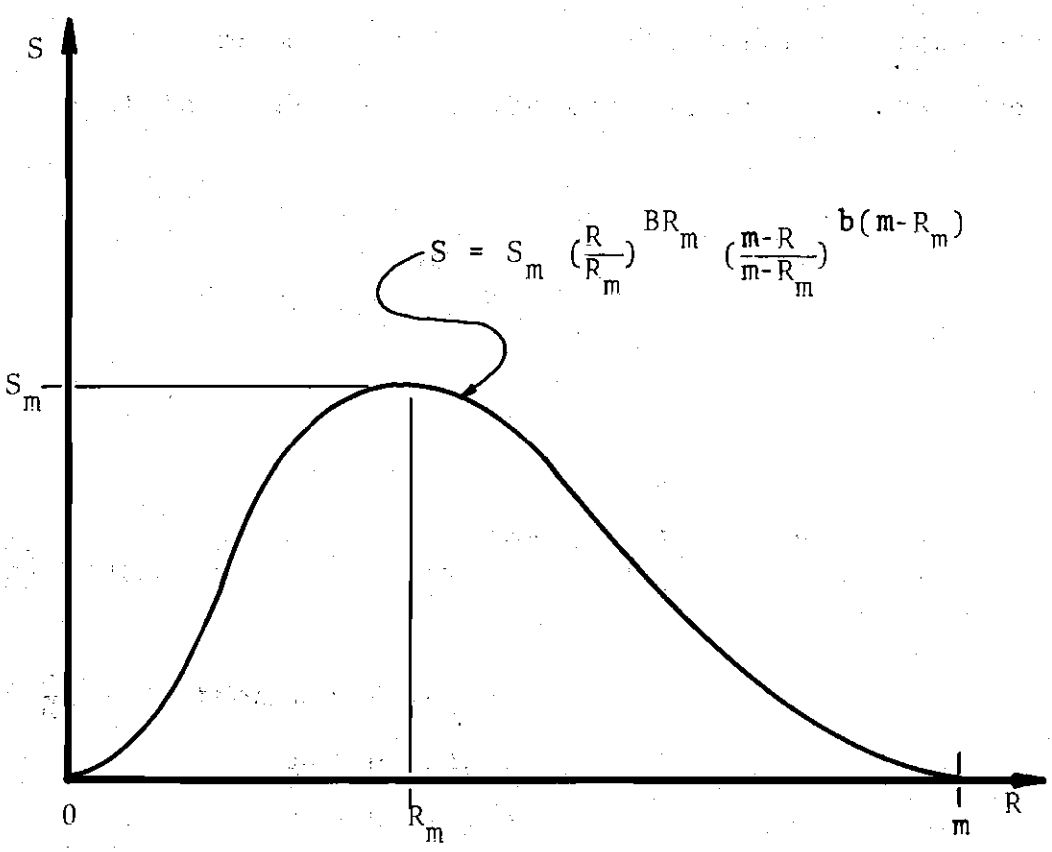

Figure 4-26. Graphical Meaning of Model Parameters

each of the model's parameters. The effect of each of these parameters on the shape of a typical strength profile is presented in Figure 4-27.

The extrema are obtained by differentiating the model with respect to R and setting the derivative equal to zero: If

$$S = S_m \left(\frac{R}{R_m}\right)^{BR_m} \left(\frac{m-R}{m-R_m}\right)^{B(m-R_m)}$$

Then

$$\frac{ds}{dR} = S_m \left\{B\left(\frac{R}{R_m}\right)^{BR_m} \left(\frac{m-R}{m-R_m}\right)^{B(m-R_m)} \left[\left(\frac{R_m}{R}\right) - \left(\frac{m-R_m}{m-R}\right)\right]\right\}$$

And if $\frac{ds}{dR} = 0$, then $R = 0$ (min)

$R = m$ (min)

$R = R_m$ (max)

Subjectively estimated equal strength contours of the predicted values of the model are shown in Figure 4-28. A detailed record of the model development procedure appears in the following appendices:

Appendix A: The Reparameterization of the Beta Distribution in Deriving the Strength Model

Appendix B: The Procedure Used in Estimating the Parameters of the Final Model

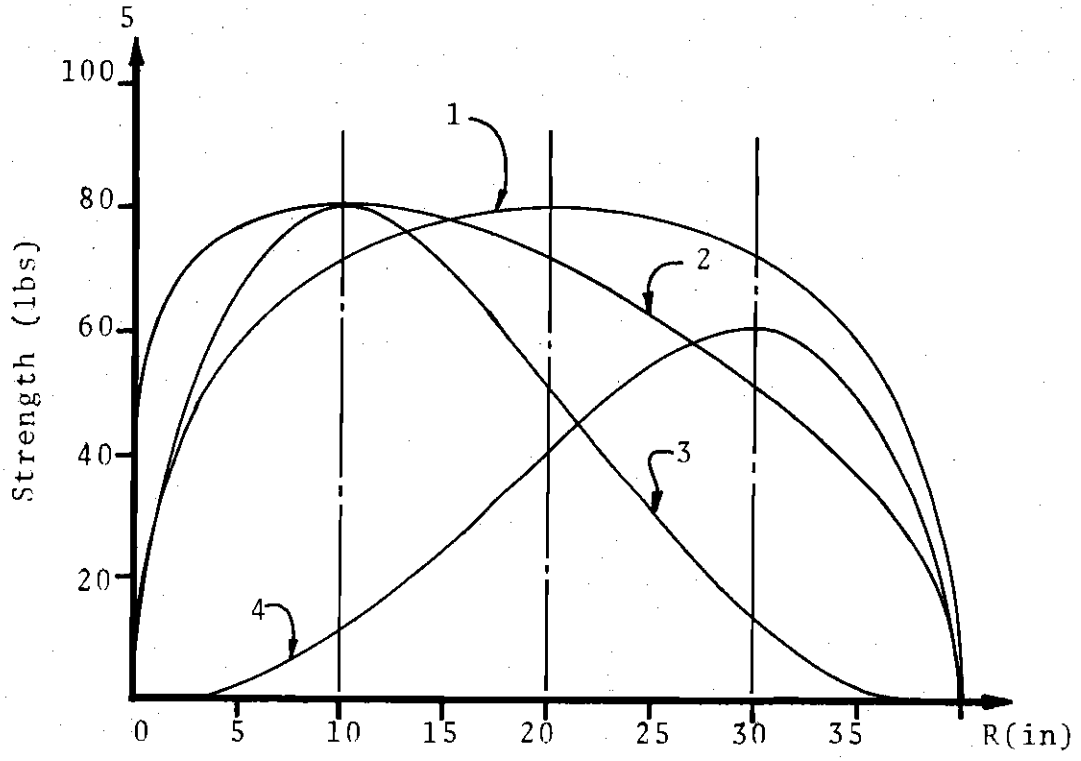

Curve No	1	2	3	4
S_m	80	80	80	60
R_m	20	10	10	30
B	.02	.02	.08	.08
m	40	40	40	40
Skew	None	Left	Left	Right

Figure 4-27. Effect of Parameters on Strength Profile Shape

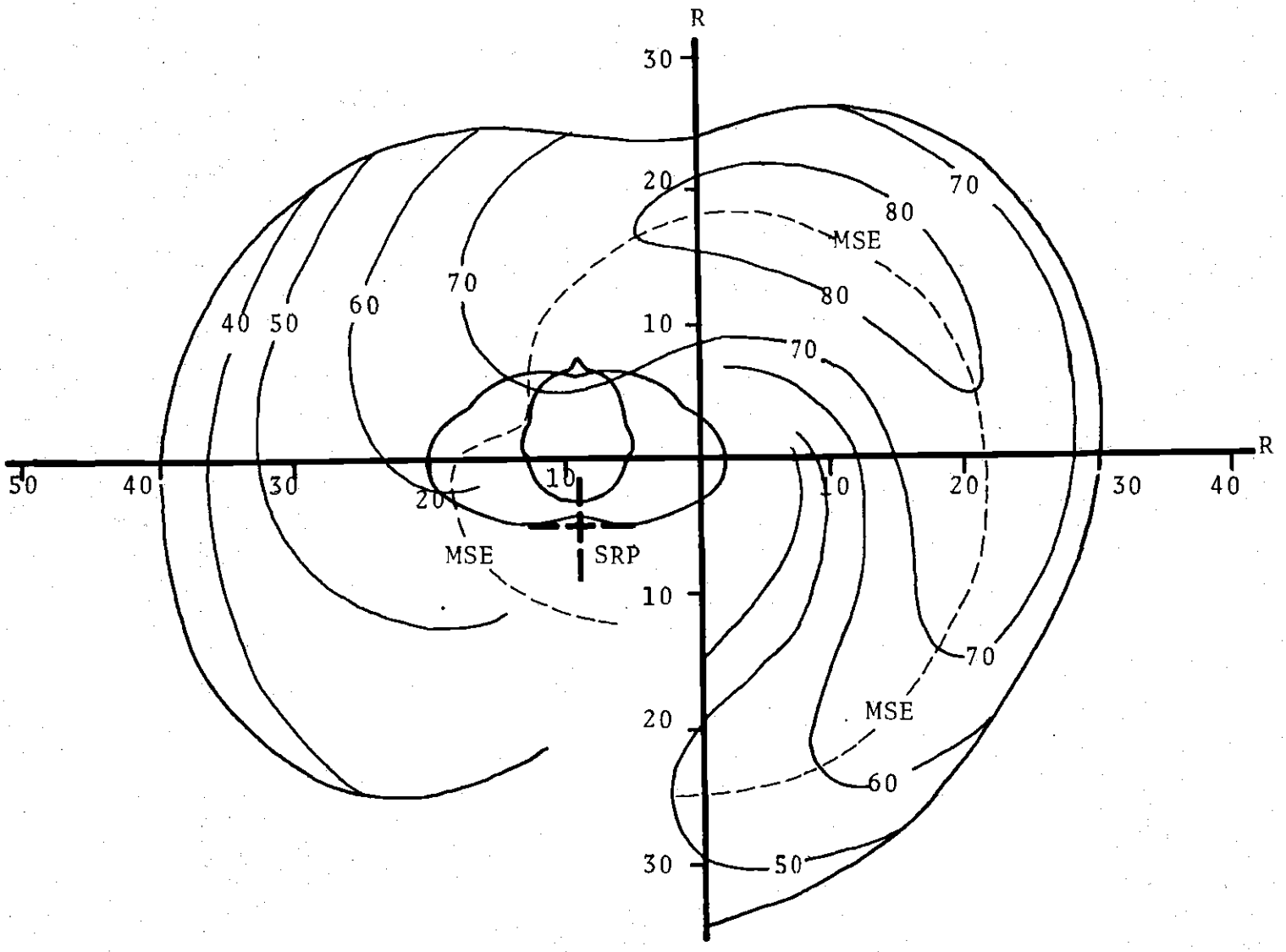

Figure 4-28. Strength Contours Generated by Final Model

Appendix C: Determining the Adequacy of Fit of the Final Model

Secondary Effects Sub-Study

The strength values obtained from the test positions collected at the beginning and end of each test session are presented in Table 4-4. The analysis of variance was run on the following model:

$$S = m + P_i + T_j + F_k + L_\ell +$$

$$[\text{first order interactions}] + \varepsilon_{m(ijk\ell)}$$

where

P_i = test period (1 = morning, 2 = afternoon)

T_j = test position (1 = "A", 2 = "B")

F_k = fatigue (1 = before, 2 = after-data collection)

L_ℓ = learning (day 1-10)

The analysis of variance model was fit on the data in Table 4-4. The table for this model is given in Table 4-5. All three or four way interactions were pooled to form the residual sum of squares. From the table it can be seen that main effects due to test position, fatigue and learning were significant at the $\alpha = .01$ level. Parameter estimates for main effects and two-way interactions appear in Table 4-6.

Table 4-4. Data for Secondary Effects Sub-Study

P_i	T_j	F_k / L_ℓ	1		2	
			1	2	1	2
1	1	1	76	81	67	83
		2	77	80	62	70
2	1	1	65	76	63	78
		2	67	72	66	70
3	1	1	70	80	66	73
		2	65	70	58	65
4	1	1	64	77	67	76
		2	69	62	62	69
5	1	1	65	71	65	77
		2	65	75	66	65
6	1	1	55	72	63	80
		2	60	67	61	75
7	1	1	53	68	60	66
		2	57	66	58	68
8	1	1	60	67	62	55
		2	60	64	60	61
9	1	1	66	66	63	67
		2	61	65	57	71
10	1	1	64	70	56	71
		2	63	62	60	66

Table 4-5. Analysis of Variance: Secondary Effects Sub-Study

*Significant at $\alpha = .01$
**Significant at $\alpha = .05$

Source of Variation		Sum of Squares	DF	Mean Square	F
Main Effects					
T		1073.113	1	1073.113	84.199*
P		25.312	1	25.312	1.986
F		154.012	1	154.012	12.084*
L		1148.612	9	127.624	10.014*
Two-Way Interactions					
T	P	15.312	1	15.312	1.201
T	F	78.013	1	78.013	6.121**
T	L	191.012	9	21.224	1.665
P	F	13.613	1	13.613	1.068
P	L	283.312	9	31.479	2.470**
F	L	106.612	9	11.846	.929
Residual		471.563	37	12.745	
Total		3560.487	79	45.069	

Table 4-6. Parameter Estimates from Secondary Effects Sub-Study

Grand Mean = 66.76

Main Effects (deviations from grand mean)

P_1 = .56	L_1 = 7.74	L_9 = -2.26
P_2 = -.56	L_2 = 2.86	L_{10} = -2.76
	L_3 = 1.61	
T_1 = 3.66	L_4 = 1.49	
T_2 = -3.66	L_5 = 1.86	
	L_6 = - .14	
F_1 = 1.39	L_7 = -4.76	
F_2 = -1.39	L_8 = -5.64	

Two-Way Interactions

	P_i		T_j		F_k	
	1	2	1	2	1	2
T_1	.43	-.43				
T_2	-.43	.43				
F_1	.37	.37	-.94	.94		
F_2	-.37	-.37	.94	-.94		
L_1	3.43	-3.43	.66	-.66	.91	-.91
L_2	-.20	.20	.28	-.28	-.47	.47
L_3	2.3	-2.3	1.03	-1.03	2.53	-2.53
L_4	-.82	.82	1.91	-1.91	1.41	-1.41
L_5	-.20	.20	1.28	-1.28	-.47	.47
L_6	-3.70	3.70	-2.22	2.22	-.47	.47
L_7	-1.57	1.57	-.34	.34	-1.59	1.59
L_8	1.05	-1.05	4.03	-4.03	-1.47	1.47
L_9	- .57	.57	1.91	-1.91	-.34	.34
L_{10}	.18	-.18	1.41	-1.41	-.09	.09

CHAPTER V

DISCUSSION

Strength Patterns Affecting General Variability in the Raw Data

Basic Strength Profile Shapes

From examining the three-dimensional view of the raw data (Figure 4-25) it is obvious that two basic strength patterns occur. From a point in front of him and to his left (radian 19 in Figure 3-6) to a point directly behind him (radian 12), the strength profiles show a definite "humped" form. Other radians--those across his body to the left and behind his left shoulder--show profiles which start high but decrease at increased distances from his right shoulder. The humped profiles on his right side are probably due to basic characteristics of the musculo-skeletal structures between the shoulder and hand which are involved in pushing. These characteristics include the mechanical advantage gained from bone angles and muscle attachment points, and the tendency of the muscles involved to be stronger at points between their maximum and minimum elongation. Because of these biomechanical characteristics, the arm, shoulder, wrist, and hand develop maximal efficiency in pushing at points between their minimum and maximum reach

distances (Astrand, Rodahl, 1970).

Possible reasons for the decreasing pattern of the left side profiles are less clear. At these points the twisting of the trunk is more of a factor in pushing. In order to reach hand locations on the left side, the more ideal shoulder and elbow angles used on the right side must be replaced with angles which are less mechanically efficient.

This awkwardness and mechanical inefficiency increases on each radian as the hand moves farther from the body. This effect causes the decreasing strength pattern seen in those areas.

Movement of the Maximum Strength Ellipse

Another general strength pattern can be seen in the maximum strength ellipse of Figure 4-1. Starting behind the subject's left shoulder and proceeding clockwise around this body, the position of the maximum strength slowly moves farther from the right shoulder. This effect is initially consistent with the decreasing curves mentioned above and their gradually blending into the "humped" curves in the vicinity of radian 19 (see Figure 3-6). From this point on, going around the subject to his right, the location of the "hump" shifts away from the shoulder point. Here, again, the reasons are not clear.

It is possible that the shift in maximum strength occurs because of the general shift in maximum reach in this area. Note that, for points in front of the subject (radians one through seven), the maximum reach distances are shortened

by the push criteria, which specifies that one point on the back should touch the chair back at all times. As the hand moves from radian eight to 12, maximum reach distances actually increase as a result of being able to stretch more while keeping one point of the back on the chair. At these angles, the body is twisted and the point of the back which touched the chair back was almost under the subject's arm. This is illustrated by the silhouette on the strength profiles for radians eight through 12 (Figures 4-10 through 4-14).

Another reason for the maximum strength ellipse's moving away from the shoulder in a clockwise direction involves the body support provided by the chair. At locations in front of the subject, the chair back provides a large part of the medium through which force is transferred to the floor. Because the back flexes two to three inches before stabilizing, the resulting maximum strength location on each forward radian is biased rearward. When pushing to the rear (over the back of the chair), however, force is transferred more directly through the subject's buttocks and feet to the floor, and there is no resultant forward bias of the maximum strength location on the rearward radians.

Location of Highest Strength Values

Figure 4-1 shows another general strength pattern, which is that the location of the highest strength values, that is, the 80 pound contour, is in front and to the right of the subject. This effect can be attributed to the

biomechanical structures involved in the push. At these locations, muscle-bone moment arms are not most efficient and bone alignment through the joints is most conducive to large exertions.

The subject's back is firmly planted against the seat back in the front right quadrant. In other locations, there is a varying degree of trunk twist, which tends to reduce the toggle effect mentioned by Hugh-Jones (1947). With the back firmly planted against the flexible chair back, the subject occasionally could "snap" his elbow into a slightly hyper-extended attitude, thereby noticeably gaining force. This is because of the more advantaneous mechanics associated with the toggle effect. This effect could only occur in the right forward radians and partially contributed to the higher strength values in that area.

Comfort is another factor which probably contributed to the larger values in the right forward radians. In other directions, there was either a body twist, the top of the chair back dug into the subject's back, or both. These conditions may have caused discomfort and resistance force resulting in lower recorded forces on these radians.

The feeling of stability gained by having the back firmly planted on the chair is another psycho-physical factor, which, when decreased, as in the more awkward radians, could have had a decremental effect on strength.

Variability of Raw Data Along Each Radian

The variability of the data along each radian has been shown in two forms: the plot of the running average σ values along each radian, which appears at the bottom of each strength profile (Figures 4-3 through 4-24); and the contours of the running average coefficient of variation values (CV_R) found in Figure 4-2.

The Free Push Criteria

The basic reason for the degree of variability evidenced in the data is the free push criteria used. Note that in Table C-1 the average inherent standard deviation is 8.0 pounds, which, on first examination, seems to be rather high.

It was the philosophy behind the free push criteria which justifies the increase in variability. The only stabilization restrictions the free push has on the subject are that both feet are on the floor, both buttocks are on the seat, and one point of the back is on the seat back at all times. These criteria are more representative of a real industrial situation (without back or torso assists) than those used in other studies.

The more restricted or stabilized procedures such as those used in other studies (Schanne, 1972; Garg, Chaffin, 1975; Thordsen, et al. 1972) lose appeal because of their departure from real life situations.

Also departing from real life is the practice of isolating muscle groups in studying strength. An example of

this practice would be the isolation of the biceps in an arm strength study. The free push philosophy makes no attempt to isolate any muscle groups, because, on some radians, twisting of the trunk and awkward reaching must occur in order to push in the desired directions. Radian 13 is an extreme example of such an awkward position. Because of interaction between muscle groups, it would be impossible to isolate muscle groups in such a complex body position.

The flexible chair back in this study served to generally locate the body and rarely gave consistent firm support to the trunk in exertions.

Variation Patterns on Each Radian

The running average standard deviation and coefficient of variation plots in Figures 4-3 through 4-24 and Figure 4-2 show the following characteristics of variation.

1. The variation on the subject's right side seems to follow a regular, predictable pattern. These radians have high variance close to and far away from the body, and smaller variance near the middle of each radian. This is due to the more awkward body positions required for pushing at extremely close and extremely distant points. At medium range hand locations, the subject can assume a more natural, comfortable body position, which results in lower variance.

2. The variation on the subject's left side seems to have little or no regular pattern. This is due to the fact that the subject rotates his trunk to reach these positions,

and variance is thereby introduced. Because of the complex twisting motion involved, no obvious patterns in variance are seen in these radians.

Subject Variability

The analysis of variance table resulting from the subject variability sub-study (Table 4-5) shows significant main effects due to test position, fatigue, and "learning."

The Test Position Effect

The two test positions, A = (-11,10) and B = (20,22), were chosen in different regions around the subject. At that time it was assumed that there would be significant strength differences due to location. Therefore, the $\alpha = .01$ significance level from the ANOVA table was not surprising.

The Fatigue Effect

The fatigue parameter indicated a statistically significant decrement in strength over the time span of each test session. The main effect for fatigue (in Table 4-6) of 1.39 indicates that this effect had little practical significance. Other contributing reasons for fatigue are the temperature and humidity in the closet-like test room and the fact that the subject moved the apparatus between exertions himself. Although these factors were not excessive, the confines of the small space did create some discomfort for the subject. Residual soreness from previous testing

could have indirectly affected the fatigue effect by gradually decreasing his motivation during the test session. Each session, lasting approximately two hours, was composed of four-minute rests and five-second exertions. Because of the large percentage of idle time in the session, the subject experienced some boredom, which could have indirectly affected his performance during the session.

The Learning Effect

The "learning" parameter was somewhat paradoxical. Examination of Table 4-6 and Figure 5-1 shows a negative effect over the course of the 10 day experiment. That is, the strength values decreased over the course of the experiment. A positive effect had been expected. This would have been primarily due to a training effect caused by the physical conditioning of the muscles involved. Also, a positive learning effect would have been expected as the subject developed techniques for use in pushing on this apparatus.

Figure 5-1 is a plot of strength predicted by the ANOVA model versus the day on which the testing occurred. Because position effect does not have direct bearing on this discussion, the effect of position (T) was omitted. The "learning" trend is clearly illustrated in this plot by a steady decrease until day seven or eight. At this point there seems to be a stabilizing trend. This could be due to subject motivation gained by nearness to the end of the experiment. Also, there may be an influence here due to a

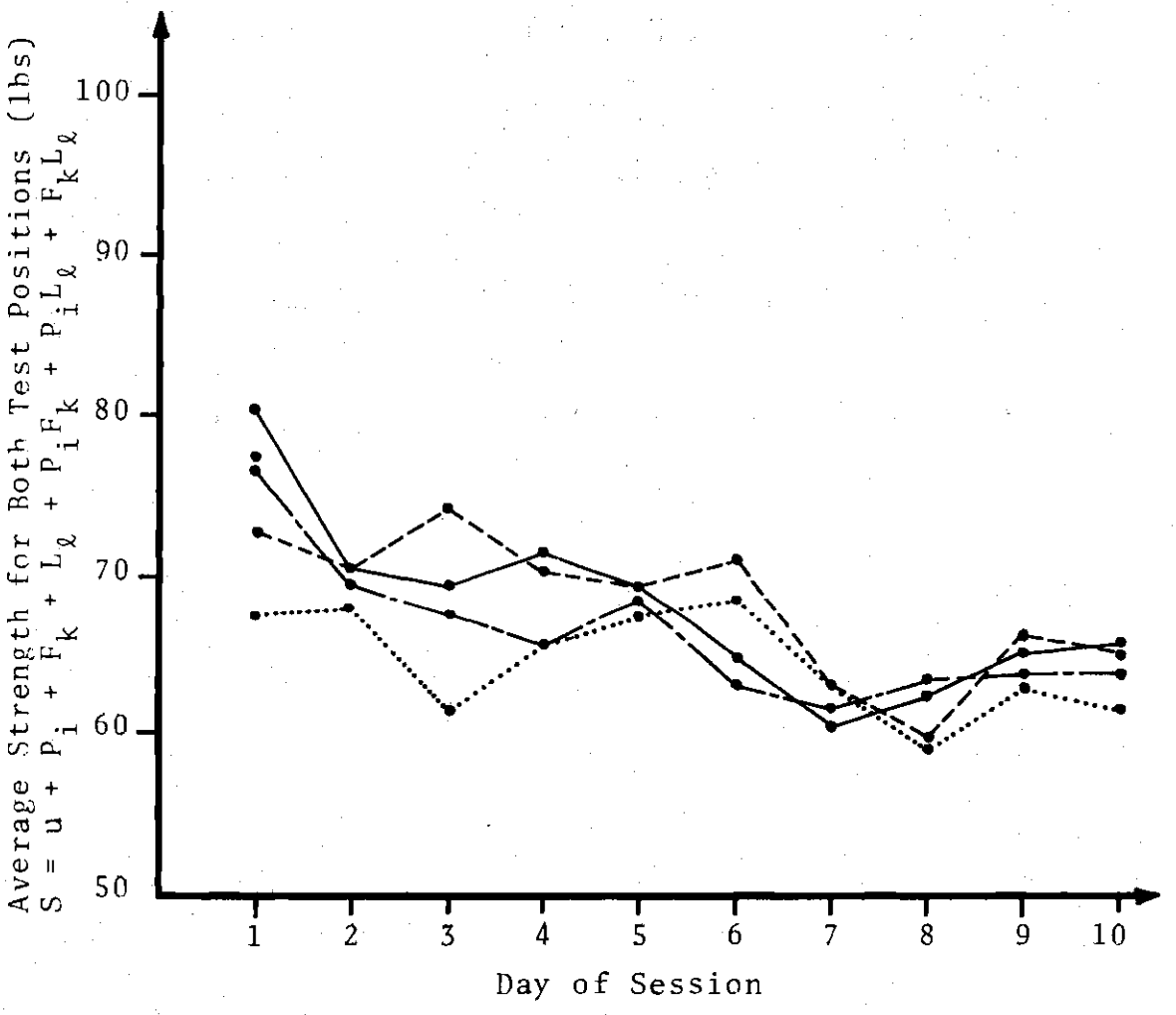

Figure 5-1. Negative "Learning" Effect on Strength

delayed acquisition of skill in the pushing task.

There are two viable reasons for the significant negative trend in force as the experiments progressed: First, the subject, who was not accustomed to this type of repeated exertion, did experience a substantial amount of soreness. The soreness appeared after the first few days of the experiment. This soreness could have caused a motivational drop with accompanying decrements in performance. Secondly, a general motivation effect could have caused the negative trend. When the experiment began, the subject was highly motivated. As the experiment progressed, however, the monotony of the exertion cycle began to affect the subject's concentration.

Another less obvious contributor to the negative "learning" effect could have been residual fatigue from the prior day's testing.

The Use of One Subject for Data Collection

The data from one subject was used to derive the model. There are two justifications for this decision:

1. The final model is in the form of a general structure. This structure can be applied to larger subject populations with the same crescent-shaped-ellipse prediction contours resulting. The way the general model is to be expanded is by the manipulation of the equations for parameters S_m, R_m, and B. This manipulation will require

the inclusion of percentile factors in the equations. Note, however, that the general model structure derived from the one-subject data will not need to be altered.

2. Because of the large number of data collected (430 points total) it was logistically impossible to involve more than one subject in the experiment. With one subject, completion of the data collection required 10 full days.

CHAPTER VI

CONCLUSIONS AND RECOMMENDATIONS

Conclusions

Several conclusions may be drawn from this study. These conclusions fall into the following categories:

1. Conclusions regarding strength patterns
2. Conclusions concerning sources of variability in strength
3. Conclusions regarding the methodology used to predict strength.

Strength Patterns

In the transverse plane located 20 inches above the SRP, a right-handed subject develops maximum push strength in the frong right quadrant. The distance in each radial direction to the location of maximum strength is minimal behind the left shoulder, and increases as the hand moves clockwise around the body.

Two general profiles of strength occur in pushing. In some angles around the body, the subject is strongest at hand locations closest to his body. At other angles, the subject is strongest at a point located between his minimum and maximum reach distance.

Equal strength contours drawn on an aerial view of the

subject are crescent-shaped ellipses which are bent around the shoulder point.

Predictive Model

Strength can be predicted by the following model with acceptable accuracy:

$$S = S_m \left(\frac{R}{R_m}\right)^{BR_m} \left(\frac{m-R}{m-R_m}\right)^{B(m-R_m)} \qquad (6\text{-}1)$$

where:

S = strength

S_m = maximum strength in one direction

R_m = distance to maximum strength in one direction

B = shape parameter of strength profile

m = maximum reach in one direction

R = distance from hand to shoulder

Secondary Effects

Secondary effects on push strength were found to be the position of the hand, fatigue, and learning effects. Such factors as soreness, motivation, and residual fatigue tend to affect strength data collection. Apparatus-induced variance probably contributes to overall variance. The free push methodology used also contributed to the overall variance. This methodology is mentioned below.

Methodology

"Free push" criteria were used in the data collection. The restrictions imposed on the subject were as follows:

Both feet on the floor, both buttocks on the seat, and one point of the subject's back on the chair back at all times.

The increased variability in the model caused by these minimally constrained criteria was not great enough to offset the advantages which resulted from the criteria. The primary advantage was the similarity of the data collection techniques to real-life pushing situations.

The model building methodology used in this study was effective insofar as it resulted in an intuitively appealing model. The methodology consisted of examining the raw data and detecting trends, such as the skewing of strength profiles as they rotated around the body. A structure for the model was chosen which would skew in either direction as a result of manipulation of its parameters. The data was then fit on a radian-by-radian basis. Finally, the model was integrated into a single expression by developing expressions for the parameters which were functions of the angles of the radians.

Recommendations

Because of the limited scope of this thesis, there are several areas into which the basic model can be expanded.

Increased Number of Parameters

The number of parameters in the general model would probably need to be increased. Currently, the model has three parameters for curve location and skewness (S_m, R_m, m) and one parameter for shape (B). The model would probably

benefit from another shape parameter, say parameter "A". With two shape parameters it may be possible to control each side of the strength profile individually. This would yield a finer degree of control for skewing, kurtosis, and general profile shape. A good candidate for the new model would include the new parameter "A" in the exponent of the third factor:

$$S = S_m \left(\frac{R}{R_m}\right)^{BR_m} \left(\frac{m-R}{m-R_m}\right)^{A(m-R_m)} \qquad (6\text{-}2)$$

Inclusion of Percentile Factor

The model also needs to be generalized to a larger population. The current model is a sound framework for a more general model. The addition of a percentile factor would be necessary to expand the model. Hopefully, the basic structure of the model, that is:

$$S = S_m \left(\frac{R}{R_m}\right)^{BR_m} \left(\frac{m-R}{m-R_m}\right)^{B(m-R_m)}$$

would remain unaltered, and the percentile factor could be integrated into the S_m and R_m equations [Eqs. (B-1) and (B-2)].

Expanded Range of Prediction

More obvious areas for expansion are in the range over which the model predicts. Currently, it is designed only for pushing in the 20 inch transverse plane. In the future it should be revised to predict values anywhere in the

reach sphere. It should also be made flexible enough to make separate predictions for pushing, pulling, left- and right-directed arm forces.

Further expansions for the model could be made in age and sex differences. This type of expansion would require validation on much larger subject population sizes.

APPENDICES

APPENDIX A

REPARAMETERIZATION OF THE BETA DISTRIBUTION IN DERIVING THE STRENGTH MODEL

Background

The present strength model is a modification of the beta distribution which is used in statistics. The most general form of the beta density function is

$$P(Y) = \frac{1}{B(p,q)} \frac{(Y-a)^{p-1}(b-Y)^{q-1}}{(b-a)^{p+q-1}} \qquad (A-1)$$

for $Y \in (a,b)$

and $p>0$, $q>0$

The term $B(p,q)$ is the beta function which can be defined in terms of gamma functions or equivalently in terms of factorials as follows:

$$B(p,q) = \frac{\Gamma(p)\Gamma(q)}{\Gamma(p+q)} = \frac{(p-1)!(q-1)!}{(p+q-1)!} \qquad (A-2)$$

The standard form of the beta distribution is obtained by using the substitution $x = (Y-a)/(b-a)$, and takes the form

$$P(x) = \frac{1}{B(p,q)} X^{p-1} (1-x)^{q-1} \qquad (A-3)$$

for $x \in (0,1)$

and $p>0$, $q>0$

Various other distributions used in statistics are subcases of Eq. A-3 as follows:

Transformation	Distribution
$p = q-1$	Rectangular
$p = q = 1/2$	Arc-sine
$q = 1$	Power function
$T = x/(1-x)$	Pearson Type VI
$F = v_2 T/v_1$	F

where $v_1=2p$

$v_2=2q$

Distribution Form

Figure A-1 shows the flexibility of the beta distribution and that the skewness of the distribution can be altered by modifying the parameters p and q. In initially reviewing the strength data collected in the present study, several modifications in the beta distribution (Eq. A-3) seemed appropriate. The resulting reparameterization of the beta distribution is reviewed in Table A-1 and resulted in the following strength model:

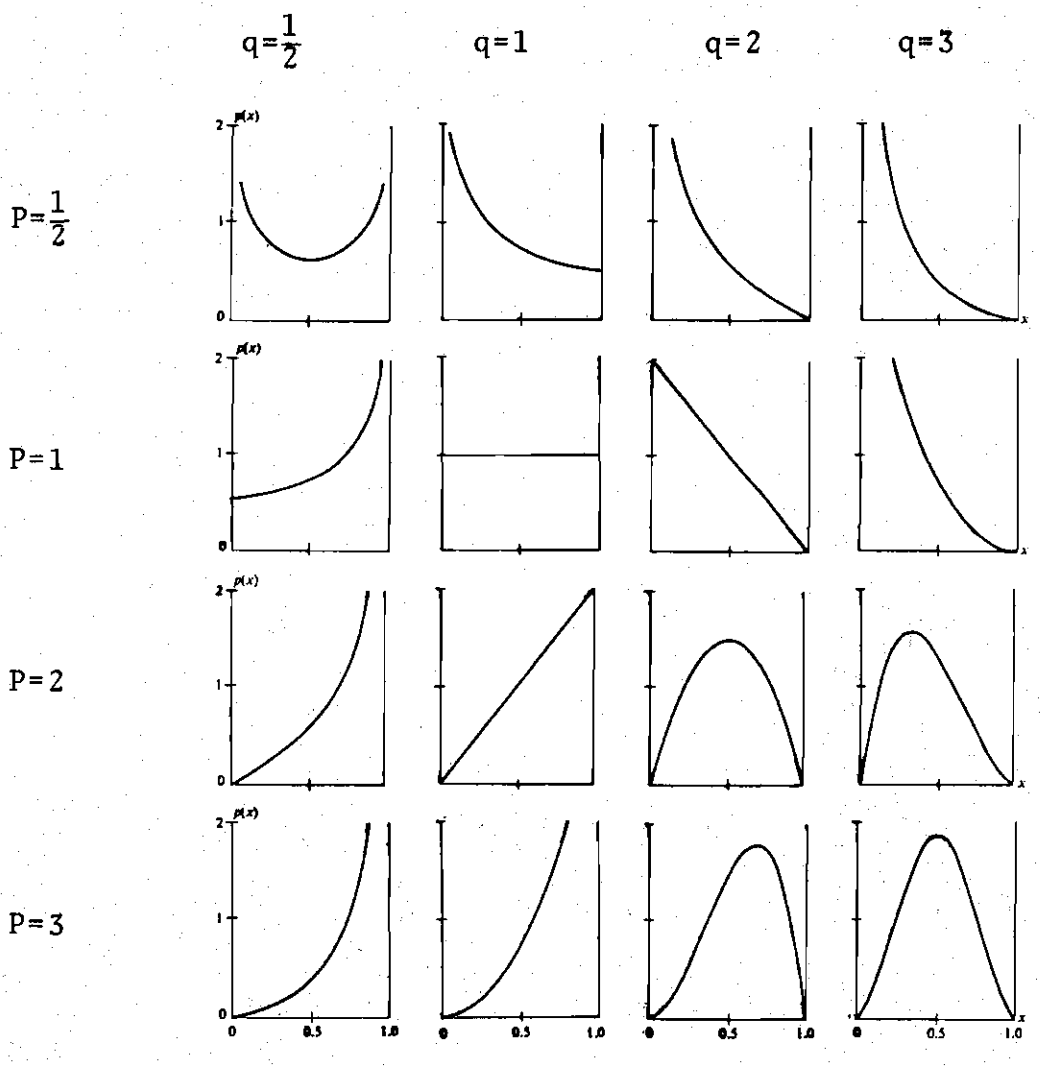

Figure A-1. Forms of the Beta Distribution (after Johnson and Kotz, 1970)

Table A-1. Direct Modifications in Beta Distribution

Modification	Rationale
$S = P(x)$	The dependent variable is strength, S, rather than a probability density, P(x)
$R = x$	The independent variable of the strength model is radial reach distance, R
$M = 1$ $R \varepsilon (0,m)$	The independent variable, R, is not confined to the unit interval but can vary from 0 to M, the maximum reach distance
$K = 1/B(p,q)$	The present model is not a probability density. The integral of the model over the range of the independent variable does not have to equal one. As a result, a constant can be substituted for the beta function, B(p,q)
$b = p-1$ $d = q-1$ with $b \geq 1$ $d \geq 1$	The curves shown in the lower right hand corner of Figure A-1 are the most appropriate forms for the strength model. Thus, values of p and q less than 1 do not have to be considered, and the model can be reparameterized in terms of the parameters b and d

$$S = K(R)^{b}(m-R)^{d} \qquad \text{(A-4)}$$

for $R \in (0,m)$

$b \geq 1$ and $d \geq 1$

Further Modification

The strength model given in equation A-4 has four parameters; however, only the parameter m, the maximum reach distance, has a heuristic interpretation. The remaining parameters, k, b, and d, are simply estimation parameters which have no direct meaning. As a result, the model was reparameterized into a more interpretable form.

Differentiating Eq. A-4 with respect to R yields

$$\frac{ds}{dR} = kR^{b}\ (m-R)^{d}\ [-d/(m-R) + b/R]. \qquad \text{(A-5)}$$

Setting this differential equal to zero it is found that the dependent variable S assumes a minimum value of zero when R = 0 or R = m. The maximum occurs when the condition

$$-b/(m-R) + b/R = 0 \qquad \text{(A-6)}$$

is satisfied. Solving for R in equation A-6 yields

$$R = R_{m} = bM/(b+d) \qquad \text{(A-7)}$$

The R value when S is maximum is denoted R_m. Similarly, the maximum value of S can be denoted as S_m and is found by substituting the expression for R_m in Eq. A-7 into Eq. A-4. This substitution yields

$$S_m = KM^{b+d}[b/(b+d)]^b[d/(b+d)]^d \qquad \text{(A-8)}$$

Eqs. A-7 and A-8 can be inverted to yield

$$d = \frac{b(m-R_m)}{R_m} \qquad \text{(A-9)}$$

and

$$K = S_m/[m^{b+d}(b/(b+d))^b(d/(b+d))^d] \qquad \text{(A-10)}$$

If these two equations are substituted into Eq. A-4, the arbitrary parameters d and k are eliminated, and after rearranging terms, the model takes the form

$$S = S_m \left(\frac{R}{R_m}\right)^b \left(\frac{m-R}{m-R_m}\right)^{b(m-R_m)/R_m} \qquad \text{(A-11)}$$

Finally, if the equation

$$b = BR_m \qquad \text{(A-12)}$$

is substituted in Eq. A-11, the final form of the model is obtained.

This last substitution is somewhat arbitrary and is only done to give the equation a more symmetric appearance. The final form of the model is

$$S = S_m \left(\frac{R}{R_m}\right)^{BR_m} \left(\frac{m-R}{m-R_m}\right)^{B(m-R_m)} \qquad \text{(A-13)}$$

for $R \in (0,m)$

$B \geq 1/R_m$ and $1/(m-R_m)$

where

R = distance to hand

m = maximum reach distance

S_m = maximum strength

R_m = reach distance to maximum strength

B = shape parameter

APPENDIX B

PROCEDURE FOR ESTIMATING PARAMETERS IN THE MODEL

The fitting of a model to the data was a three-step sequential process:

Step one: First prediction of R_m, S_m, and B for each radian

Step two: Development of expressions for R_m and S_m as functions of ϕ

Step three: Development of expression for B as function of ϕ

Step One: The Four Parameter Model

The method used to estimate parameters was a computer routine which will be referred to as the "net search routine." This routine was a Fortran program which ennumerated large numbers of combinations of parameters, and, for each combination, calculated an S prediction, a residual, and the sum of the squares of the residuals (which will be referred to as the "SS error") for each radian. The goodness of fit of each combination of parameters was shown by directly comparing the SS error associated with various combinations of parameters.

A non-linear regression computer package was utilized prior to using the net search routine. This program employed

the Marquardt or Gaussian technique. Its use was abandoned because it would not converge on optimal parameters.

The net search routine was first used on a radian-by-radian basis to find the values of S_m, R_m, and B which yielded a minimum SS error. The fourth parameter, m, was set equal to 40.0. This number was an approximation of the maximum reach distance. The ranges and increments of this search are as follows:

Parameter	Range	Increment
B	.005 - .80	.005
R_m	10.0 - 30.0	2.0
S_m	40.0 - 100.0	5.0
M	40.0 (fixed)	

The predictions are listed in Table B-1. Plots were made of these predictions versus ϕ (Figure B-1). The ϕ notation evolved from these plots. By locating the origin of these plots at radian B, the smooth forms for the S_m and R_m plots were evident. The S_m curve is a smooth, well defined second degree curve, and the R_m plot is clearly a line with a slight upward slope. For this reason the angle of radian 13 was designated $\phi = 0$. The angle of radian 13 in the θ notation is 210 (see Figure 3-6).

At this point, the plot of B versus ϕ remained somewhat difficult to characterize. The net search routine was used later to re-predict B.

Table B-1. Parameter Estimates from Net Search Routine

	Radian	1	2	3	4	5	6	7	8	9	10	11	12	13	14	15	16	17	18	19	20	21	22
4 Param. Model	SM	80	80	75	80	85	85	85	70	70	65	60	55	40	45	55	55	65	65	70	70	80	85
	RM	16	16	18	18	18	18	22	22	22	22	24	30	10	14	14	30	10	14	10	22	20	18
	B	.080	.080	.055	.055	.070	.075	.045	.050	.030	.050	.045	.020	.025	.010	.010	.005	.005	.005	.005	.020	.045	.075
	SS	969	1134	1165	1374	1878	2100	707	1084	3153	882	1209	843	232	827	987	1076	691	788	484	1181	2952	1804
1 Param. Model	B	.07	.075	.075	.06	.055	.055	.04	.06	.03	.05	.06	.02	--	.01	.005	.005	.005	.005	.01	.02	.03	.065
	SS	1208	1823	1867	1329	2034	2490	866	1183	3091	967	1334	1023	--	818	1062	1594	715	920	566	2139	3541	2027
Final Model	SS	2213	3235	3185	2025	2438	2753	980	1399	3430	887	1346	2179	503	1204	1018	2680	1578	2422	1017	2139	3610	2873

Step Two: Fitting Functions to R_m and S_m

Because of its well-defined shape, the plot of S_m versus ϕ was fit with a second degree linear regression model. This function was

$$S_m = 30.0 + .4759\phi - .0013\phi^2 \qquad \text{(B-1)}$$

This expression fit the data with an R-square value of .92 (see Figure B-1). There was some concern, however, about the tendency for the S_m data to "dip" in the area from radian one to six (see Figure B-1), to evaluate the potential effects of these large residuals on further use of this expression for S_m, error SS values were checked at the S_m values predicted by the regression equation (B-1). These sums of squares were not substantially higher than those resulting from the original net search predictions, so the "dip" tendency was considered to be acceptable.

The net search predictions for R_m showed a linear trend which was fit by a straight line. Instead of using a weighted least squares procedure, a line was fit to the data "by eye." Then, on radians with questionably large residuals, the SS error checking procedure which was used in the "dip" problem above was used. This technique eliminated the need to weight residuals on a radian-to-radian basis. The weighting of residuals would have been in relation to the SS error increase associated with each residual. The checking

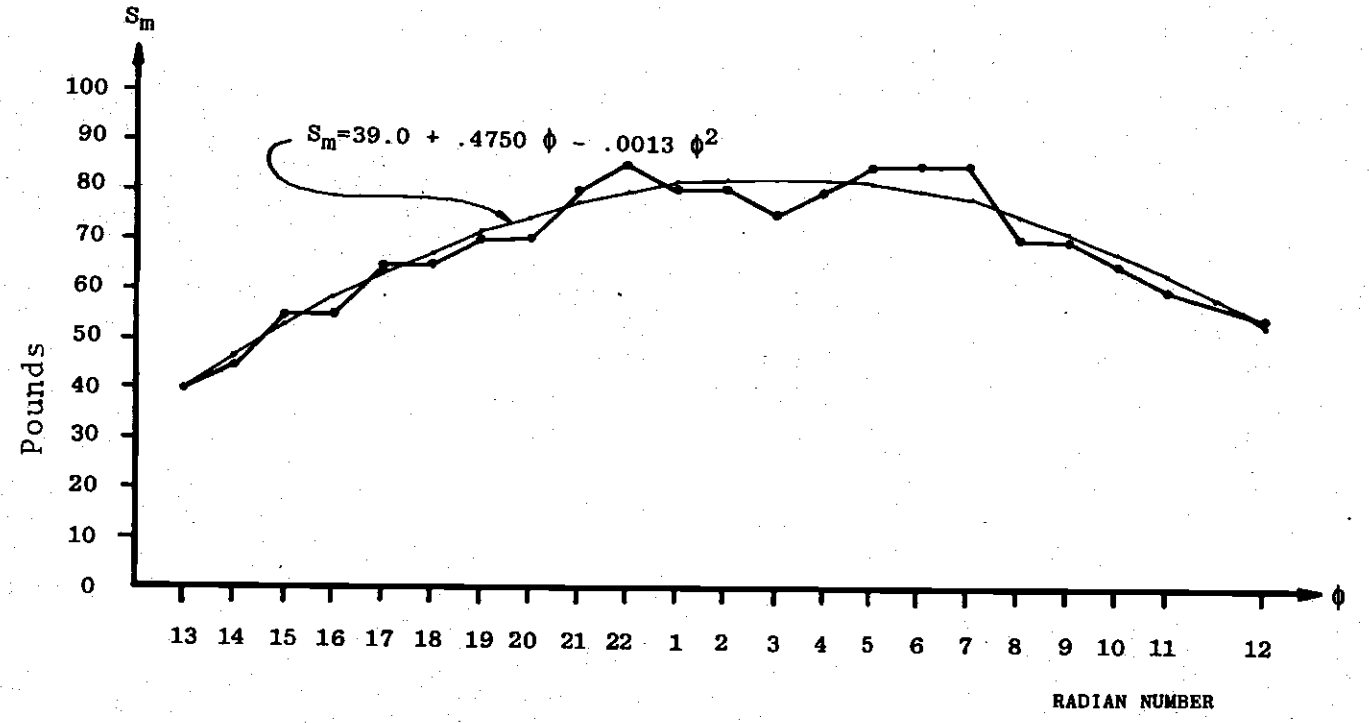

Figure B-1. Parameter Estimates from Net Search Routine

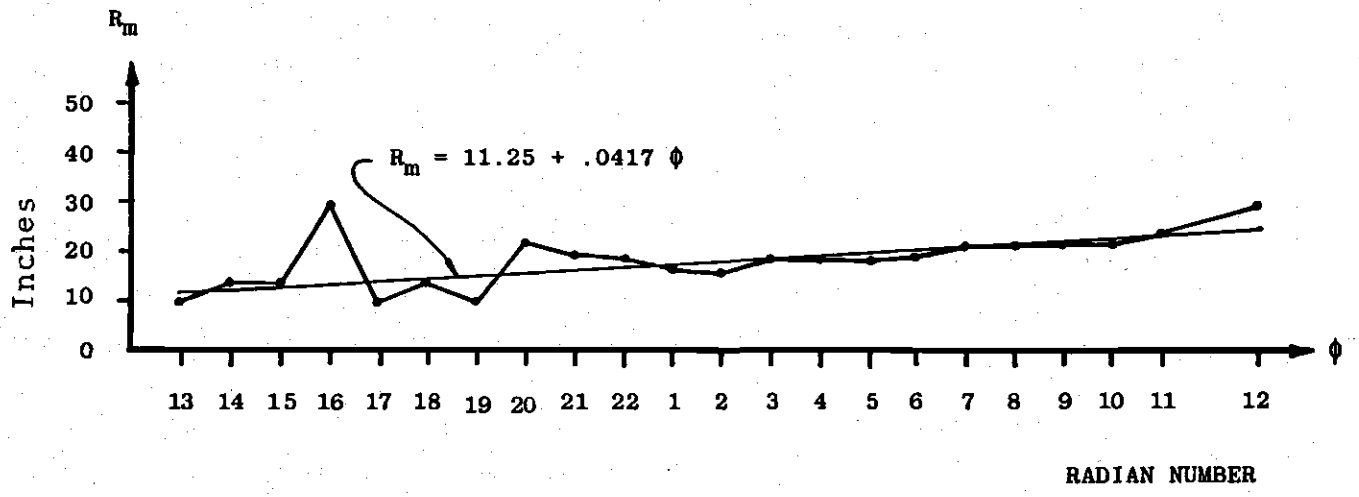

Figure B-1 (continued)

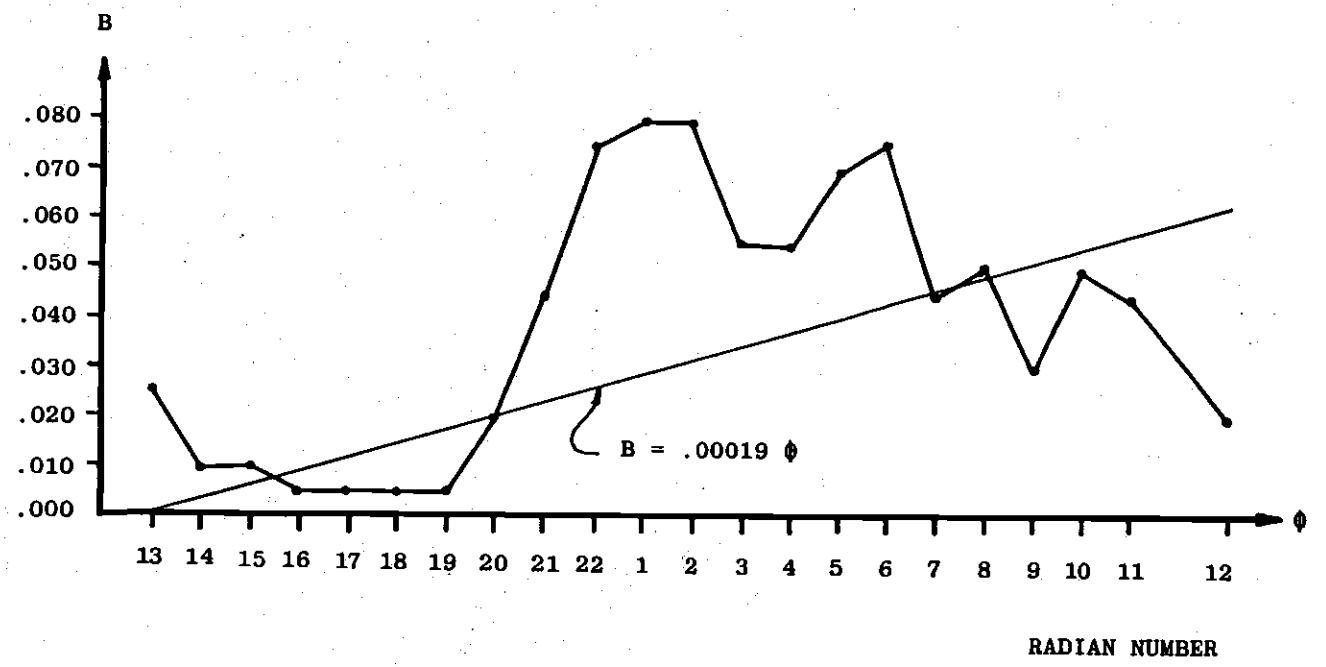

Figure B-1 (continued)

procedure yielded the same result as weighting of residuals. None of the increases in SS error was considered to be serious enough to abandon the use of a straight line for predicting R_m as a function of ϕ.

The equation for the line was

$$R_m = 11.25 + .0417\phi \qquad \text{(B-2)}$$

Graphs of these expressions (Eqs. (B-1) and (B-2)) are superimposed on the original net search predictions in Figure B-1.

Step Three: Deriving the Function for B

The first step in deriving the B versus ϕ function was to repredict B with the original net search routine, now modified to iterate only over values of B, with the S_m and R_m loops being replaced by Eqs. (B-1) and (B-2). Similar ranges and increments were used in this net and its prediction of B values are shown in Table B-1 and Figure B-2.

Note that very little smoothing of the B versus ϕ curve occurred as a result of the new net predictions. (Compare Figure B-1 with Figure B-2.)

SS error contours were drawn over the B versus ϕ plot. These contours indicated the shape of a curve which would predict B with the smallest SS error on each radian (Figure B-3). Typical proposed curves appear as dashed

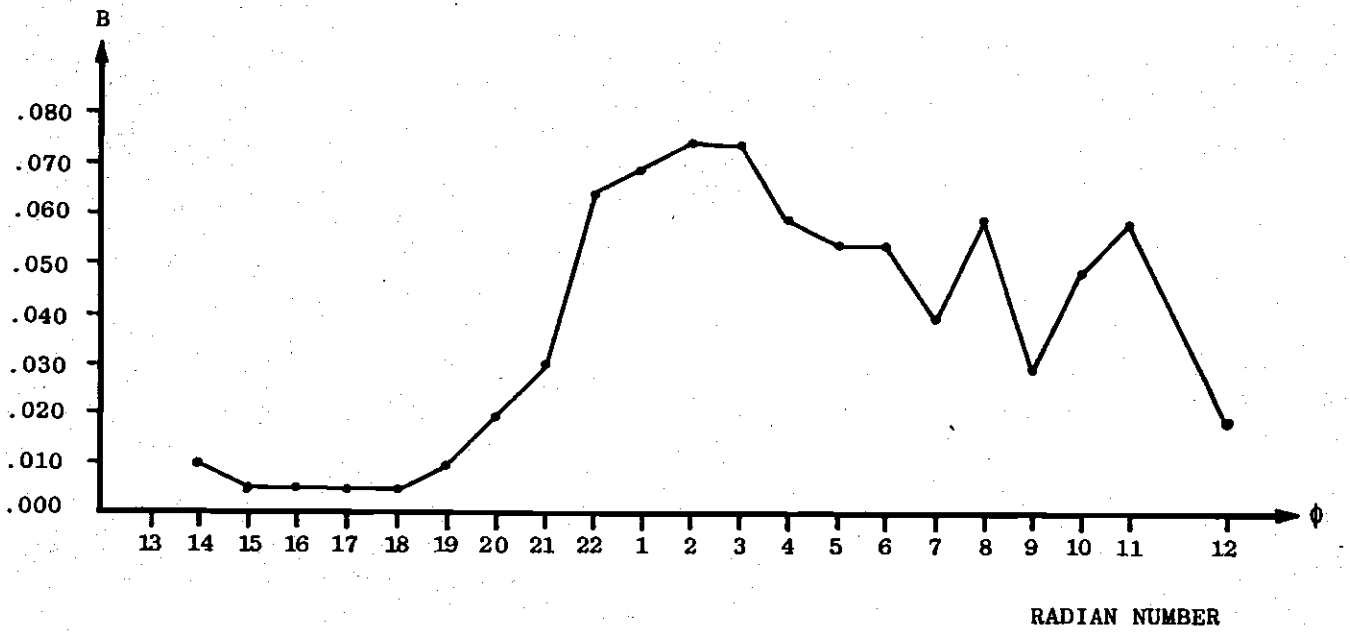

Figure B-2. Estimates for B from one Parameter Net Search Routine

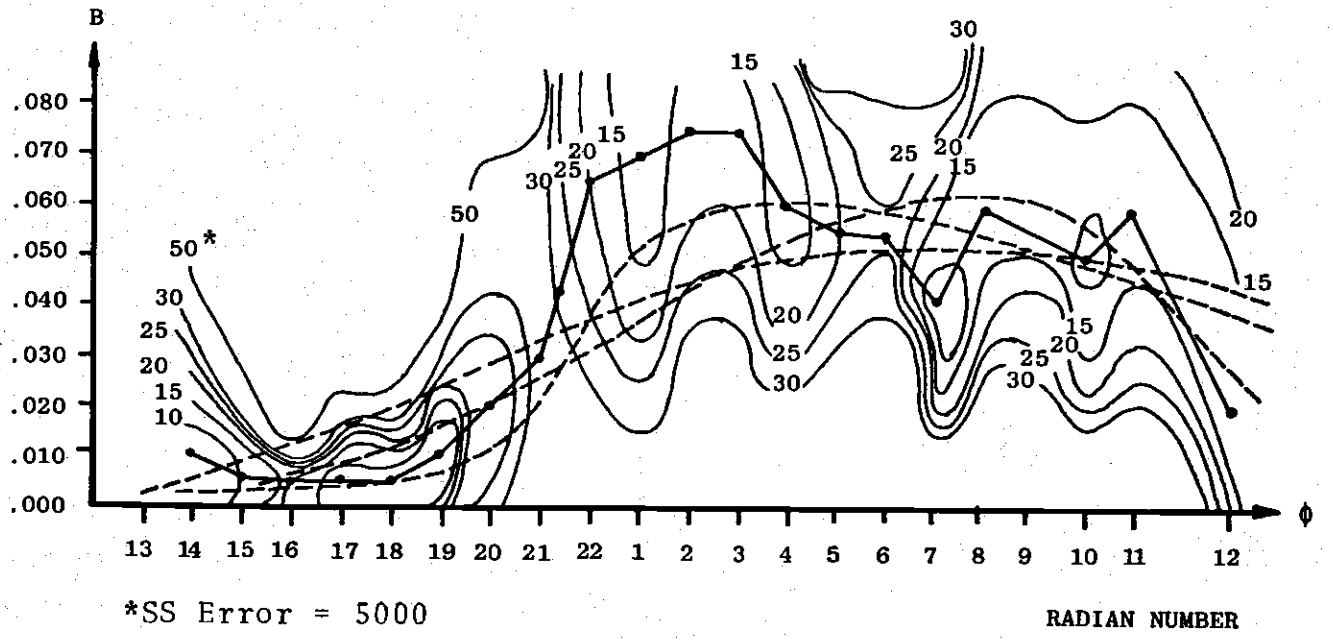

Figure B-3. SS Error Contours for Estimates of B

lines in Figure B-3.

The most promising curves appeared to be a line, a second degree curve, and a third degree curve. The third degree curve was abandoned because its marginally better fit would be offset by its complexity. Also, it would have been overfitting for this model, which was derived from data from just one subject.

Several second degree curves were fit to the plot with reasonable R-square values, but, in order to find the curve with the least SS error, another net search routine was performed. This net iterated over the three parameters of a second degree curve to find the combinations of parameters which would yield B values which, in turn, would yield minimum SS error. This net search also tested various straight lines and constants.

The ranges, increments, optimal models, and accompanying sums of squares can be seen in Table B-2. Note that the net search demonstrated that minimum SS error results from the use of a straight line to predict B rather than a second degree curve or a constant. This was because the line could predict the left side of the B versus ϕ plot (Figure B-3), which was sensitive to SS error, and get reasonable results on the right side, without going below zero at radian 13.

The equation for this line was

Table B-2. Summary of Results of the B Function Net Search Routine

Model: $\hat{B} = C + D\phi + E\phi^2$

Parameter	Range	Increment	Min SS Error	Parameter Estimate
C	.00001-.0046	.00001	45,137.5	.00001
D	.00011-.00080	.00001		.00019
E	(-).00000001-(-).0000041	.00000001		.00000001

Model: $\hat{B} = D\phi$

Parameter	Range	Increment	Min SS Error	Parameter Estimate
D	.00015-.00024	.00001	45,101.0	.00019

Model: $\hat{B} = C$

Parameter	Range	Increment	Min SS Error	Parameter Estimate
C	.0001-.1	.0001	71,359.6	.02

$$B = .00019\phi \qquad \text{(B-3)}$$

The plot of Eq. (B-3) is shown superimposed on the original predictions in Figure B-1.

APPENDIX C

ADEQUACY OF THE FIT OF THE MODEL

The inherent standard deviations of the data, which are given in Table C-1, are computed as follows:

$$\sigma_I = \sqrt{\frac{\sum_{i=1}^{10} \sum_{u=1}^{2} (Y_{iu} - \bar{Y}_i)^2}{10}}$$

where

i = location of hand or radian

u = number of the data point at that location

To determine the adequancy of the final model, the error sums of squares was divided by the appropriate degrees of freedom to give an estimate of the variance of the model. There was some uncertainty as to what number should be used for the degrees of freedom.

According to the convention used in ANOVA, the degrees of freedom for each radian would be the number of data points minus the number of parameters, or

20-4 = 16 degrees of freedom

The variance estimate would then be:

Table C-1. Variability of Model During Development

Radian	1	2	3	4	5	6	7	8	9	10	11	12
Raw Data σ_I	7.63	7.76	9.5	9.8	10.7	11.6	6.6	7.0	11.6	6.4	7.2	5.2
4 Param. Model σ	9.8	10.6	10.8	11.7	13.7	14.5	8.4	10.4	17.8	9.4	11.4	9.2
1 Param. Model σ	11.0	13.5	13.7	11.5	14.3	15.8	9.3	10.9	17.6	9.8	11.5	10.1
Final Model σ	14.9	18.0	17.8	14.2	15.6	16.6	9.9	11.8	18.5	9.4	11.6	14.8

Radian	13	14	15	16	17	18	19	20	21	22	Average
Raw Data σ_I	5.9	7.1	7.5	6.6	4.65	3.63	5.81	8.17	13.7	11.7	7.99
4 Param. Model σ	4.8	9.1	9.9	10.4	8.3	8.9	7.0	10.9	17.2	13.4	10.80
1 Param. Model σ	--	9.0	10.3	12.6	8.5	9.6	7.5	14.6	18.8	14.2	12.10
Final Model σ	7.1	11.0	10.1	16.4	12.6	15.6	10.1	14.6	19.0	16.9	13.93

$$\frac{\text{total SS - model SS}}{16}$$

This approach resulted in variances which were very close to, and sometimes less than, the inherent variability of the data--a result which did not seem to be intuitive.

A second approach was used. This approach considers the model degrees of freedom to be 10. At each of the 10 locations on each radian there are two data points. Therefore, there are 10 levels of the independent variable, resulting in 10 degrees of freedom. Theoretically, a 10 parameter polynomial would give a perfect fit to the data. Hence, the error degrees of freedom were calculated as:

$$20\text{-}10 = 10 \text{ degrees of freedom}$$

and the variance estimate for each radian was:

$$\frac{\text{error SS}}{10}$$

Table C-1 shows the standard deviations of each radian at each step in the model fitting process. Note that the raw data variances are the smallest, and that, as the model progressed to its final form, the variances increased. This is due to the addition of more parameters and the increasing sample size involved in going from individual radians to

all radians. The average standard deviation of the final model is approximately six pounds higher than the average standard deviation inherent in the raw data.

APPENDIX D

SAMPLE STRIP CHART RECORDING AND DATA FORM

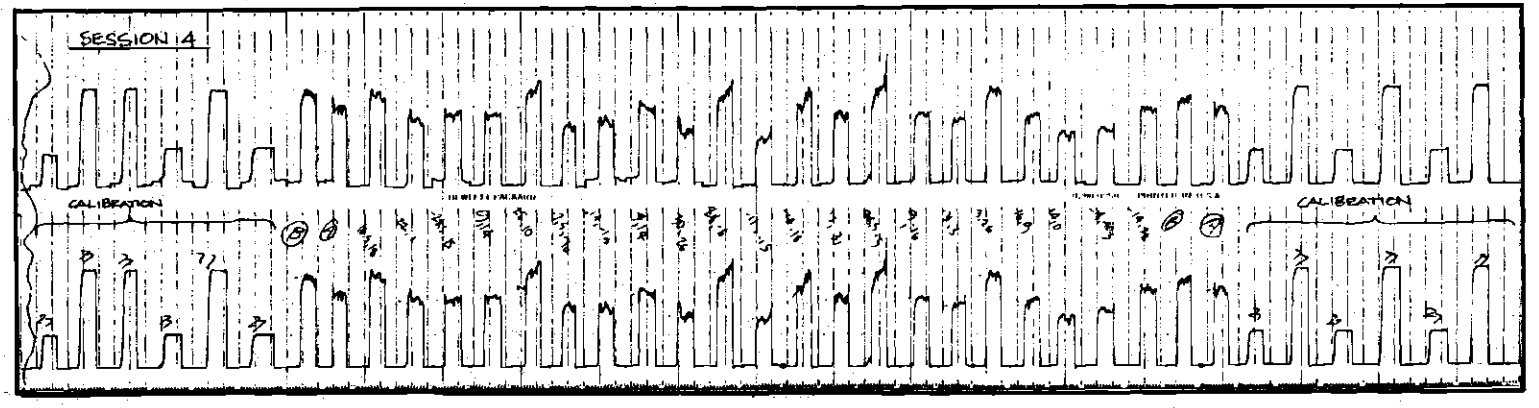

Figure D-1. Sample Strip Chart Recording of Data

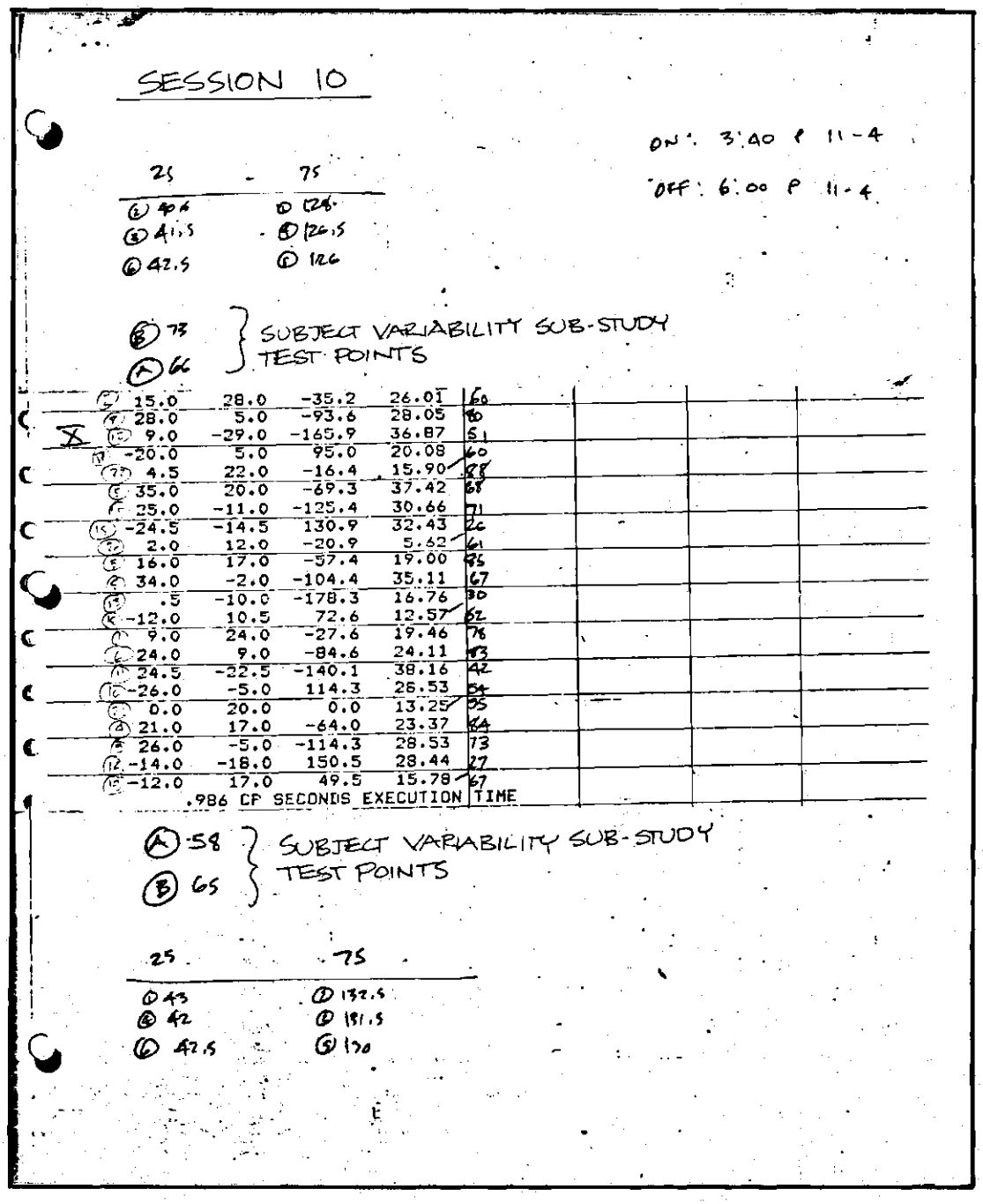

SESSION 10

ON: 3:40 P 11-4

OFF: 6:00 P 11-4

25	75
(E) 40.5	(D) 126
(G) 41.5	(B) 126.5
(C) 42.5	(F) 126

(B) 73 (A) 66 } SUBJECT VARIABILITY SUB-STUDY TEST POINTS

(5)	15.0	28.0	-35.2	26.01	60
(9)	28.0	5.0	-93.6	28.05	80
X (12)	9.0	-29.0	-165.9	36.87	51
(1)	-20.0	5.0	95.0	20.08	60
(11)	4.5	22.0	-16.4	15.90	88
(E)	35.0	20.0	-69.3	37.42	68
(F)	25.0	-11.0	-125.4	30.66	71
(13)	-24.5	-14.5	130.9	32.43	26
(14)	2.0	12.0	-20.9	5.62	61
(B)	16.0	17.0	-57.4	19.00	85
(C)	34.0	-2.0	-104.4	35.11	67
(15)	.5	-10.0	-178.3	16.76	30
(A)	-12.0	10.5	72.6	12.57	62
(C)	9.0	24.0	-27.6	19.46	76
(6)	24.0	9.0	-84.6	24.11	83
(7)	24.5	-22.5	-140.1	38.16	42
(10)	-26.0	-5.0	114.3	28.53	54
(3)	0.0	20.0	0.0	13.25	95
(4)	21.0	17.0	-64.0	23.37	84
(8)	26.0	-5.0	-114.3	28.53	73
(12)	-14.0	-18.0	150.5	28.44	27
(15)	-12.0	17.0	49.5	15.78	67

.986 CP SECONDS EXECUTION TIME

(A) 58 (B) 65 } SUBJECT VARIABILITY SUB-STUDY TEST POINTS

25	75
(D) 43	(D) 132.5
(E) 42	(F) 131.5
(C) 42.5	(G) 130

Figure D-2. Sample Data Form

APPENDIX E

HAND LOCATION COORDINATE CONVERSION COMPUTER PROGRAM

```
      PROGRAM SETUP(INPUT,OUTPUT,TAPE5=INPUT,TAPE6=OUTPUT)
C
C     THIS PROGRAM TAKES THE X AND Y COORDINATES OF HAND LOCATIONS
C     AS INPUT VARIABLES. THESE VALUES ARE THEN CONVERTED TO
C     THE VARIABLES 'CHANG' AND 'RPRPRI'.'CHANG' IS THE ANGLE
C     WHICH THE CHAIR MUST BE ROTATED TO FOR A GIVEN HAND LOCATION.
C     'RPRPRI' IS THE DISTANCE TO WHICH THE TROLLEY MUST BE MOVED.
C     BOTH OF THESE VARIABLES ARE READ DIRECTLY FROM SCALES MOUNTED
C     ON THE TEST EQUIPMENT. THE SHOULDER-HAND DISTANCE (R) IS ALSO PRINTED OUT.
C
      DIMENSION X(216),Y(216),CHANG(216),RPRPRI(216),R(216)
      DO 3 I=1,216
      READ(5,1) X(I),Y(I)
1     FORMAT(F6.1,F6.1)
      P=6.75
      Q=57.296
      IF(X(I).GT.0.0.AND.Y(I).GE.0.0)GO TO 9
      IF (X(I).LT.0.0.AND.Y(I).GE.0.0)GO TO 10
      IF(X(I).GT.0.0.AND.Y(I).LT.0.0)CHANG(I)=
     *(3.1415927-ATAN(-X(I)/(Y(I)-P)))*Q*(-1)
      IF(X(I).LT.0.0.AND.Y(I).LT.0.0)CHANG(I)=
     *(3.1415927-ATAN(X(I)/(Y(I)-P)))*Q
      IF(X(I).EQ.0.0.AND.Y(I).EQ.6.75)GO TO 8
      GO TO 2
9     IF(Y(I).LT.P)GO TO 11
      CHANG(I)=(ATAN(X(I)/(Y(I)-P)))*Q*(-1.)
      GO TO 2
10    IF(Y(I).LT.P)GO TO 12
      CHANG(I)=(ATAN(X(I)/(Y(I)-P)))*Q*(-1.)
      GO TO 2
11    CHANG(I)=(3.1415927-ATAN(X(I)/(P-Y(I))))*Q*(-1.)
      GO TO 2
12    CHANG(I)=(3.1415927-ATAN(-X(I)/(P-Y(I))))*Q
      GO TO 2
8     CHANG(I)=0.0
2     R(I)=SQRT((X(I)-9.)**2+(Y(I)-5.)**2)
3     RPRPRI(I)=SQRT(X(I)**2+(Y(I)-P)**2)
      PRINT 4
4     FORMAT(//,3X,'X',7X,'Y',4X,'CHANG',3X,'RPRPRI',5X,'R')
      PRINT*,'      '
      DO 6 I=1,216
6     PRINT 5,X(I),Y(I),CHANG(I),RPRPRI(I),R(I)
5     FORMAT(F6.1,2X,F6.1,2X,F6.1,2X,F6.2,2X,F6.2)
      STOP
      END
```

BIBLIOGRAPHY

Asmussen, E., Heebol-Nielson, K., "Isometric Muscle Strength of Men and Women," Danish National Association for Infantile Paralysis, Testing and Observation Institute, Communications, No. 11, 1961.

Ayoub, M., McDaniel, J., "Effects of Operator Stance on Pushing and Pulling Tasks," AIIE Transactions, Sept. 1974.

Astrand, P., Rodahl, K., Textbook of Work Physiology, McGraw-Hill Book Co., N.Y., 1970.

Caldwell, L. S., "Body Stabilization and the Strength of Arm Extension," Human Factors, June, 1962.

Caldwell, L. S., Chaffin, D., et al., "A Proposed Standard Procedure for Static Muscle Strength Testing," American Industrial Hygiene Journal, April 1974.

Chaffin, D. B., "Biomechanical Strength Models," Old World, New World, One World, Proceedings of the 6th Congress of the International Eronomics Association and Technical Program for the 20th Annual Meeting of the Human Factors Society, 1976.

Chaffin, D. B., Herrin, G., "The Effectiveness of Pre-Employment Strength Testing for Manual Materials Handling Jobs," Old World, New World, One World, Proc. of 6th Congress of International Ergonomics Association, 1976.

Chaffin, D. B., "Ergonomics Guide for the Assessment of Human Static Strength," American Industrial Hygiene Association Journal, July, 1975.

Clarke, H. H., Muscular Strength and Endurance in Man, Prentice Hall, 1966.

Diffrient, N., Tilley, A. R., Bardagjy, J. C., Humanscale 1/2/3, MIT Press, Cambridge, Mass., 1974.

Garg, A., Chaffin, D. B., "A Biomechanical Computerized Simulation of Human Strength," AIIE Transactions, March 1975.

Gaughran, G. R. L., Dempster, W. T., "Force Analyses of Horizontal Two-Handed Pushes and Pulls in the Sagittal Plane," Human Biology 28, 1956.

Draper, N., Smith, H., Applied Regression Analysis, John Wiley and Sons, New York, 1966.

Hines, W. W., Montgomery, D. C., Probability and Statistics in Engineering and Management Science, Ronald Press Co., N.Y., 1972.

Hugh-Jones, P., "The Effect of Limb Position in Seated Subjects on Their Ability to Utilize the Maximum Contractile Force of the Limb Muscles," Journal of Physiology, 105, 1947.

Hunsicker, P. A., "Arm Strength at Selected Degrees of Elbow Flexion," A.F. Project No. 7214-71727, WADC-TR-54-548, WPAFB, 1955.

Johnson, N. L., Kotz, S., Distributions in Statistics, Continuous Multivariate Statistics, John Wiley and Sons, N.Y., 1972.

Kilpatrick, K. E., "A Biokinematic Model for Workplace Design," Human Factors, 14(3), 1972.

Kroemer, K. H. E., "Horizontal Push and Pull Forces Exertable when Standing in Working Positions on Various Surfaces," Applied Ergonomics, June 1974.

Kroemer, K. H. E., Howard, J. M., "Toward Standardization of Muscle Strength Testing," Medicine and Science in Sports, 2(4), 1970.

Kroemer, K. H. E., "Push Forces Exerted in Sixty-Five Common Working Positions," AMRL-TR-68-143, Aug. 1969, AD695 040.

Laubach, L. L., "Muscular Strength of Women and Men, a Comparative Study," AMRL-TR-75-32, May 1976, AD A025 793.

Laubach, L. L., Kroemer, K. H. E., Thordsen, M. L., "Relationships Among Isometric Forces Measured in Aircraft Control Locations," Aerospace Medicine, July, 1972.

Leeper, R. C., "Study of Control Force Limits for Female Pilots," FAA-AM-73-as, Dec. 1973, AD 777839.

Lower, R. S., Schutz, R. K., Sadosky, T. L., "A Prediction Model of Arm Push Strength in the Transverse Plane," Proceedings of the Human Factors Society, 21st Annual Meeting, San Francisco, 1977.

Lower, R. S., "A Mathematical Predictive Model of Arm Strength," Master's Thesis, Georgia Institute of Technology, June, 1976.

Martin, J. B., Chaffin, D. B., "Biomechanical Computerized Simulation of Human Strength in Sagittal Plane Activities," AIIE Transactions, March 1972.

Montgomery, D. C., Design and Analysis of Experiments, John Wiley and Sons, New York, 1976.

Nie, N. H., Hull, C. H., Jenkins, J. G., Steinbrenner, K., Bent, D. H., Statistical Package for the Social Sciences, 2nd Ed., McGraw-Hill, N.Y., 1970.

Carley, C. O., Calculus: A Modern Approach, Barnes and Noble, New York, 1971.

Pearson, J. R., McGinley, D. R., Butzel, L. M., "A Dynamic Analysis of the Upper Extremity: Planar Motions," Human Factors, Feb., 1963.

Roebuck, J. A., Kroemer, K. H. E., Thomson, W. G., Engineering Anthropometry Methods, John Wiley and Sons, New York, 1975.

Schanne, F., "A Three Dimensional Hand Force Capability Model for a Seated Person," unpublished dissertation for Ph.D. in Industrial Engineering, University of Michigan, Ann Arbor, Mich., 1972.

Thordsen, M. L., Kroemer, K. H. E., Laubach, L. L., "Human Force Exertions in Aircraft Control Locations," AMRL-TR-71-119, Feb. 1972, AD 740 930.

Van Cott, H. P., Kinkade, R. G., Human Engineering Guide to Equipment Design, Revised Edition, Joint Army, Navy, Air-Force Steering Committee, Washington, D. C., 1972.